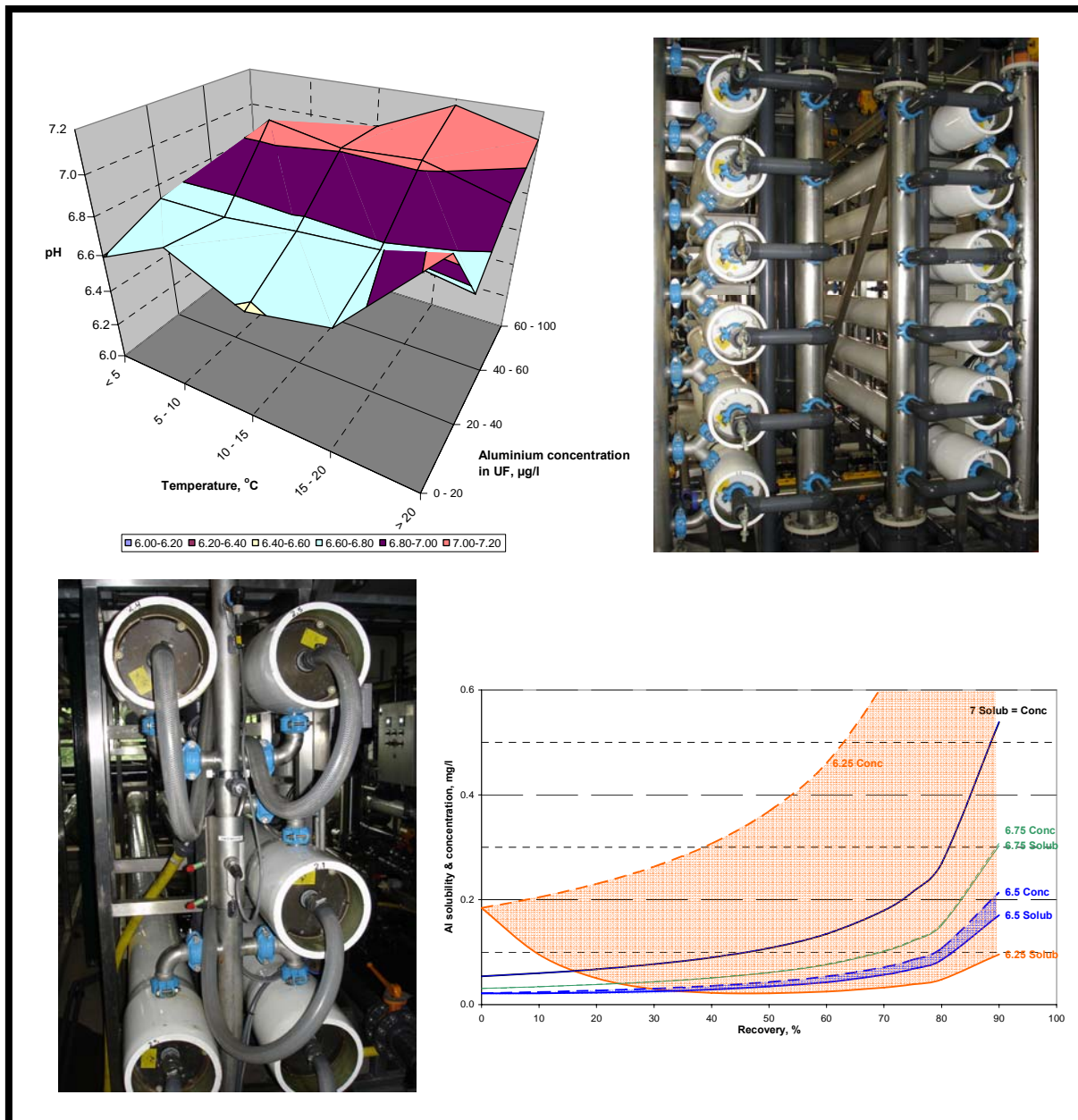


UNESCO-IHE INSTITUTE FOR WATER EDUCATION



Role of Coagulant in an Integrated Membrane System: Case Study on a UF/RO plant, Drenthe

SERGIO GENARO SALINAS RODRÍGUEZ

MSc Thesis MWI 2006-26
April 2006

UNESCO-IHE
Institute for Water Education



Role of Coagulant in an Integrated Membrane System: Case Study on a UF/RO plant, Drenthe

Master of Science Thesis
by
Sergio Genaro Salinas Rodríguez

Supervisor
Prof. Jan C. Schippers M.Sc., Ph.D. (UNESCO-IHE)

Mentor
Maria D. Kennedy, Ph.D. (UNESCO-IHE)

Examination committee
Prof. Jan C. Schippers M.Sc., Ph.D. (UNESCO-IHE), Chairman
Maria D. Kennedy, Ph.D. (UNESCO-IHE)
Ir. Aleid Diepeveen (WMD)

This research is done for the partial fulfilment of requirements for the Master of Science degree at the UNESCO-IHE Institute for Water Education, Delft, the Netherlands

Delft
April 2006

The findings, interpretations and conclusions expressed in this study do neither necessarily reflect the views of the UNESCO-IHE Institute for Water Education, nor of the individual members of the MSc committee, nor of their respective employers.

To my parents

Abstract

In 2000, the Water Company of Drenthe (WMD) built the Klazienaveen Treatment Plant, located in Klazienaveen (Assen) in the north east of The Netherlands in order to supply the NORIT plant (manufacturer of Activated Carbon) with boiler feed water ($Cl^- < 5\text{ ppm}$, $TDS < 20\ \mu\text{S/cm}$, $5.5 < \text{pH} < 7$). The nominal production capacity is $60\ \text{m}^3/\text{hr}$ ($17\ \text{l/s}$) and the annual production is $380,000\ \text{m}^3$. Pre-treatment includes coagulation, whereby *Poly Aluminium Chloride* (PAC) ($14\ \text{ppm}$ in 2005) is employed as a coagulant. The filtration process is performed in two parallel in a continuous process using Astrasand filters. After filtration, PAC is again dosed ($1\ \text{ppm}$) before the *Ultrafiltration* units (UF). The UF system comprises four units or skids in parallel. A UV meter is employed to monitor the UF permeate, and the PAC dose is adjusted depending on the UV reading. The UF permeate is fed to three *Reverse Osmosis* units (RO) units in a two-stage arrangement, with a total recovery of 75%. The frequency of cleaning of the reverse osmosis membranes can be as often as once every two weeks, particularly in warm periods, which suggests that membrane fouling (organic, biological, particulate) and/or scaling (inorganic fouling) may be occurring in the reverse osmosis system.

This research was focused on the affects of coagulant in the integrated membrane (UF & RO) system. The approach taken involved determination of the optimum dose of coagulant for the process, evaluation of the efficiency of UV and DOC removal by coagulation and simulation of the aluminium solubility and aluminium concentration in the RO system. The available data, which comprised monthly/weekly measurements for a period of six years of operation, was studied and analyzed and an attempt was made to draw some conclusions for the plant.

The study of the chemical dosing control (CDC) revealed that the use of simple and robust online sensors like UV measurement allows automatic dosing control. However, it was found that the actual target value of $20\ \text{Abs/m}$ produces substantial over dose of coagulant – 90 % of the time – when UV removal is considered only. In 2005, the PAC dose was ca. $14\ \text{mg/l}$. However, for coagulant doses in excess of $5\ \text{mg/l}$, the additional removal of UV is less than 2.5 % per mg coagulant/l, which suggests that the current dose is on the high side.

Poly aluminium chloride is a very complex compound. The species that are produced during coagulation cause a change in pH along the RO units, but this change is constant for any given recovery, e.g. at 75% recovery, the pH change between the RO feed water and concentrate water is 0.6. It was found that the optimum pH (6.6) for coagulation for this plant was similar in the summer and winter periods, although this is based on limited data. The simulation of aluminium solubility and concentration along RO systems were done on basis of three aluminium species, Al_{13}^{7+} , $\text{Al}(\text{OH})_4^-$, $\text{Al}(\text{OH})_2^+$. Two temperatures were simulated, $20\ ^\circ\text{C}$ to represent the summer (warm period) and $5\ ^\circ\text{C}$ to represent the winter (cold period). Results showed that for cold periods ($5\ ^\circ\text{C}$) an RO feed water pH of at least 7.2 and for warm periods ($20\ ^\circ\text{C}$), a feed water pH of at least 6.7 are required respectively, to avoid scaling of aluminium on the membranes.

A deposition factor was calculated in the RO plant and this suggested that ca. 21 % of the aluminium fraction that theoretically can precipitate on the RO membranes actually resulted in membrane scaling. $\text{MFI}_{0.45}$ results gave an indication of leakages or broken fibres on UF modules. Integrity tests revealed that 0.1 % of the fibres were leaking per module.

In conclusion, theoretical simulation of aluminium solubility and results of deposition factor showed that aluminium more than likely plays a role in fouling of the RO membranes and could be a reason for the frequent cleaning. Actual doses of coagulant produce not significant additional UV removal and in that sense a reduction from $14\ \text{mg/l}$ (2005) to ca. $7\ \text{mg/l}$ could be considered.

Keywords: PAC, ultra filtration, Reverse osmosis, fouling.

Acknowledgements

To the Great Architect of the Universe, nothing is possible without him.

For their support, permanent guide and wise advice I am grateful to Prof. Jan C. Schippers and Dr. Maria D. Kennedy from UNESCO-IHE.

To the Water Company of Drenthe (WMD) for funding this project, especially to Aleid Diepeveen, Simon Dost; and to Hilde Prummel and Marcel Boorsma from Water Laboratory Noord (WLN).

To NUFFIC for let me to go further in my academic life.

To my family for encourage and help me to be steadfast in this *journey*.

Table of Contents

Abstract	i
Acknowledgements	ii
1 Introduction and Objectives	1
1.1 Introduction	1
1.1.1 Source water quality	3
1.2 Goal and Objectives	4
1.2.1 Assumptions of the research.....	4
1.2.2 Hypothesis of the project.....	5
2 Theory and Literature Review	6
2.1 Natural Organic Matter	6
2.1.1 Characterization of Natural Organics	6
2.1.2 UV absorbance	7
2.1.3 Aromaticity and Reactivity.....	8
2.1.4 Size of NOM.....	8
2.1.5 Solubility and aggregation of Natural Organics	8
2.2 Coagulation	9
2.2.1 Coagulation Mechanism.....	9
2.2.2 Chemistry of particulates.....	10
2.2.3 Chemistry of NOM.....	11
2.2.4 Coagulant Chemistry	12
2.3 Factors affecting Coagulation	15
2.3.1 Alkalinity, pH.....	15
2.3.2 NOM.....	19
2.3.3 Advances in coagulation process control.....	19
2.4 UF, RO and membrane characteristics	20
2.4.1 Ultrafiltration.....	20
2.4.2 Membrane characterization	21
2.5 Effects of parameters on membrane fouling	22
2.5.1 Hydrophobicity effects	22
2.5.2 Ionic effects	22
2.6 Membrane flux decline and fouling	22
2.6.1 UF dead end, membrane flux model.....	23
2.6.2 Membrane fouling by NOM.....	23
2.6.3 Membrane fouling mechanisms.....	25
2.6.4 Membrane cleaning	25
3 Materials and Methods	27
3.1 Materials and general operation	27
3.1.1 WMD “Norit” Klazienaveen plant	27
3.1.2 PAC dosing.....	27
3.1.3 UF Membrane Module	28
3.1.4 UF Feedwater	29
3.1.5 UF Backwashing	29
3.1.6 RO Membrane module	30
3.1.7 RO feed water.....	31

3.1.8	RO chemical cleaning.....	31
3.2	Methods	31
3.2.1	Data Analysis.....	31
3.2.2	Coagulant dosage efficiency.....	31
3.2.3	Simulating Solubility change in RO.....	32
3.2.4	Deposition factor calculation.....	32
3.2.5	UF Integrity test.....	34
3.2.6	Specific resistance of aluminium.....	34
4	Results and Discussion.....	37
4.1	Rate of floc formation.....	37
4.2	PAC dose.....	39
4.2.1	UV removal.....	41
4.2.2	DOC removal.....	43
4.3	Phosphate removal.....	45
4.4	Organic matter complexation with Aluminium	46
4.5	Characterising of the coagulant.....	47
4.5.1	Equations of aluminium species in PAC	47
4.6	Aggressivity against CaCO₃ (LSI) for permeate UF.....	49
4.7	Aluminium solubility changes in RO	50
4.8	Solubility of aluminium – UF permeate.....	50
4.8.1	Dependence on temperature	50
4.8.2	Optimum pH for coagulation.....	52
4.9	Simulation of Aluminium.....	53
4.9.1	Simulation of Aluminium solubility.....	53
4.9.2	Simulation of Aluminium concentration and solubility.....	55
4.10	Aluminium scaling - precipitation.....	56
4.10.1	Particle Deposition Factor, Ω	56
4.10.2	Modified Fouling Index (MFI)	57
4.10.3	Specific resistance.....	58
4.10.4	Integrity tests	59
5	Conclusions and Recommendations.....	61
5.1	Conclusions.....	61
5.2	Recommendations.....	61
6	References.....	62
7	Appendixes.....	65
7.1	Annex 1	65
7.1.1	Summary of chemical parameters analysis.....	65
7.1.2	Ionic Balances	65
7.1.3	Flocculation, G & Gt values	66
7.1.4	Theoretical Solubility of Aluminium.....	66
7.1.5	Sampling Points for LCOCD test.....	67
7.2	Annex 2 - Equations for aluminium solubility and concentration along R.O. systems.....	67
7.2.1	Determining aluminium species solubility	68
7.2.2	Determining aluminium species concentration.....	71

7.3	Annex 3 – Simulation of Al solubility and concentration.....	75
7.3.1	T = 20°C	75
7.3.2	T = 5°C	78
7.4	Annex 4. Aluminium soluble in water.....	80
7.5	Annex 5. Deposition factor, pH and Temperature.....	82
7.6	Annex 6 - The Modified Fouling Index (MFI).....	82
7.7	Annex 7 - Specific Resistance.....	86

Tables Index

Table 1-1	Chemical costs report (till end of July 2005).....	2
Table 1-2	Average removal efficiencies in the plant (%).....	3
Table 1-3	Source water quality fluctuations.....	3
Table 1-4	Requirements of quality for boiler feed water.....	4
Table 2-1	Guidelines on the nature of NOM and expected TOC removals.....	12
Table 2-2	Summary of Coagulant solubility	14
Table 2-3	Raw water parameters affecting Coagulant dosage and selection.....	15
Table 2-4	Filtration processes size particle exclusion	20
Table 2-5	Schematic description of the effect of solution chemistry on the conformation of NOM macromolecules (Hong and Elimelech, 1997).....	24
Table 3-1	Characteristics Coagulant Mixing Tank.....	27
Table 3-2	Characteristic of X-flow UF module (source: Technical data manufacturer)	29
Table 3-3	Operational and cleaning parameters of X-flow UF module	29
Table 3-4	Characteristic of RO membranes (source: Technical data manufacturer).....	30
Table 3-5	Operational parameters of RO module.....	30
Table 3-6	Solubility Equations for several Aluminium species (mol/l)	32
Table 3-7	Concentration Equations for several Aluminium species (mol/l).....	32
Table 4-1	Data and results. G, Gt estimation.....	38
Table 4-2	Average dose in mg Al/l	40
Table 4-3	Aluminium Species equations, log Al in mol/l	49
Table 4-4	Particle Deposition factor in Klazienaveen plant, Ω	57
Table 4-5	Klazienaveen MFI _{0.45} results.....	58
Table 4-6	Klazienaveen plant Integrity test results, 16/03/06	59
Table 7-1	Summary of Coagulant solubility	67

Figures Index

Figure 1-1	Treatment scheme of Klazienaveen Plant.....	2
Figure 1-2	Fluctuation of DOC in time (mg/l)	4
Figure 2-1	Composition of an average river water (5 mg/l DOC) (Thurman, 1985).....	6
Figure 2-2	Continuum of particulate and dissolved organic carbon in natural waters (Aiken and Leenheer, 1993).....	7
Figure 2-3	Conceptual view of coagulation reactions (Pernitsky and Edzwald, 2003).....	9
Figure 2-4	Modes of bridging between NOM and aluminium ions (Gregor et al., 1997).....	10
Figure 2-5	Surface Chemistry of a clay particle (Pernitsky and Edzwald, 2003).....	10
Figure 2-6	Electrochemical behaviour of hydroxyl groups (Pernitsky and Edzwald, 2003).....	11
Figure 2-7	Typical NOM structure.....	11
Figure 2-8	Concentration of soluble Al species in equilibrium with amorphous hydroxides. (Al_T represent total soluble species) (Pernitsky and Edzwald, 2003).....	13
Figure 2-9	Distribution of monomeric Al hydrolysis products as a function of pH	14
Figure 2-10	Effects of pH on floc charge	16
Figure 2-11	Effects of pH on NOM removal.....	17
Figure 2-12	Influence of pH (Delgado et al., 2003)	17
Figure 2-13	Theoretical solubility of amorphous $Al(OH)_3$ in water at zero ionic strength and at 298 K, polynuclear complexes not included. (Schrader et al. 2005).....	18

Figure 2-14	Influence of pH on the removal of colour with coagulation with aluminium salts	18
Figure 2-15	Double layer of membrane surface (Elimelech et al., 1994).....	22
Figure 2-16	Membrane fouling mechanisms (Peavy, 1984).....	25
Figure 3-1	Source water canal – upstream and downstream of the intake.....	27
Figure 3-2	Water intake and rough filter	27
Figure 3-3	PAC dosing tank and pumps.....	28
Figure 3-4	Scheme of UF in Klazienaveen plant.....	28
Figure 3-5	Scheme of the RO in Klazienaveen plant	30
Figure 4-1	Treatment scheme – Klazienaveen Plant	37
Figure 4-2	Influence of suspension pH on the flocculation rate (Zhang et al., 2004a).....	38
Figure 4-3	PAC dosage	40
Figure 4-4	UV removal efficiency vs. PAC dose and Coagulant dose vs UV removal efficiency per mg of Al per litre.....	42
Figure 4-5	Added value of coagulant dosage	43
Figure 4-6	DOC removal vs. PAC dosage and DOC removal vs. UV removal	43
Figure 4-7	DOC removal (%) per mg of aluminium and Added value for DOC removal	44
Figure 4-8	UV/DOC ratio.....	44
Figure 4-9	Solubility of metal phosphates (Stumm and Morgan, 1996)	45
Figure 4-10	LSI in permeate UF.....	49
Figure 4-11	pH in RO concentrate vs Recovery and vs. pH RO feed	50
Figure 4-12	Total Aluminium solubility varying temperature	51
Figure 4-13	Aluminium concentration in RO feed water depending on temperature compared with theoretical PAC solubility	51
Figure 4-14	Solubility of Aluminium in permeate UF. November to April (“winter”) and May to October (“summer”).....	52
Figure 4-15	Optimum pH for minimum solubility of Aluminium.	53
Figure 4-16	Simulation of solubility for $\text{pH}_{\text{feed RO}} = 6.5$ and $T = 20^\circ\text{C}$	54
Figure 4-17	Simulation of Total Aluminium solubility, $T=20^\circ\text{C}$ and $T=5^\circ\text{C}$	54
Figure 4-18	Simulation Aluminium solubility and concentration, $T= 20^\circ\text{C}$ and $T = 5^\circ\text{C}$	55
Figure 4-19	Recovery (%) vs. $C_{\text{concentrate}}$ ($\mu\text{g/l}$) for different Particle Deposition Factors (Ω).....	56
Figure 4-20	Deposition factor, Ω (Recovery = 75 %, $\text{CF} = 4$) (without outliers).....	57
Figure 4-21	UF scheme – Klazienaveen plant.....	59
Figure 7-1	Theoretical solubility for Al species in equilibrium with $\text{Al}(\text{OH})_3(\text{am})$ indicated by solid (20°C) and dashed (5°C) lines. (Pernitsky et al., 2003).....	66
Figure 7-2	Proposed sampling points for LC-OCD test	67
Figure 7-3	Simulation Al solubility and Al concentration ($\text{pH}_{\text{feed RO}} = 6$), $T = 20^\circ\text{C}$ (a)	75
Figure 7-4	Simulation Al solubility and Al concentration ($\text{pH}_{\text{feed RO}} = 6$), $T = 20^\circ\text{C}$ (b).....	75
Figure 7-5	Simulation Al solubility and Al concentration ($\text{pH}_{\text{feed RO}} = 6.5$), $T = 20^\circ\text{C}$ (a)	76
Figure 7-6	Simulation Al solubility and Al concentration ($\text{pH}_{\text{feed RO}} = 6.5$), $T = 20^\circ\text{C}$ (b).....	76
Figure 7-7	Simulation Al solubility and Al concentration ($\text{pH}_{\text{feed RO}} = 7$), $T = 20^\circ\text{C}$ (a).....	76
Figure 7-8	Simulation Al solubility and Al concentration ($\text{pH}_{\text{feed RO}} = 7$), $T = 20^\circ\text{C}$ (b).....	77
Figure 7-9	Simulation Al solubility and Al concentration ($\text{pH}_{\text{feed RO}} = 7.5$), $T = 20^\circ\text{C}$ (a)	77
Figure 7-10	Simulation Al solubility and Al concentration ($\text{pH}_{\text{feed RO}} = 7.5$), $T = 20^\circ\text{C}$ (b).....	77
Figure 7-11	Simulation Al solubility and Al concentration ($\text{pH}_{\text{feed RO}} = 6$), $T = 5^\circ\text{C}$ (a)	78
Figure 7-12	Simulation Al solubility and Al concentration ($\text{pH}_{\text{feed RO}} = 6$), $T = 5^\circ\text{C}$ (b).....	78
Figure 7-13	Simulation Al solubility and Al concentration ($\text{pH}_{\text{feed RO}} = 6.5$), $T = 5^\circ\text{C}$ (a)	78
Figure 7-14	Simulation Al solubility and Al concentration ($\text{pH}_{\text{feed RO}} = 6.5$), $T = 5^\circ\text{C}$ (a).....	79
Figure 7-15	Simulation Al solubility and Al concentration ($\text{pH}_{\text{feed RO}} = 7$), $T = 5^\circ\text{C}$ (a)	79
Figure 7-16	Simulation Al solubility and Al concentration ($\text{pH}_{\text{feed RO}} = 7$), $T = 5^\circ\text{C}$ (b).....	79
Figure 7-17	Simulation Al solubility and Al concentration ($\text{pH}_{\text{feed RO}} = 7.5$), $T = 5^\circ\text{C}$ (a).....	80
Figure 7-18	Simulation Al solubility and Al concentration ($\text{pH}_{\text{feed RO}} = 7.5$), $T = 5^\circ\text{C}$ (b).....	80
Figure 7-19	Aluminium concentration (data) and Al solubility in RO feed water, $\mu\text{g/l}$	81
Figure 7-20	Aluminium concentration and Al solubility in RO concentrate water, $\mu\text{g/l}$	81
Figure 7-21	Deposition factor (Ω) as function of pH (Recovery = 75 %, $\text{CF}_{\text{hyp}} = 4$).....	82
Figure 7-22	Deposition Factor (Ω) as function of Temperature (Recovery = 75 %, $\text{CF}_{\text{hyp}} = 4$).....	82

1 Introduction and Objectives

1.1 Introduction

The use of reverse osmosis (RO) in production of boiler feed water can cut chemical costs by reducing the frequency of ion exchange regeneration. A complete system, including RO and ion exchange is typically more cost effective system when compared to systems that do not use RO. However, conventional RO systems require pre-treatment units, which obviously add to the total cost of the system (NewLogicResearchInc., 2003).

Silicate and colloidal deposits decrease boiler efficiency and also cause premature failure of turbines. Ultrafiltration (UF) can remove more than 99% of colloidal silica, as well as precipitated iron and aluminium. The reduction in particulate matter, suspended solids and total organic carbon (TOC) also enhance turbine and boiler efficiency. However, the use of conventional membrane technologies can suffer from substantial membrane fouling problems (NewLogicResearchInc., 2003).

The influent water to a plant can come from a variety of sources, including groundwater well (aquifer), surface water or wastewater, and has to be treated to meet the quality requirements for boiler feed water. For boiler feed water treatment, depending on its requirements, a number of processes can be used, including chemical treatment/lime softening, dual media filtration, carbon adsorption, conventional RO membrane filtration and final ion exchange resin polishing. However, significant waste is generated from these unit operations, including spent carbon and spent regenerating chemicals from the ion exchange resins if it is the case. To avoid scaling in the boilers, power plants normally utilize a multi-step process to remove the hardness of the incoming water, i.e. chemical treatment or ion exchange, as well as other less advanced methods, such as multimedia filtration (NewLogicResearchInc., 2003).

The manufacturing works of activated carbon in the north of Holland by NORIT requires high water quality for the boiler. To satisfy this requirement as in quality as in quantity the Water Company of Drenthe built a treatment plant “Norit” Klazienaveen with high technical and multi step processes; this plant started to operate in 2000. “Norit” Klazienaveen Treatment Plant is located in Klazienaveen (Assen) in the north east of The Netherlands. It has a nominal production capacity of 60 m³/hr (17 l/s), a maximum production capacity of 75 m³/hr (21 l/s) and the yearly actual production is 380,000 m³. The treatment units of the plant are shown in Figure 1-1. The operation of the treatment plant is the responsibility of BètaWater, supplier of water utilities and part of the drinking water supply company Waterleidingmaatschappij Drenthe (WMD).

Pre-treatment includes coagulation (adding polyaluminium chloride, PAC, (10 ppm) as a coagulant). The filtration process is performed in two parallel units in a continuous process using Astrasand filters. After filtration, PAC is again dosed (1 ppm) before the Ultra Filtration units (UF). The UF system comprises four units or skids in parallel. For chemical cleaning of the UF Divos, NaOH and NaCl are used. A UV meter monitors the UV of the UF permeate. The desired value of the UV of the UF permeate is 20 Abs/m, and if the reading is higher/lower than this value, the PAC dose is changed accordingly. Thereafter, the UF permeate is fed to three reverse osmosis units (RO) in a two-stage arrangement with a total recovery of 75 %.

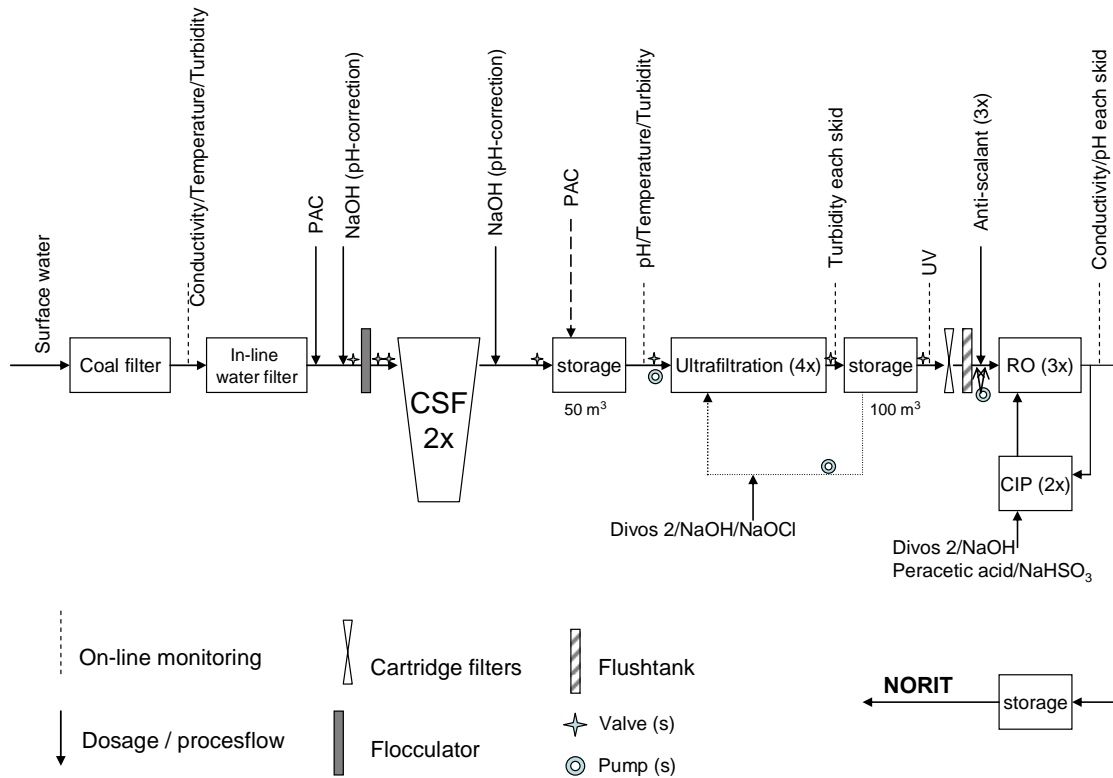


Figure 1-1 Treatment scheme of Klazienaveen Plant

The monitoring system takes place across the plant, for measuring the electrical conductivity, temperature, pH, UV extinction, and turbidity.

The treatment plant is actually facing an optimization plan. Thus, a main concern for this plan it is to reduce the costs for chemicals. In the table below it is shown that the coagulant is the more expensive item in the treatment for chemicals.

Table 1-1 Chemical costs report (till end of July 2005)

Overview Chemical costs	2005	2004
Cleaning UF: "NaOCl"	€ 527,34	€ 518,87
Cleaning RO: "Sodium Bisulfate"	€ 642,07	€ 963,09
Cleaning RO: "Peracetic acid"		€ 1.365,38
Cleaning UF/RO: "Divos2"	€ 4.606,74	€ 15.745,52
Cleaning UF(?): "Oxaalzuur"	€ 637,50	
Conditioning RO: Anti-scalant	€ 8.970,00	€ 14.160,00
Conditioning pH-correction: "Caustic soda"		€ 4.243,04
Coagulant PAC	€ 15.918,10	€ 23.956,60
Total	€ 31.301,75	€ 60.952,50
Produced/delivered (till 04/07/'05)	187.558 m3	
Estimate (till 28/07/05)	211.558 m3	
Total produced 2004		361.694 m3
Costs of chemicals per m ³	€ 0,148	€ 0,169

In general the costs of chemicals can be divided in three main issues: cleaning of membranes (UF/RO), conditioning of (process) water (pH, etc) and coagulant dosing (PAC). According to the table above last year the major costs were for coagulant dosing, 40% and for cleaning and conditioning both 30%. In 2004 a connection for the

delivery of sodium hydroxide is made to the system of Norit (client), who deliver this chemical for free.

In 2005 the costs for coagulant dosing are even higher, e.g. 50% than 2004. The other chemical costs are for cleaning, e.g. 20% and conditioning e.g. 30%.

It is expected that with the optimisation in the coagulation step, through an appropriate dosage and pH correction the UV and possibly NOM removal will increase and therefore the coagulant dose will reduce. Optimum coagulation conditions are those that maximize pathogen removals (not the case), produce low turbidities and particle counts, and minimize residual Aluminium.

Table 1-2 Average removal efficiencies in the plant (%)

Process	UV	DOC	Turbidity
After CSF	70.7	36.0	33.1
After UF	80.5	60.1	99.8

Table 1-2 shows that UF is very important for DOC and turbidity removal. It is possible to say that at least 60 % of the DOC has size bigger than the porous size of UF membranes. Figure 2-2 shows the size of different types of compounds.

1.1.1 Source water quality

In general the policy of the Dutch water sector does not allow the industry sector consumes groundwater, only surface water.

The source water for the plant change with the season, for summer – from April to October - is canal water with an average 16 mg/l of DOC and in winter – November to march - the NOM presence is even higher. During the winter period the plant uses the canal water, which running through an area with peaty, high iron and organic matter concentrations and a high turbidity. In the summer period, the plant uses another source of water, the Ijssel Lake. This water has a relatively low turbidity and low concentration of iron and organic matter and a high TDS. The change between the two water types is gradual and occurs in April and October. The water quality of both sources needs charismatic process to meet the client standard.

With the time a lot of data and experience has been collected by the plant during the six years of operation. The raw water quality changes as the source change between the direct canal and the lake. That means high variation in all water quality parameters. The Table 1-3 shows the water quality as maximum and minimum for the most effect parameters in the treatment process.

Table 1-3 Source water quality fluctuations

Parameter	Unit	Min	Max
Temperature	°C	2	22
DOC	mg C/l	12	35
Turbidity	FTU	12	80 (120)
UV extinction	abs/m	35	165
Suspended solids, SS	mg/l	4	40

The source water quality fluctuates with the seasons. It is in winter that the worse situation is present where the NOM presence is higher and with high values of EC. The Figure 1-2 shows the variation with time of organic matter in source water. The period where the temperatures are colder present more DOC content than in “summer” period.

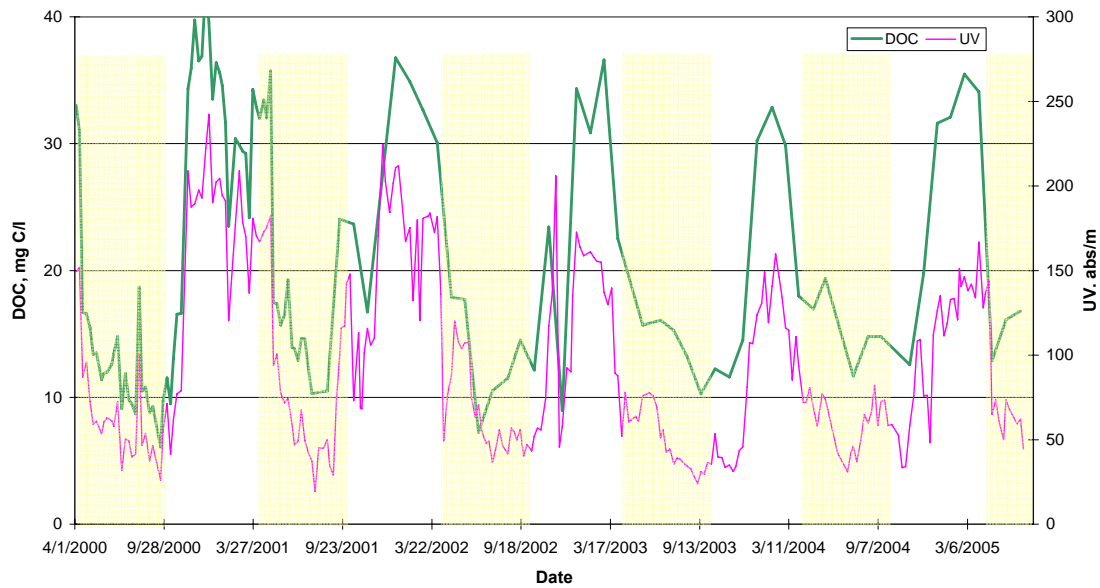


Figure 1-2 Fluctuation of DOC in time (mg/l)

The client has a special water quality standard, with low total dissolved salts (TDS) and other parameters. This standard must meet by the “Norit” Klazienaveen water product not only the quality but also the quantity. The quality requirements are shown in Table 1-4.

Table 1-4 Requirements of quality for boiler feed water

Requirement	Value
Electrical Conductivity, ($\mu\text{S}/\text{cm}$)	< 20
Chloride concentration, Cl^- (ppm)	< 5
pH	5.5 - 7

The requirements are very demanding. These force to the operator to use as much coagulant as necessary in order to obtain the required quality product.

1.2 Goal and Objectives

The main *goal* of this study is to study the role of coagulant in an integrated membrane system specifically in Klazienaveen treatment plant.

The *specific objectives* are:

- Analyse the water treatment process in Klazienaveen Plant.
- Evaluate chemical dosing control (CDC) in terms of removal efficiency of UV and DOC.
- Determine the optimum conditions for coagulation. (Maximize particle and turbidity removal, Maximize TOC removal, and Minimize residual aluminium).
- Simulate change in solubility and change in concentration of aluminium in reverse osmosis systems

1.2.1 Assumptions of the research

1. Total dose of PAC in front of CSF and UF is governed by the ratio $\text{UV}/\text{TOC} < 2.5$.
2. Fouling RO membranes and cleaning frequency is governed by fouling.

1.2.2 Hypothesis of the project

1. Adapting G and Gt- value in the flocculation unit prior to UF will improve the effectiveness of PAC. As a result a lower dose will be required.
2. It is possible to reduce the dose and/or cost of PAC by 50%, without affecting the performance of UF and RO plant. pH plays a dominant role in optimizing PAC dose.
3. Precipitation and/or deposition of Aluminium plays a substantial role in fouling RO membranes in Klazienaveen plant.
4. PAC reduces substantially NOM fractions responsible for organic fouling in UF and RO and fouling in RO.
5. PAC reduces the concentration of: phosphate, silica, aluminium. Dose and pH play a dominant role.

2 Theory and Literature Review

2.1 Natural Organic Matter

Natural organics, especially humic acid (HA) and fulvic acid (FA) contribute to the natural colour of water, which becomes visible if the dissolved organic carbon (DOC) concentration is higher than approximately 5 mg/l. It is for that reason that natural organics removal is often referred to as colour removal. Surface water DOC contains about 45 % FA, 5 % HA, 25 % low molecular weight (LMW) acids, 5 % neutral compounds, 5 % bases and 5 % contaminants (Thurman, 1985). An average organic composition of natural water is shown in Figure 2-1. However, the quantitative amount of each fraction is case specific.

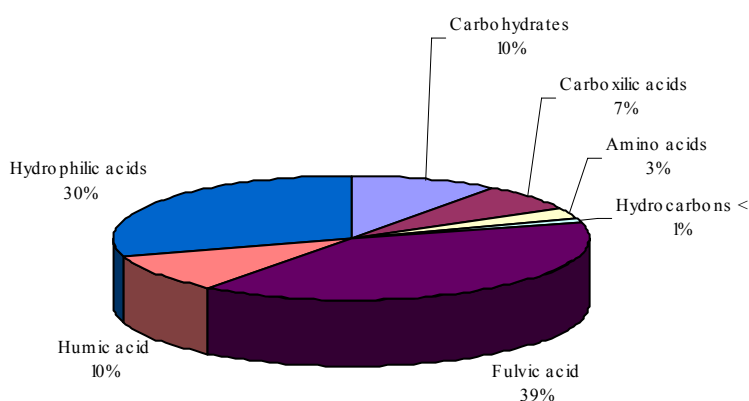


Figure 2-1 Composition of an average river water (5 mg/l DOC) (Thurman, 1985)

Three different compounds make up humic substances (HSs): Humin (defined insoluble), humic acid (HA, insoluble at a pH of 1) and fulvic acid (FA, soluble at any pH) (Schafer, 2001). In general, NOM is the complete content of organics in natural water as shown in Figure 2-1. This NOM is generally obtained by concentration or drying a surface water sample. HA and FA are fractions of NOM that require a fractionation process for separation.

2.1.1 Characterization of Natural Organics

The characterization of natural organics is important in order to understand treatment behaviour and to compare results to other waters. The main characteristics of natural organics are molecular weight, functional groups, hydrophobicity and charge. Results obtained are often relative, depending on the method used and thus vary greatly, even for identical compounds (Schafer, 2001). It is recommended that where possible apply different methods.

2.1.1.1 Organic Carbon

A sum parameter for organic matter is total organic matter (TOC) or dissolved organic carbon (DOC). However DOC or TOC will not give any information about the HS content if mixed organic substances are used, such as NOM. DOC/TOC analysis can be problematic, especially at low concentrations (several 100 µg/l), where contamination can be higher than the value of interest.

Different methods of DOC/TOC analysis are available, but only the UV/persulfate oxidation method appears successful for determination of low concentrations (Greenberg et al. 1992). Kainulainen et al (1994) determined correlation coefficients for different analytical methods (TOC, KMnO_4), colour, and fractions of humic matter were determined.

Fractionation of natural organics is required to link characteristics to treatment behaviour. Particulate organic carbon (POC) can be easily separated from dissolved organic matter using a $0.45 \mu\text{m}$ filter. This operation distinguishes the parameters TOC and DOC by definition. POC is the fraction of the TOC that is retained on a $0.45 \mu\text{m}$ porosity membrane. DOC is the organic carbon smaller than $0.45 \mu\text{m}$ in diameter. POC generally represents a minor fraction (below 10%) of the TOC (Thurman, 1985).

Figure 2-2 shows the division between dissolved and particulate organic carbon, based of filtration through a $0.45 \mu\text{m}$ filter. But overlapping the dissolved and particulate fractions is the colloidal fraction. According to IUPAC (1971), the term colloidal refers to a state of subdivision, implying that the molecules or polymolecular particles dispersed in a medium have at least in one direction a dimension roughly between $0.001 \mu\text{m}$ and $1 \mu\text{m}$, or that in a system discontinuities are found at distances of that order. Therefore colloids have a size between $0.001 \mu\text{m}$ and $1 \mu\text{m}$. (Figure 2-2 presents and equivalence of 10 kDa for $0.001 \mu\text{m}$.)

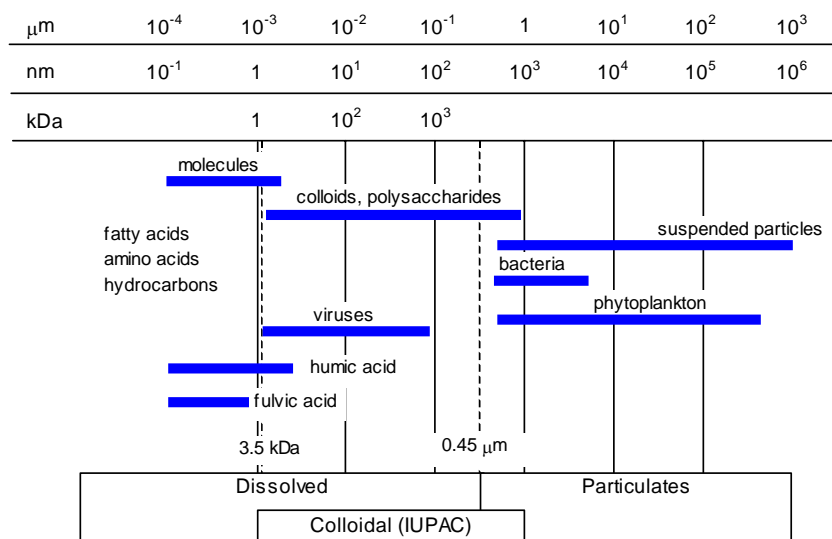


Figure 2-2 Continuum of particulate and dissolved organic carbon in natural waters (Aiken and Leenheer, 1993)

2.1.2 UV absorbance

UV absorbance has been used for reasons of simplicity in many pilot plant studies. However, UV measures the aromaticity of compounds preferentially and does not give correct results if the aromaticity is altered, as is the case in most treatments. Values will be overestimated, as most treatment processes preferentially remove aromatic compounds. UV absorbance can therefore not be used to measure treatment efficiency (Schafer, 2001).

The UV/TOC ratio is often used to determine the humic fraction in the organic matter or to determine the aromaticity of a sample.

2.1.3 Aromaticity and Reactivity

UV absorbance at particular wavelengths can be related to the presence of specific chromophores. Absorbance at 254 nm can be mainly correlated to the amount of double bonds in aromatic rings (Pettersen et al., 1994) and, thus, to the aromaticity of a sample. HA is more aromatic than FA, and FA is more aromatic than hydrophilic acids (Krasner et al., 1996). Absorbance was observed to be highly pH dependent (Abbt-Braun et al., 1990).

For monitoring and representing NOM concentration and the humic content or aromaticity of NOM, Ultraviolet absorbance at 254nm (UVA₂₅₄) is used.

Specific Ultraviolet Absorbance SUVA is defined as $SUVA = UVA_{254} / DOC$; SUVA is an index of aromaticity of water. The SUVA of fulvic acid is higher than natural bulk waters. In case of comparing ozonated water and raw water, ozonated water exhibit lower SUVA than a corresponding raw water because of the break down of aromatic structure by ozone. It shows that the aromatic structure of NOM can absorb more UV light than an aliphatic structure.

2.1.4 Size of NOM

Size, molecular weight, radii of gyration and polydispersity are interrelated. Size is an important characteristic in water treatment, as diffusion coefficients and removal efficiencies are directly dependent on the size of a solute. A large number of methods exist to measure these important parameters though results vary greatly. Each method has its own limitations (Schafer, 2001).

The more common methods are: Chromatographic techniques, Ultrafiltration fractionation and Dialysis, Ultracentrifugation, Flow field-flow fractionation, Dynamic light scattering, Membrane osmometry, Electron microscopy, etc.

NOM size is expressed as the molecular weight (MW) by using high performance liquid chromatography - size exclusion column (HPLC-SEC) methods. However this method also has some limitations (Yangali, 2005).

In general, hydrophilic DOC appeared to have a smaller MW size. It is hypothesized that hydrophobic NOM can be rejected more easily by a membrane than other components due to size (steric) exclusion. This size exclusion effect can be improved by electrostatic exclusion because hydrophobic NOM exhibits a negative charge density (Cho et al., 2000).

2.1.5 Solubility and aggregation of Natural Organics

The solubility of natural organics is an important issue in membrane processes where concentration polarisation is a common effect. Concentration polarisation may lead to gel formation if the solubility is exceeded. Solubilities of mixtures are difficult to determine. Many parameters influence solubility; FA is, by definition, more soluble than HA at low pH. The complexation with metal ions also influences solubility.

Aggregation occurs due to an increase in ionic strength, which shields organic charge. The high MW components aggregate preferentially (Schafer, 2001). Calcium can enhance aggregation of NOM.

2.2 Coagulation

The term “coagulation” narrowly defined, refers to the destabilization of a colloidal suspension, but it is often used in a broader sense that includes the addition of a coagulant and perhaps one or more coagulant aids (e.g., acid or base for pH adjustment) as well as the process used to remove the destabilized particles. Coagulants typically used for treating drinking water include metal-salt coagulants (e.g., alum, ferric sulphate, ferric chloride), polymerized metal-salt coagulants (e.g., polyaluminium chloride (PAC)), and organic polymers that may be cationic, anionic, and non-ionic. These coagulants not only destabilize particles, but also remove a fraction of the natural organic matter present in natural waters.

Coagulation involves reaction between coagulant chemicals, NOM molecules, and the surfaces of particles. This section reviews the fundamental chemistry of particulates, NOM, and coagulants, and describes the coagulation mechanism through which these reactions occur.

Among the most challenging conditions for treatment by coagulation/filtration are very cold water, about 5 °C or colder, waters with turbidities of less than 10 NTU, and low alkalinity waters. Another very difficult condition for water treatment by coagulation/filtration is the combination of high colour and moderate to high turbidity (Pernitsky and Edzwald, 2003).

2.2.1 Coagulation Mechanism

The removal of dissolved natural organic matter (NOM) and colloidal particles in drinking water coagulation is thought to occur via four primary mechanisms:

- Enmeshment
- Adsorption
- Charge neutralization / destabilization
- Complexation / precipitation

These mechanisms are presented conceptually in Figure 2-3, and will be referred to in the following sections. These coagulation mechanisms have been studied extensively, and many good references are available (Amirtharajah and Mills, 1982, Dempsey, 1994).

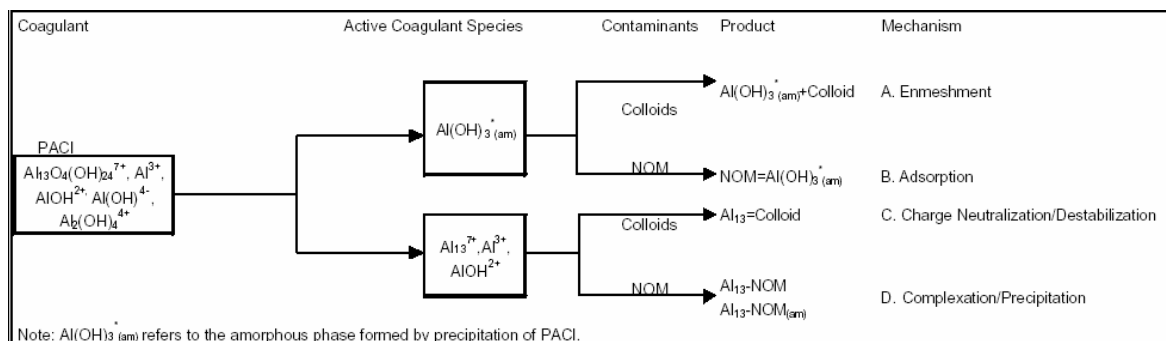


Figure 2-3 Conceptual view of coagulation reactions (Pernitsky and Edzwald, 2003)

Figure 2-4 shows pictorially how NOM forms complexes with aluminium ions, and how these complexes change shape and size with changing pH. At very low pH, very few NOM molecules can be accommodated around each aluminium ion because NOM contains few anionic sites below pH 2, and the NOM is tightly wound. As the pH is

raised, more anionic sites are generated by deprotonation of acidic carboxyl groups, and at the same time, the molecules unwind and become more linear, which is the result of repulsion of the many negative charges.

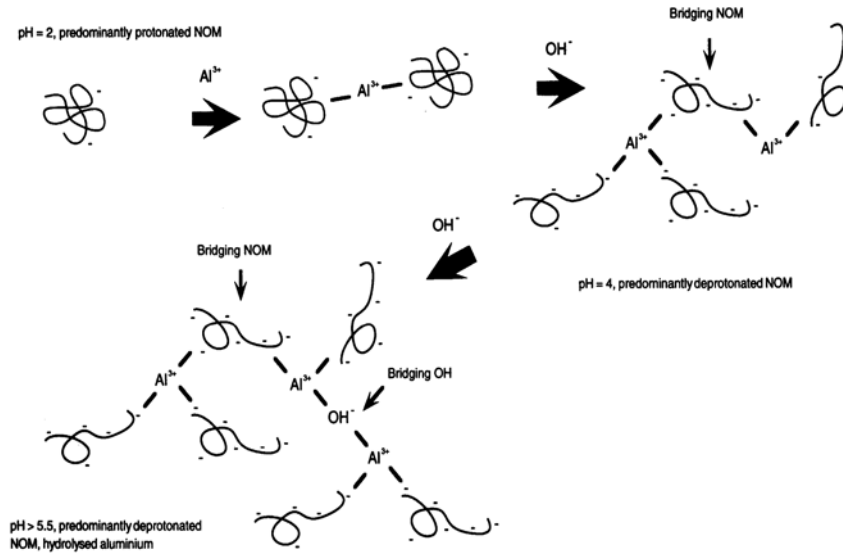


Figure 2-4 Modes of bridging between NOM and aluminium ions (Gregor et al., 1997)

2.2.2 Chemistry of particulates

Inorganic particles such as clays make up a large proportion of the particles present in natural waters. These particles may consist of iron oxides, silicates, calcites, clays, aluminium oxides, and, many other minerals (Weisner and Klute, 1997). Although the particles in each watershed are unique, all show similar electrochemical behaviour, since their surfaces are generally covered with surface hydroxyl (OH) groups, as shown in Figure 2-5.

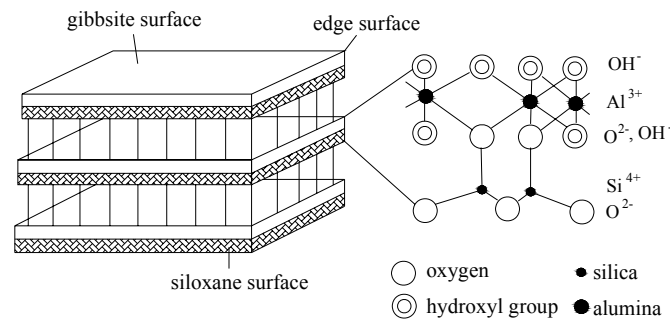


Figure 2-5 Surface Chemistry of a clay particle (Pernitsky and Edzwald, 2003)

Depending on the pH of solution, the charge of these hydroxyl groups may be positive or negative, as shown in Figure 2-6. Similar surface chemistry is also found on organic particles such as bacteria, as shown in Figure 2-6. Under the pH conditions of most natural waters, these particles have a negative surface charge, typically in the range of 0.11 to 1 $\mu\text{eq}/\text{mg}$ (Thurman, 1985).

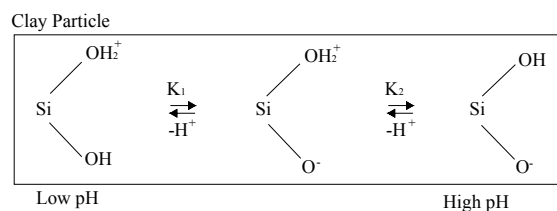


Figure 2-6 Electrochemical behaviour of hydroxyl groups (Pernitsky and Edzwald, 2003)

Under certain conditions, particles can be effectively destabilized by the neutralization of this surface charge by positively charged coagulant species as shown in pathway C of Figure 2-3. Coagulants that destabilize particles by charge neutralization will have dosage dependence related to turbidity. For example, water with 10 mg/l of clay turbidity having a negative charge of 0.5 $\mu\text{eq}/\text{mg}$ will have a positive charge demand of 5 $\mu\text{eq}/\text{l}$.

In many instances, an amount of coagulant in excess of that required for reaction with particle charge is required to react with NOM. Or, excess coagulant is added to produce large amounts of floc that will settle rapidly. In these situations, suspended particles are removed by enmeshment into precipitated floc particles (“sweep floc”), and turbidity has little effect on the required coagulant dose. This is illustrated by pathway A of Figure 2-3.

2.2.3 Chemistry of NOM

Natural Organic Material (NOM) is a heterogeneous mixture of organic compounds that enter the water column from decaying vegetation, organic soils, and biological activity. NOM from different source materials has different characteristics. In general, NOM molecules are large and contain many functional groups that affect their chemical behaviour. One example structure is shown in Figure 2-7, which highlights some of the common functional groups present. The charge on these functional groups can also change with pH. Several comprehensive references on NOM chemistry are available (Thurman, 1985).

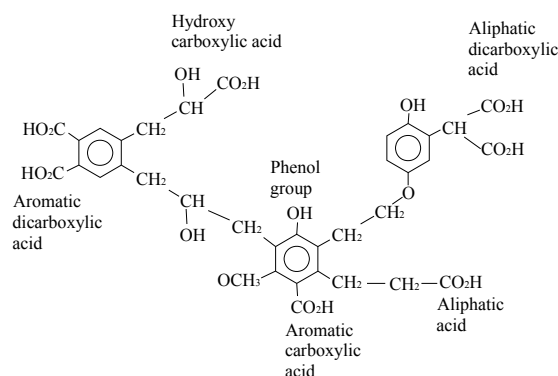


Figure 2-7 Typical NOM structure

Although much research has been devoted to the coagulation of inorganic particles, it has been shown that for most surface waters, coagulant doses are controlled by NOM concentration rather than by turbidity (Edzwald and Benschoten, 1990). Positively charged coagulant species can complex negatively charged functional groups forming Al-NOM precipitates that can be removed in subsequent solids separation processes, as shown in pathway D of Figure 2-3. The charge density of these NOM functional groups is typically 10 to 100 times greater than the charge density of inorganic particles discussed above. For example, a water containing only 3 mg/l DOC with a negative

charge of 10 $\mu\text{eq}/\text{mg}$, will have a positive charge demand of 30 $\mu\text{eq}/\text{l}$, six times that of the 10 mg/l clay turbidity case discussed above (Edzwald and Benschoten, 1990).

In addition to the amount of NOM present, the nature of the NOM has a significant effect on whether NOM controls coagulant dosages and on how much NOM is removed by coagulation. Coagulation has been shown to be most effective in removing NOM in the high and intermediate molecular weight ranges (Sinsabaugh et al. 1986, Chadik et al. 1987). Complex analytical techniques are available to fractionate NOM on the basis of molecular weight, hydrophobicity, and acidity. However, these techniques are exceedingly complex, and do not lend themselves to routine monitoring and control of coagulation in water treatment plants.

The concept of Specific UV absorbance (SUVA) has been developed as an operational indicator of the nature of NOM and the effectiveness of coagulation in removing NOM, TOC, and DBP precursors (Edzwald and Benschoten, 1990). SUVA values offer a simple characterization of the nature of the NOM based on measurements of UV absorbance and DOC. SUVA is defined as the normalized UV absorbance of a water sample with respect to the DOC. It is expressed in units of m^{-1} of absorbance per mg/l of DOC.

$$SUVA = \frac{UV_{254} \text{ (cm}^{-1}\text{)} \times 100}{DOC \text{ (mg/l)}}$$

Guidelines for the interpretation of SUVA values are presented in Table 2-1. For supplies with low SUVA (2 or less), TOC will not control coagulant dose. For water supplies with SUVA greater than 2, the amount of NOM typically exerts a greater coagulant demand than the amount of particles. For these waters, the required coagulant dose increases with increasing TOC.

Table 2-1 Guidelines on the nature of NOM and expected TOC removals

SUVA	Composition	Coagulation	DOC Removals
< 2	Mostly Non-Humics	NOM has little influence	< 25 % for Alum,
	Low Hydrophobicity,	Poor DOC removals	Little greater for Ferric
	Lower molecular weight		
2 - 4	Mixture of Aquatic Humics and other NOM,	NOM influences	25-50 % for Alum
	Mixture of Hydrophobic and Hydrophilic NOM,	DOC removals should be Fair to Good	Little greater for Ferric
	Mixture of Molecular Weights		
> 4	Mostly Aquatics Humics,	NOM controls	> 50 % for Alum
	High Hydrophobicity	Good DOC removals	Little greater for Ferric
	High Molecular Weight		

Source: (Edzwald and Tobiason, 1999)

2.2.4 Coagulant Chemistry

The coagulation mechanisms described above involve either charge neutralization or precipitation by positively charged, *dissolved* coagulant species, or enmeshment in or adsorption on the surfaces of *precipitated* floc particles. To understand coagulation, one must understand the conditions under which dissolved versus solid-phase species are present, and the charge on these species.

Under water treatment conditions, alum chemistry can be described by the presence of three species: Al^{3+} , $\text{Al}(\text{OH})^{2+}$, and $\text{Al}(\text{OH})_4^-$ in equilibrium with an amorphous

$\text{Al(OH)}_{3(\text{am})}$ solid phase (Hayden et al. 1974, Van Benschoten et al. 1990). The distribution of these species as a function of pH is shown in Figure 2-8. The figure shows that alum is least soluble at pH 6.0. This means that at pH 6.0, the maximum amount of coagulant is converted to solid-phase floc particles. At pH values higher or lower than this pH of *minimum solubility*, dissolved Al levels in the treated water will increase. As well, the figure also shows that at pH values less than the pH of minimum solubility, the highly charged Al^{3+} and Al(OH)^{2+} species are most prevalent dissolved species. The solid phase formed upon precipitation, $\text{Al(OH)}_{3(\text{am})}$, has a surface charge that is dependent on pH, due to the hydroxyl groups present. As was described for inorganic particles and NOM, the surface charge is more positive at lower pH. This has implications for the adsorption of NOM onto the floc surface, and the filterability of the floc.

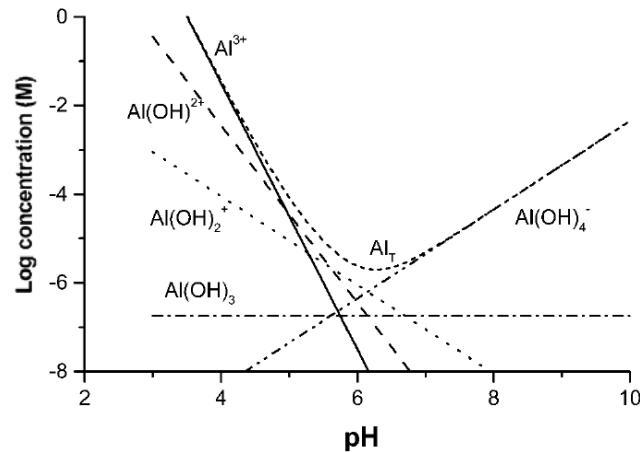


Figure 2-8 Concentration of soluble Al species in equilibrium with amorphous hydroxides. (Al_T represent total soluble species) (Duan and Gregory, 2003)

Polyaluminium chloride (PAC) chemistry is similar to that of alum, except that PAC contains highly charged polymeric aluminium species as well as the monomers described above. An Al_{13} species with the formula $\text{Al}_{13}\text{O}_4(\text{OH})_{24}(\text{H}_2\text{O})_{12}^{7+}$ (abbreviated as Al_{13}^{7+}) has been shown to be the dominant polymeric species (Parthasarathy and Buffle, 1985).

Polyaluminium coagulants are characterized by their degree of neutralization (r), or basicity.

$$r = [\text{OH}^-] / [\text{Al}_T]$$

$$\text{Basicity} = (r / 3) * 100 \%$$

Where $[\text{OH}^-]$ represents the quantity of base added during production. The value of r can vary from zero to three, corresponding to basicities of 0 to 100 %. Commercial PACs are generally available with basicities between 15 and 85 %. The basicity affects the alkalinity consumption of the coagulant, as well as the amount of polymeric species present. In general, the higher the basicity, the greater the Al_{13}^{7+} fraction, up to an r of approximately 2.1 (70 % basicity) (Bottero and Cases, 1980).

Significant differences exist between the solubility characteristics of PACs and alum (Pernitsky and Edzwald, 2003, vanBenschoten and Edzwald, 1990). PACs are more soluble and have a higher pH of minimum solubility than alum. For different PACs, the pH of minimum solubility increases with increasing basicity. It is important to note that the pH of minimum solubility for PACs with high basicity is significantly higher than that for alum. This means that these PACs can be used at higher pH values without

resulting in elevated dissolved Al levels, and that the highly charge Al_{13}^{7+} species is present over a higher pH range. Due to the presence of the Al_{13} polymer, the surface charge on PAC floc has a larger positive charge density than alum floc. Further details of PAC chemistry can be found elsewhere (Pernitsky and Edzwald, 2003).

For all metal coagulants, it is important to note that the pH of minimum solubility increases as temperature decreases as shown in Table 2-2.

Table 2-2 Summary of Coagulant solubility

Coagulant	Minimum Solubility			
	20 °C		5 °C	
	pH	µg/L Al	pH	µg/L Al
Alum	6	16	6.2	3
Polyaluminium Sulfate (PAS)	6	28	6.4	6
PAC low basicity non sulfated (LBNS)	6.2	27	6.7	4
PAC medium basicity sulfated (MBS)	6.3	29	6.5	4
PAC high basicity non-sulfated (HBNS)	6.4	36	6.8	9
PAC high basicity sulfated (HBS)	6.4	52	6.9	5
Aluminium-Chlorohydrate (ACH)	6.7	101	7.6	53

Source: (Pernitsky and Edzwald, 2003)

When solution pH is higher than 3, the hydrolysis of Al^{3+} begins. With a low OH/Al value (<0.5) and a low Al_t concentration of $10^{-2} - 10^{-5}$ mol/l, Al_1 are formed according to following reactions:

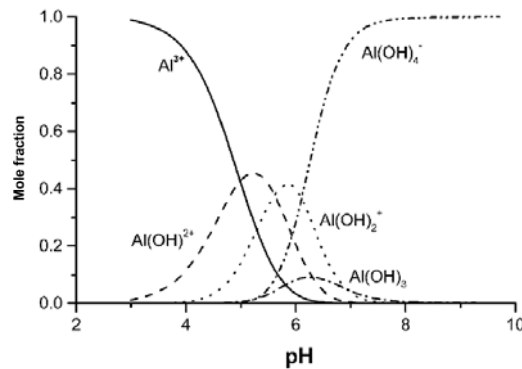
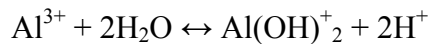
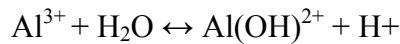
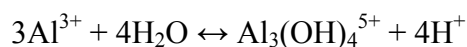
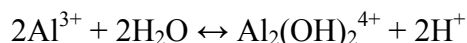


Figure 2-9 Distribution of monomeric Al hydrolysis products as a function of pH (Gregory and Duan, 2001)

Within the OH/Al value between 0.5 and 2.46, polymerisation of aluminium species occurs and different polymeric species, for example, $Al_2(OH)_2^{4+}$, $Al_3(OH)_4^{5+}$, $Al_{13}O_4(OH)_{24}^{7+}$ (Al_{13}) etc., are formed (Zhang et al., 2004b).



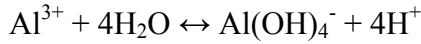
Through hydrolysis and polymerisation the solution of polymeric hydroxide complexes can reach equilibrium and be stable indefinitely. In fact, this is a metastable state

between different aluminium species and hydroxide precipitates (Baes and Mesmer, 1976).

With the OH/Al value over 2.5 and the Al_i concentration higher than 10⁻² mol/l, polymeric species change to gels and precipitate as Al(OH)₃ (Zhang et al., 2004b).



In alkaline solutions Al(OH)₃ may form Al(OH)₄⁻ (Baes and Mesmer, 1976).



2.3 Factors affecting Coagulation

For all raw water types, here are several water quality parameters that affect coagulation performance, including the amount of particulate material, the amount and nature of the NOM present, and the bulk chemical and physical properties of the water. These parameters are listed in Table 2-3. The effects of each of these parameters, and guidelines for selecting proper coagulation conditions (coagulant type, dose, and pH) are discussed below.

Table 2-3 Raw water parameters affecting Coagulant dosage and selection

Factor	Coagulant Demanding Substances	Nature of NOM	Bulk water properties
Measured or Calculated Parameter	Turbidity	SUVA	pH
	TOC		Alkalinity
	UV ₂₅₄		Temperature

2.3.1 Alkalinity, pH

Alkalinity refers to the acid-neutralizing capacity of water, and is a general indication of water's buffering capacity. Alkalinity and pH are related; higher alkalinity waters have higher pH. Metal coagulants are acidic, and coagulant addition consumes alkalinity. For low alkalinity waters, coagulant addition may consume all of the available alkalinity, depressing the pH to values too low for effective treatment. High alkalinity waters (highly buffered) may require high coagulant additions to depress the pH to values favourable for coagulation. Alum and ferric chloride are more acidic than PAC, and therefore result in greater alkalinity consumption after addition. For PAC, alkalinity consumption is related to basicity. *Higher basicity PACs will consume less alkalinity than low or medium basicity ones.*

The pH at which coagulation occurs is the most important parameter for proper coagulation performance, as it affects the:

- Surface charge of colloids
- Charge of NOM functional group
- Charge of the Dissolved-phase coagulant species
- Surface charge of floc particles
- Coagulant solubility

For aluminium-based coagulants the best coagulation performance is generally seen at pH values that are as close as possible to the pH of minimum solubility of the coagulant. This controls dissolved Al residual, as well as maximizing the presence of floc particles for adsorption of NOM.

The effects of coagulation pH are illustrated in Figure 2-10, which shows the relationship between electrophoretic mobility (EPM), a measure of particle surface charge, and coagulant dose for two pH conditions for a low turbidity, low TOC water. At pH 6.3, near the pH of minimum solubility for alum and PAC, the charge of the NOM is neutralized at a relatively low coagulant dose of 1.5 mg/l as Al (this corresponds to a dry alum dose of approximately 16 mg/l), and a floc of neutral to positive charge results. At pH 7.5 much higher coagulant doses are required to react with the NOM. At all alum doses tested, the resulting floc has a negative charge, which can be difficult to filter through negatively charged grains of a sand filter. In contrast, the floc formed with the high basicity non-sulfated PAC exhibits a higher positive charge at this elevated pH.

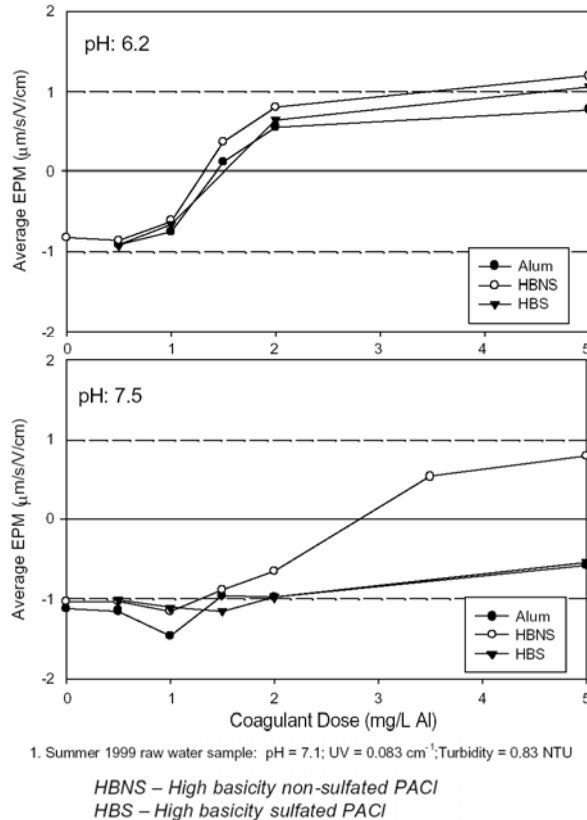


Figure 2-10 Effects of pH on floc charge

Very low pH (pH 5.5) is often recommended to maximize TOC removal for alum. PACs, on the other hand, do not require pH this low. This is shown in Figure 2-11, which shows the effects of pH adjustment on the performance of a high basicity PAC for the sample. The sample has moderate to high TOC concentrations, low turbidity, and moderate concentrations of alkalinity. Without pH adjustment, coagulation pH with the PAC varied between 7.6 and 7.8. By adjusting the pH to 7.0, dramatic increases in NOM removals were seen. Further pH reductions showed diminishing returns.

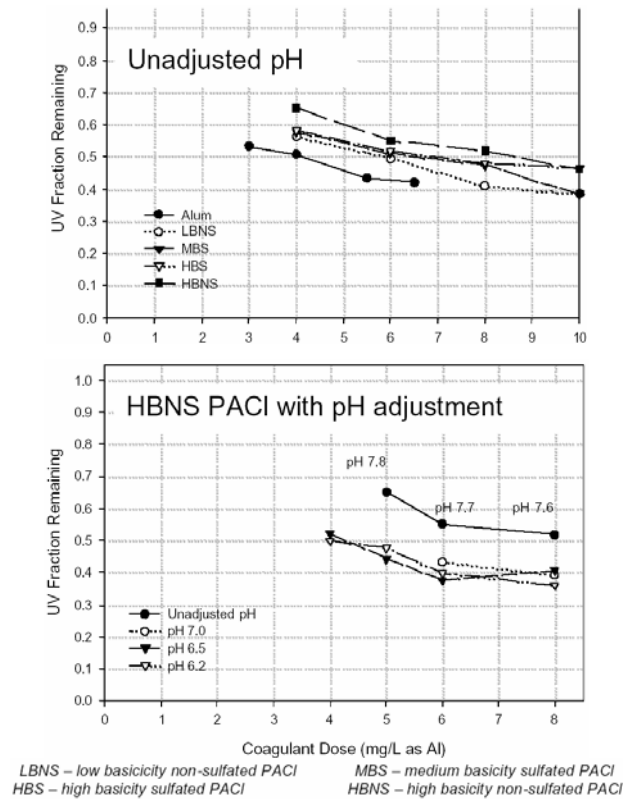


Figure 2-11 Effects of pH on NOM removal

In general, as the coagulant dosage increases, the precursor removal increases; however if the pH is not independently controlled, restabilization can occur (due to very low pH) and precursor removal will be less than optimal. Coagulant dose is one of the most common variables studied during jar tests, and results from numerous studies are cited in the literature, and results are specific to the source water and season being tested.

The solution pH during coagulation is a significant variable that can be controlled to maximize precursor removal under a given set of conditions. Coagulation using iron or aluminum salts in the pH range of 5.5 to 6.5 generally corresponds to maximum precursor removal; however the optimum pH for iron salts is typically 0.5 to 1.0 pH unit higher than for alum.

The *effect of pH* on the effectiveness of coagulation is illustrated on the hand of two examples: Removal of kaoline and removal of colour.

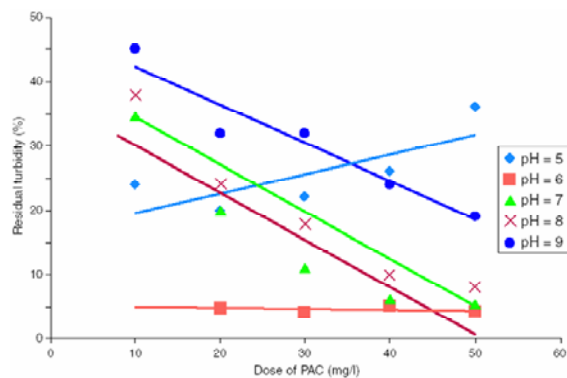


Figure 2-12 Influence of pH (Delgado et al., 2003)

Kaolinite is a group of minerals, which forms the main part of clay minerals. These minerals are insoluble. At pH values around 7 or higher the kaolinite particles have a negative charge.

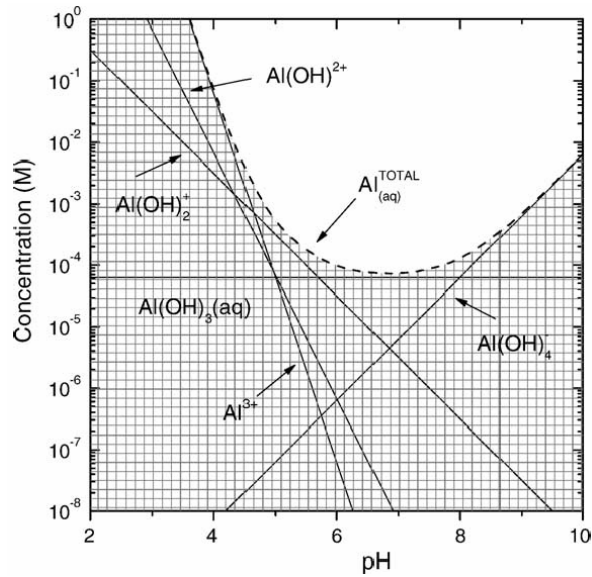


Figure 2-13 Theoretical solubility of amorphous $\text{Al}(\text{OH})_3$ in water at zero ionic strength and at 298 K, polynuclear complexes not included. (Schrader et al. 2005)

True *colour* in natural waters consists mainly of humic substances e.g. Fulvic acids. An important part of these substances will form insoluble compounds with Al/Fe. These substances are generally weak acids. (Schipper and Buiteman, 2005). The dissociated FA is able to form with positively charged hydrolyzed $\text{Al}^{3+}/\text{Fe}^{3+}$ ions insoluble compounds.

From experiments and practice it is known that the effectiveness of colour depends on pH (see Figure 2-14). For an efficient removal of colour the concentration of fulvate has to be high and the hydrolyzed Al^{3+} has to be positively charged. Consequently the optimum pH is between high and low.

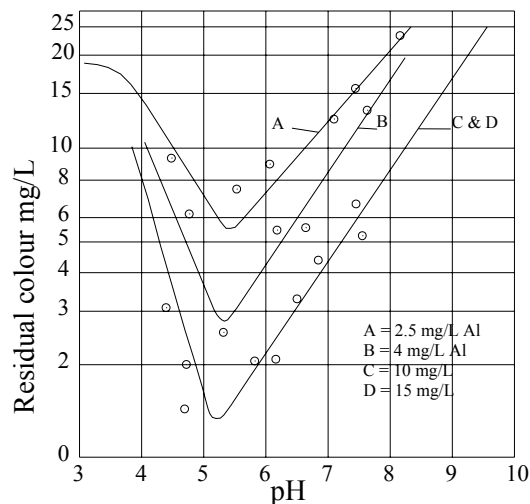


Figure 2-14 Influence of pH on the removal of colour with coagulation with aluminium salts

2.3.1.1 pH depression

The addition of 1 mg/l of alum results in the consumption of 0.5 mg/l of alkalinity (as CaCO_3). If the raw water alkalinity is low, the alum dose required to achieve proper

treatment may depress the pH to below the pH of minimum solubility, requiring subsequent base addition for proper coagulation performance and residual Al control. pH depression is less of a problem with PACs, as they are already partially neutralized, and therefore consume less alkalinity. Among PACs, alkalinity consumption is inversely proportional to basicity. For example, a PAC with 50 % basicity will consume only 0.25 mg/l of alkalinity (as CaCO₃). This makes high basicity PAC well suited to low alkalinity waters.

Using the alkalinity consumption associated with a given coagulant and the raw water alkalinity, the resulting coagulation using various coagulant doses can be predicted using computational models (Pernitsky and Edzwald, 2003).

2.3.2 NOM

Sufficient coagulant must be added to satisfy the charge demand of the raw water NOM for effective treatment to occur. SUVA guidelines can be used to predict whether NOM will influence or control coagulant doses, and the degree of NOM removal expected. In most situations where NOM is present, it is more important for determining coagulant dosage than turbidity or others parameters. However, the amount or type of NOM present is less important for choosing an individual coagulant (for example, a high versus medium basicity PAC) than the raw water alkalinity. For most waters, alum, PACs, and FeCl₃ can achieve similar TOC removal when used at the appropriate pH. NOM removal will be less at higher pH for all coagulants. The required coagulant dose for NOM removal will also likely increase as water temperature decreases.

2.3.2.1 Turbidity

For low TOC raw waters in which turbidity controls coagulation, sufficient coagulant must be added to destabilize suspended colloids or to create a good settling floc. SUVA guidelines can be used to predict whether turbidity will influence or control coagulant doses. However, raw water turbidity is less important for coagulant selection and dosage than the raw water NOM or alkalinity. Coagulant doses are generally higher when raw water turbidity increases, although the relationship is not linear.

2.3.2.2 Temperature

Low temperature affects coagulation and flocculation processes by altering coagulant solubility, increasing water viscosity, and retarding the kinetics of hydrolysis reactions and particle flocculation. Higher coagulant doses, the addition of flocculation or filter aids, longer flocculation times, and lower flotation, sedimentation, and/or filtration rates are often required to produce low turbidity treated water. Sedimentation processes are most affected.

Polyaluminium coagulants are thought to be more effective than alum in cold waters as they are pre-hydrolyzed. The superiority of PAC compared to alum under cold-water conditions has been widely reported (Dempsey, 1994, Odegaard and Fettig, 1990).

2.3.3 Advances in coagulation process control

2.3.3.1 UV254

As discussed above, coagulation doses are often set by NOM removal requirements. NOM removal in water treatment processes is typically quantified by TOC measurements, which can be time consuming and expensive. Because the double bonds in organic molecules absorb ultraviolet light at 254 nm (UV254), UV absorbance

measurements can provide a quick estimate of the organic carbon content of raw or treated water samples. The operator effort required to analyze UV254 is similar to that required to measure turbidity. This process is done online.

Although the numerical relationship between UV absorbance and TOC is unique to each raw water, a change in TOC can always be detected as a change in UV absorbance. This makes UV absorbance measurements well suited to monitoring changes in NOM concentration. Daily monitoring of raw water UV absorbance can provide valuable information to operators about changing raw water TOC concentrations, and pending impacts to the required coagulation dose. Changes in raw water TOC often occur without any change in raw water turbidity, and operators are often not aware that their coagulant dose is insufficient to react with the increased NOM levels until after clarifier or filter turbidity increases.

Tracking the removal of UV absorbing substances across the treatment process can also provide a benchmark for coagulation performance. Coagulant dose can be adjusted to achieve a certain UV absorbance removal, and this removal percentage used as an operational setpoint, similar to a streaming current detector (SCD). Like an SCD, the UV absorbance removal set point to be used should be the UV absorbance removal achieved by the plant when it is running well. This set point may vary seasonally, but should be somewhere between 40 and 60 % UV absorbance removal.

$$UV_{removal} (\%) = \frac{(UV_{raw} - UV_{post\ coagulation})}{UV_{raw}} \times 100\% \quad , \text{ where } UV = UV \text{ absorbance at } 254 \text{ nm}$$

UV absorbance removal can also be quickly checked during routine jar tests. For waters in which NOM concentrations influence or control coagulation, UV absorbance measurements may provide more useful information for selecting coagulant doses than settled turbidity measurements alone.

2.4 UF, RO and membrane characteristics

2.4.1 Ultrafiltration

In water treatment, UF can be defined as a clarification and disinfection membrane operation. UF membranes are porous and allow only the macromolecules to be rejected and with better reason, all types of microorganisms as viruses and bacteria, or all type of particles. Pore size of UF is between 0.05 to 1 μm , operating under a pressure of 0.5 to 5 bars (Mallevalle et al., 1996).

Table 2-4 Filtration processes size particle exclusion

Filtration Process	μm	nm
Microfiltration, MF	0.02 – 10	20 – 10.000
Ultrafiltration, UF	0.005 - 0.02	5 – 20
Nanofiltration, NF	< 0.001	< 1
Reverse osmosis, RO*	< 0.001	< 1

*Pores in RO membranes are smaller than in NF membranes

In UF membrane, removal of solute is mainly performed by sieving effect, as broad as pore size distribution; contrasting with NF, RO membrane operations performed by diffusion and sorption or partitioning.

2.4.2 Membrane characterization

Membrane can be characterized by hydrophobicity, pore size, and surface charge. These factors play important role in membrane rejection and fouling.

2.4.2.1 Contact angle for hydrophobicity

Contact angle is an index of hydrophobicity of membrane surface; it can be measured by captive bubble and sessile drop methods. Higher contact angle means higher hydrophobicity of the membrane surface.

The contact angle is increased by hydrophobic foulants due to the provision of more hydrophobic foulants on the membrane surface, while hydrophilic foulants reduce the contact angle (Cho et al., 1998). This means that hydrophobic NOM components increase the membrane surface charge (less negative) by coating negatively charged functional groups. On the other hand, in case of hydrophilic NOM foulants, its polysaccharide or polysaccharide – like substances reduce the negative charge causing reducing the contact angle.

Membranes are made from several different polymers such as regenerated cellulose (RC), polyamide (PA), and polysulfone (PSf) or polyethersulfone (PES). Cellulose is relatively hydrophilic and is a polysaccharide in terms of its material properties. Aromatic polyamide is relatively hydrophobic, and polysulfone is the most hydrophobic.

2.4.2.2 Membrane MWCO (Molecular Weight Cut-Off)

Membrane MWCO is a starting point to understand NOM rejection and other solute separations by membrane filtration, because size exclusion is the main rejection mechanism of membrane processes. MWCO is the molecular weight of the particles that are 90% rejected by a membrane. Manufacturers provide the MWCO information for each membrane from results of solute rejection tests using macromolecules.

2.4.2.3 Membrane surface charge

In case of negatively charged particles exist in the solution, unsolvated cations are absorbed on the membrane surface and it is called Stern layer. And also solvated cations are attracted to the Stern layer due to the negative charge of the surface layer.

A diffuse layer is formed on the stern layer and its concentration of cations is higher than anions in the diffuse layer, as shown in Figure 2-15.

Cations near the stern layer keep higher concentration. The concentration of cations reach the equilibrium with bulk solution, due to the more distance from the Stern layer. The boundary between the Stern layer and the diffuse layer is called Shear boundary and Zeta potential is described at the difference with potential between the Shear boundary and the bulk solution. When ionic strength is increased, the depth of double layer is decreased because of ions existing in the each layer is also increased (Elimelech et al., 1994).

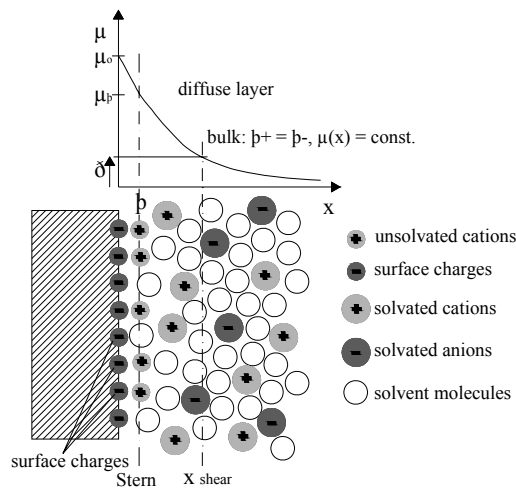


Figure 2-15 Double layer of membrane surface (Elimelech et al., 1994)

2.5 Effects of parameters on membrane fouling

In order to maintain a high flux, negative charged membrane are ideal to reject NOM acids, which also have a negative charge, inhibiting adsorption of NOM. Electrostatic repulsion between NOM and the membrane surface, and also NOM adsorption, can be influenced by water quality, including, pH, ionic strength, and divalent cations (Ca^{2+}) (AWWA, 2001).

2.5.1 Hydrophobicity effects

Hydrophobic interactions are important factors in flux declines; Nilson et al. (1996) conducted a research to study the flux decline affected by different NOM fraction, which were isolated by XAD resin by using NF membrane. As a result of this experiment, the hydrophobic NOM fraction was responsible for nearly the entire flux decline. The hydrophilic fraction of NOM was rejected rather poorly when compared with the hydrophobic NOM. However, the mechanism of hydrophobic interaction is not clear until now except results of some experimental data. Braghetta (1997) reported that membrane foulants can be hydrophobic fractions of NOM when hydrophobic interactions overcome charge repulsion between NOM and the membrane surface.

2.5.2 Ionic effects

Membrane fouling and rejection is affected by inorganic ions contained in water. Hydrophobic and hydrophilic NOM can be adsorbed onto calcium surfaces and adsorption of humic acid on the hydrophobic membranes can be improved by calcium (Clark and Jucker, 1993). Ion binding (such as with Ca^{2+}) would decrease the double layer and allow functional groups to approach closer to each other.

2.6 Membrane flux decline and fouling

Flux decline and fouling of membranes are important factors for selecting the membrane process due to the cost of operating a membrane system. Negative charged membrane is profitable to reject negative charged NOM acids inhibiting adsorption of NOM and this is caused by electrostatic repulsion between NOM and membrane surface.

There are two hypotheses for the NOM fouling and rejection. One is that only hydrophobic NOM fractions are responsible for membrane fouling due to hydrophobic interactions between hydrophobic NOM and membrane and another is that negative charged hydrophobic results in electrostatic repulsion. Through these objective concepts, it can be hypothesized that hydrophobic and hydrophilic neutrals may adsorb onto the membrane surface easily without electrostatic repulsion, resulting in NOM fouling and corresponding flux decline (i.e. accordingly as the charge density, hydrophobic NOM can be foulants or rejected by membrane).

2.6.1 UF dead end, membrane flux model

Equation 2-1, given by Hagen-Poiseuille, describes laminar flow through pores under an ideal situation, e.g. with uniformly evenly sized pores in the membrane, no fouling.

$$J = \frac{\varepsilon r^2 \Delta p}{8 \mu \tau \Delta x}, \quad [2-1]$$

Where ε is membrane porosity, τ is the pore tortuosity factor, r (m) the pore radius, and Δx is (m) the effective membrane thickness. Membrane flux is proportional to porosity and pore size and pressure. On the other hand, flux is decreased by increasing μ (i.e. low temperature) or membrane thickness.

When the sieving mechanism in UF is dominant, a cake layer of rejected particles usually forms on the membrane surface. The cake layer and membrane may be considered as two resistances in series, and the pressure-driven permeate flux is then described by equation 2-2 (Darcy's law).

$$J = \frac{dV}{Adt} = \frac{\Delta p}{\mu(R_m + R_c)}, \quad [2-2]$$

Where V (m³) is the filtrate volume, t (s) is the filtration time, A (m²) is the membrane area, Δp (Nm⁻²) is the pressure drop across the membrane, μ (Nm⁻²s) is the dynamic viscosity of the water, R_m (m⁻¹) is the hydraulic resistance of the clean membrane, and R_c (m⁻¹) is the cake resistance of the fouled membrane.

The membrane resistance clearly depends on the membrane thickness, its nominal pore size, and various morphological features such as the tortuosity, porosity, and pore size distribution. For a membrane whose pores consist of cylindrical capillaries of uniform radius perpendicular to the face of the membrane, the membrane resistance is obtained from 2-1 and 2-2 as;

$$R_m = \frac{8 \Delta x}{\varepsilon r^2}, \quad [2-3]$$

2.6.2 Membrane fouling by NOM




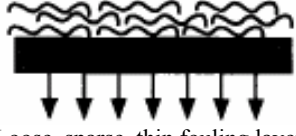
The phenomenon of fouling is very complex and difficult to describe theoretically. Especially membrane filtration flux decline due to NOM fouling and flux recovery after cleaning is felt to be less well understood than that due to other colloidal, biological and scale-related fouling (Cho et al., 1999). Although some studies dealing with NOM adsorption mechanisms can provide some insight into the adsorption mechanisms of NOM onto membrane surfaces, they cannot explain NOM fouling in membrane filtration of natural waters, because fouling mechanisms involve not only chemical interactions but also physical (hydrodynamic) interactions (Hong and Elimelech, 1997).

Mallevalle et al., (1989) characterized the fouling layer formed during microfiltration and ultrafiltration of natural waters. They reported that the fouling layer was composed of clay (kaolinite) and organic matter mostly. The organic matter was found to be packed under the inorganic fouling layer, forming a gel-like organic matrix.

Several researchers have shown that the extent of NOM fouling is greatly influenced by the hydrophobicity of the membrane and NOM. Static adsorption experiments by Jucker and Clark (1994) demonstrated that humic macromolecules adsorbed more favourably onto hydrophobic membranes. Nilson and DiGiano (1996) have investigated the effect of NOM properties on NOM fouling of NF membranes. From their work, aquatic NOM was fractionated into hydrophilic and hydrophobic components.

Fouling tests are shown that the hydrophobic fraction of NOM was mostly responsible for permeate flux decline, whereas the hydrophilic fraction caused much less fouling. Furthermore, they also concluded that only the large molecular weight fraction of NOM contributed to the formation of a fouling layer.

Table 2-5 Schematic description of the effect of solution chemistry on the conformation of NOM macromolecules (Hong and Elimelech, 1997)

Chemical conditions	Humics in solution	Humics on membrane surface	Flux decline
High ionic strength low pH, or presence of divalent ions	 Compact, coiled configuration	 Compact, dense, thick, fouling layer	Severe
Low ionic strength high pH, and absence of divalent ions	 Stretched, linear configuration	 Loose, sparse, thin fouling layer	small

Hong and Elimelech (1997) reported the filtration of three classes of isolated humic substances with a thin film composite (TFC) NF membrane (nominal MWCO < 100) and their results were summarized at Table 2-5. Cho et al. (1999) reported that feed NOM concentration and NOM aromaticity were less important factors in flux decline with relatively low flux membranes (MWCO = 400~3,000) but flux decline of relatively high flux membranes (e.g. UF) can be influenced by NOM aromaticity and membrane hydrophobicity. Amy et al. (1999) also studied interactions between NOM and membranes and the result was that inorganic water quality appeared to have little effect on flux decline, high Ca^{2+} or low pH enhanced NOM rejection and electrostatic exclusion was determined to be an important NOM rejection mechanism, particularly for higher MWCO UF versus lower MWCO NF. As a result of that study, hydrophilic NOM (polysaccharides) is major foulant but in case of water mainly composed of hydrophobic NOM (90%) the dominant foulant was hydrophobic NOM.

Cho et al. (2000), suggested that NOM molecules that are not totally excluded from the membrane's pores, but that are large enough and can adsorb near the pore openings, and are the main species leading to flux decline. These species are removed with NaOH cleaning, an observation that supports the hypothesis that they are adsorbing near the pore mouth.

2.6.3 Membrane fouling mechanisms

The mechanisms of fouling are four: complete blocking, standard blocking, intermediate blocking, and cake filtration.

Complete blocking, or called pore blocking phenomenon, represents that each particle arriving to the membrane participates in blocking some pore or pores with no superposition of particles.

Standard blocking, called internal adsorption, is described in case that each particle arriving to the membrane is deposited onto the internal pore walls leading to a decrease in the pore volume.

In *intermediate blocking*, or long-term blocking phenomenon, each particle can settle on other particle previously arrived and already blocking some pore or it can also directly block some membrane area

Cake filtration phenomenon represents that each particle locates on others already arrived and already blocking some pores and there is no room for directly obstructing some membrane area. The four fouling mechanisms are shown in Figure 2-16.

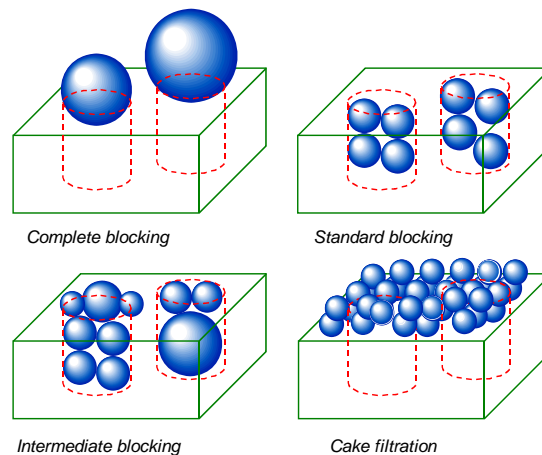


Figure 2-16 Membrane fouling mechanisms (Peavy, 1984)

2.6.4 Membrane cleaning

Membrane cleaning is an essential component of nearly all membrane processes because all membranes will foul during operation, causing the membrane performance to drop below acceptable levels. At that point the foulants must be removed using the acceptable cleaning procedure. Membrane cleaning can be divided into three categories: hydraulic, chemical and mechanical cleaning.

2.6.4.1 Hydraulic cleaning

Hydraulic cleaning, i.e., backwashing is practiced by pumping the permeate water from the permeate tank into shell of the membrane (from outside to inside). It is generally effective at removing particle cakes from the membrane surface, and it can also remove foulants from the membrane interior, particularly when performed with a chemical cleaning solution, i.e., in case of significant adsorption or tight cake formation in the membrane (so-called enhanced backwashing). Backwashing conditions, i.e. cycles and length of filtration runs, are important in UF process because shorter filtration cycles will yield an apparent increase in production, but meaning more frequent backwashing, as a result the overall water production will decrease.

2.6.4.2 Chemical cleaning

Chemical cleaning is performed when the backwashing cannot restore the flux. It involves the use of chemical compounds. Cleaning agents can be classified in the following categories:

- Acid/base (HCl, H₂SO₄/NaOH) for dissolving mineral and salt/proteins foulants.
- Oxidizing agents (H₂O₂, NaOCl) for biological foulants.
- Enzymes (Protease, Alpha amylase) for severe fouling.
- Surfactants/detergents (Ultrasil, Froclean, etc) for organic foulants.

The type of cleaning agents to use will depend on the type of foulant and membrane material. Membrane lifetime will be affected by the type of cleaner and procedure used because cleaning agents react with the membrane itself while they react with organics at the membranes, changing the permeate flux, retention characteristics and increasing the frequency of replacement.

2.6.4.3 Mechanical cleaning

Tubular membranes types can often be cleaned by forcing rubber sponges balls through the hollow spaces of the large tubes. Sponge ball cleaning is most effective at removing soft biological and organic foulants from the membrane surface, but this type of cleaning is unable to remove such materials from within the pores.

3 Materials and Methods

3.1 Materials and general operation

3.1.1 WMD “Norit” Klazienaveen plant

“Norit” Klazienaveen Treatment plant is property of WMD and is operated by WMD itself. The scheme of the plant is shown in Figure 1-1. The source is a canal whose water can vary in winter and summer (Figure 3-1). The raw water firstly passes a screen (rough filter) to remove debris and other impurities (Figure 3-2), and then the water is pumped to the plant installation. In some occasions tap water is used as source for treatment for producing the boiler feed water.



Figure 3-1 Source water canal – upstream and downstream of the intake



Figure 3-2 Water intake and rough filter

3.1.2 PAC dosing

Coagulant is prepared in a tank whose characteristics are summarized in Table 3-1.

Table 3-1 Characteristics Coagulant Mixing Tank

Parameter	Description
Material	HD-PE
Tank Dimensions	ø 2150 × 2350 mm
Volume	8 m ³
Max. volume flow	15 m ³ /hr
Working pressure	Un-pressurized
Filling medium	PAC

The volume of the tank is enough for a normal operation in the plant. Following are shown the dosing pumps and the tanks where the coagulant is prepared.



Figure 3-3 PAC dosing tank and pumps

The monitoring system records the UV absorbance of the UF permeate water and at all time, this value must be lower than the “guide” value. Therefore, in case of problems with the UV removal, then more coagulant is dosed automatically. In case of problems with the dosing of with UV removal less than needed an alarm message is shown on the remote control system for information and adequate action of the operator.

The dosing equipment do not reported any problem during use and is working properly.

3.1.3 UF Membrane Module

The X-flow UF module operates in a dead-end mode, which is schematically shown in Figure 3-4. The characteristics of the UF module are summarised in Table 3-2 , and the general operational and cleaning parameters are summarized in Table 3-3.

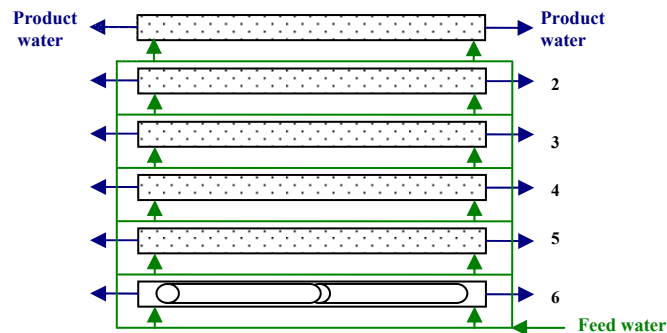


Figure 3-4 Scheme of UF in Klazienaveen plant

The ultra-filtration unit comprises four skids of six vessels each one. The length of every vessel is 3 meters and are placed horizontally one over the other. The diameter of the membranes is 8 inches. The average pore size of the membrane is 0.03 μm . The feed water passes through the membrane from inside to outside. Clean filtrate (permeate) is collected on the sides. The UF module operates under a constant flux filtration conditions, which means that the flux is generally fix at around 33 $\text{l/m}^2\cdot\text{hr}$, while the TMP increases from 0.5 bar (clean membrane) to 2 bar (fouled membrane) due to membrane fouling.

Table 3-2 Characteristic of X-flow UF module (source: Technical data manufacturer)

Criteria	Description
General information:	
Module supplier:	X-Flow
Type:	UFC
Diameter:	8 inch
Membrane area per element:	35 m ²
Length element:	1.5 m
Characteristics:	
Membrane material	Hydrophilic Polyethersulfone
Structure	Asymmetric/microporous
Geometry	Tubular
Molecular weight cutoff (kDa)	200 (on dextrans)
Capillary membrane (mm)	0.8 mm and 1.5 mm
Transmembrane pressure (kPa)	-300...+ 300
pH tolerance	2 – 12
Maximum chlorine exposure (ppm*h)	250000
Temperature (°C)	1 - 80
Configuration:	
Length pressure vessel:	3 m
Number of pressure vessel per skid:	6
Number of elements per pressure vessel:	2
Number of elements per skid:	12
Membrane area per skid:	420 m ²
Total:	
Number of skids:	4
Total number of membrane elements:	48
Total area of membranes:	1680 m ²
Nominal flow per skid:	33 m ³ /hr - 79 l/m ² .hr
Nominal flow (total):	132 m ³ /hr - 79 l/m ² .hr

Table 3-3 Operational and cleaning parameters of X-flow UF module

Group	Parameter	Data
Operational parameters	Operation mode	Constant flux
	Flux, l/m ² .hr	79
	TMP, bar	0.5 (avg)
	Feed flow for each module, m ³ /hr	33
Backwashing	Backwashing,	Every 30 min or when the maximum TMP is reached
	Backwashing peak feed pressure, bar	2
	Peak backwashing flow, m ³ /hr	120
Chemical cleaning	Chemical cleaning frequency	Enhanced backwash is 1-2 times a day with NaOH

3.1.4 UF Feedwater

The feed water of UF modules comes from a storage tank after continuous sand filters (CSF). The details of the microbial floc size were not available.

A summary of the characteristics of the UF feed water are shown in annex 7.1.1.

3.1.5 UF Backwashing

In order to control membrane fouling, periodically (30 min) the membranes are backwashed for 30 seconds by pumping a fraction of the permeate back through the membrane. The backwashing pressure is around 1.46 bar in average.

Two times a day it is performed an enhanced backwash with NaOH.

3.1.6 RO Membrane module

The RO membranes operate in a cross-flow mode, which is schematically shown in Figure 3-5. The characteristics of the RO module are summarised in Table 3-4 and the general operational parameters are summarized in Table 3-5.

The reverse osmosis unit comprises three skids of two stages every one. The first stage has three pressure vessels and the second stage has two pressure vessels. Each pressure vessel is 6 meters length and contains 6 elements of 1 meter each. The diameter of the membranes is 8 inches.

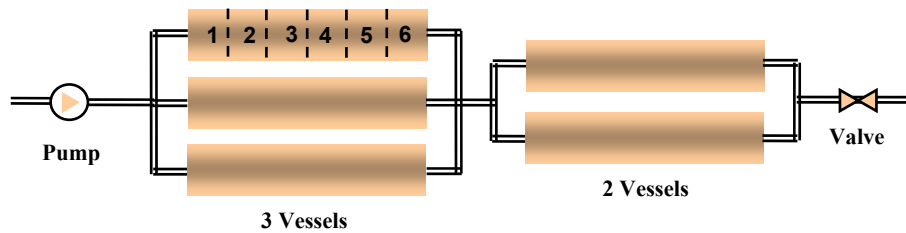


Figure 3-5 Scheme of the RO in Klazienaveen plant

The recovery of the reverse osmosis is 75 % and operate under constant flux filtration conditions, which means that the flux is generally fix at around 20 l/m².hr.

Table 3-4 Characteristic of RO membranes (source: Technical data manufacturer)

Criteria	Description
General information:	
Supplier:	Hydranautics
Type:	ESPA2
Diameter:	8 [inch]
Area/element:	37.16 [m ²]
Flux:	20 [l/m ² .hr]
Characteristics:	
Membrane material	Hydrophilic Polyethersulfone
Structure	Asymmetric/microporous
Geometry	Tubular
Molecular weight cutoff (kDa)	200 (on dextrans)
Capillary membrane (mm)	0.8 mm and 1.5 mm
Transmembrane pressure (kPa)	-300....+ 300
pH tolerance	2 – 12
Maximum chlorine exposure (ppm*h)	250000
Temperature (°C)	1 - 80

Table 3-5 Operational parameters of RO module

Criteria	Description
Configuration:	
Length pressure vessel:	6 m
Number of stages:	2
Number of pressure vessel 1 st stage:	3
Number of pressure vessel 2 nd stage:	2
Number of elements per pressure vessel:	6
Number of elements 1 st stage:	18
Number of elements 2 nd stage:	12
Total area of membranes:	1114.8 m ² (668.9 + 445.9)
Total:	
Number of RO skids:	3

Total number of membrane elements:	90 (30 each vessel)
Total membrane area installation:	3344.5 [m ²]
Feed flow for each skid:	m ³ /hr - l/m ² .hr
Permeate Flow from each skid:	m ³ /hr - l/m ² .hr
Nominal flow (total):	m ³ /hr - l/m ² .hr

Before the RO unit there is a flush tank. If the plant is stopped the RO units are flushed and biocide or other chemicals (organic peroxide) is added.

Cleaning times depend on the season. It can be once in two weeks in worst situations. In summer is once every 4 weeks, in winter once in six weeks. The fact that the cleaning frequency is higher in the summer period suggests that bio-fouling may be occurring.

3.1.7 RO feed water

The first stage of R.O. receives the UF permeate as feed water. The second stage feed water is the concentrate of the first stage. The total recovery is 75 %.

3.1.8 RO chemical cleaning

Until II/2005 it was used antiscalant (type not specified) with a dose of 3 ppm, however this was suspended. As biocide, an organic peroxide can be dosed if necessary; however if this chemical is used continuously, it yields fungi problems.

3.2 Methods

3.2.1 Data Analysis

In the WMD treatment plant parameters such as UV extinction and turbidity are monitored on-line. WMD works together with the WLN laboratory for several chemical parameters (e.g. Al, DOC, Ca, etc). Some of the parameters are measured monthly such as DOC, and others are measured weekly, such as aluminium concentration.

In annex 7.1.1, there is a summary of values and concentrations of several parameters measured and analysed by WMD/WLN with respect to the Norit plant.

During the six years of operation of the plant the amount of data recorded is enormous. For example, for aluminium the concentration was measured weekly during the period.

A full ionic balance is necessary to verify the accuracy of the laboratory analysis provided. This balance shows the sum of positive and negative ions and compares them. It is a general rule for approval of a laboratory analysis that the difference between the sum of positive ions and negative ions should be less than 10 %. Results of ionic balance for eight dates, between 21/06/05 and 08/12/04, show differences in positive and negative ions higher than 120 % and in some cases higher than 400 % as shown in annex 7.1.2. Therefore, some ions were not analysed in the analysis. Most likely the ions that are not taken into account were: Sodium, magnesium, ammonium, fluoride and nitrite.

A complete ionic balance is required in order to verify the accuracy of the analysis of macro parameters and to enable scaling calculations.

3.2.2 Coagulant dosage efficiency

The efficiency of UV removal and DOC removal is determined with next equations,

$$UV_{removal} = \frac{UV_{rawwater} - UV_{UFperm}}{UV_{rawwater}}$$

$$DOC_{removal} = \frac{DOC_{rawwater} - DOC_{UFperm}}{DOC_{rawwater}}$$

The result of the equations is a direct relation between the dosage and the removal.

Using these results can be obtained the removal per mg of coagulant. Plotting these results is possible to get the equation of the best fit line. This line is important for getting the added value, or the additional removal per extra milligram per litre of coagulant that is used in the plant.

3.2.3 Simulating Solubility change in RO

For simulating the change in solubility in R.O. elements were used next equations. These equations were determined using the aluminium species equations and definitions of recovery and pH change along the membranes.

Table 3-6 Solubility Equations for several Aluminium species (mol/l)

Species	T = 20 °C	T = 5 °C
$Al(OH)_4^-$	$Al(OH)_4^- = CF_{hyp} \times 10^{pH_{feed}} \times \left(\frac{1}{10^{12.7}} \right)$	$Al(OH)_4^- = CF_{hyp} \times 10^{pH_{feed}} \times \left(\frac{1}{10^{13.4}} \right)$
Al_{13}^{7+}	$Al_{13}^{7+} = \frac{[10^{(-7)}]^{\log(CF_{hyp})}}{[10^7]^{pH_{feed}}} \times 10^{38.55}$	$Al_{13}^{7+} = \frac{[10^{(-7)}]^{\log(CF_{hyp})}}{[10^7]^{pH_{feed}}} \times 10^{41.45}$
$Al(OH)^{2+}$	$Al(OH)^{2+} = \frac{[10^{(-2)}]^{\log(CF_{hyp})}}{[10^2]^{pH_{feed}}} \times 10^{5.7}$	$Al(OH)^{2+} = \frac{[10^{(-2)}]^{\log(CF_{hyp})}}{[10^2]^{pH_{feed}}} \times 10^{6.3}$

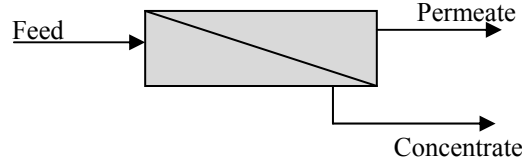
To simulate the change in concentration along the RO, were used next equations. The procedure followed to obtain these equations is shown in annex 7.2.

Table 3-7 Concentration Equations for several Aluminium species (mol/l)

Species	T = 20 °C	T = 5 °C
$Al(OH)_4^-$	$[Al(OH)_4^-] = CF_{hyp} \times \left[1 \times 10^{pH_{feed}} \times \left(\frac{1}{10^{12.7}} \right) \right]$	$[Al(OH)_4^-] = CF_{hyp} \times \left[1 \times 10^{pH_{feed}} \times \left(\frac{1}{10^{13.4}} \right) \right]$
Al_{13}^{7+}	$[Al_{13}^{7+}] = CF_{hyp} \times \frac{10^{38.55}}{[10^7]^{pH_{feed}}}$	$[Al_{13}^{7+}] = CF_{hyp} \times \frac{10^{41.45}}{[10^7]^{pH_{feed}}}$
$Al(OH)^{2+}$	$Al(OH)^{2+} = CF_{hyp} \times \frac{10^{5.7}}{[10^2]^{pH_{feed}}}$	$Al(OH)^{2+} = CF_{hyp} \times \frac{10^{6.3}}{[10^2]^{pH_{feed}}}$

3.2.4 Deposition factor calculation

Equations can be determined with a mass balance as follows,



From the scheme, doing a mass balance can be written:

$$Q_f = Q_p + Q_c \quad \text{in an ideal system}$$

$$Q_f C_f = Q_p C_p + Q_c C_c + \Omega C_f Q_p$$

But the concentration in permeate is zero ($f = 1$), therefore $C_p = 0$.

consequently,

$$Q_f * Al_{\text{feed}} = \Omega * Q_p * Al_{\text{feed}} + Q_c * Al_{\text{concentrate}}$$

$$\Omega * Q_p * Al_{\text{feed}} = Q_f * Al_{\text{feed}} - Q_c * Al_{\text{concentrate}}$$

$$\Omega = (Q_f * Al_{\text{feed}} - Q_c * Al_{\text{concentrate}}) / (Q_p * Al_{\text{feed}})$$

$$\Omega = (Q_f * Al_{\text{feed}}) / (Q_p * Al_{\text{feed}}) - (Q_c * Al_{\text{concentrate}}) / (Q_p * Al_{\text{feed}})$$

$$\Omega = (Q_f / Q_p) - (Q_c / Q_p) * (Al_{\text{concentrate}} / Al_{\text{feed}})$$

Recovery is: $R = \frac{Q_p}{Q_f} * 100$ (Assuming, $f = 1$. Salt rejection = 100 %)

So, $Q_f / Q_p = 1 / R$

and, $Q_c = Q_f - Q_p$

$$Q_c / Q_p = (Q_f - Q_p) / Q_p = Q_f / Q_p - 1$$

Replacing,

$$\Omega = 1 / R - (Q_f / Q_p - 1) * (Al_{\text{concentrate}} / Al_{\text{feed}})$$

$$\Omega = (1 / R) + (1 - (1 / R)) * (Al_{\text{concentrate}} / Al_{\text{feed}})$$

Therefore,

$$\Omega = \frac{1}{R} + \frac{Al_{\text{concentrate}}}{Al_{\text{feed}}} \cdot \left(1 - \frac{1}{R}\right)$$

where Q is the flow of feed (f), concentrate (c) and permeate (p).

It is important to notice that the formula above assume that the Recovery is assuming that the salt rejection is 100 %, this is $f = 1$. Therefore the concentration factor is not the real one but a theoretical or hypothetical (CF_{hyp}).

$$\Omega = \frac{1}{CF_{\text{hyp}} - 1} \cdot \left(CF_{\text{hyp}} - \frac{Al_{\text{concentrate}}}{Al_{\text{feed}}} \right)$$

$$CF_{\text{hyp}} = \frac{\Omega \cdot Al_{\text{feed}} - Al_{\text{concentrate}}}{Al_{\text{feed}} \cdot (\Omega - 1)}$$

$$R = \frac{Al_{feed} - Al_{concentrate}}{Al_{feed} \cdot \Omega - Al_{concentrate}}$$

$$C_{concentrate} = C_{feed} \cdot \left[CF_{hyp} - \Omega \cdot (CF_{hyp} - 1) \right]$$

From the last equation can be seen that,

Ω , % C_{brine}

0 $C_{brine} = C_{feed} * CF_{hyp}$

100 $C_{brine} = C_{feed}$ Aluminium in product water (permeate) is zero.

3.2.5 UF Integrity test

Procedure:

As a general description of the procedure can be said the following,

1. Pressure test of the chosen skid for determining which vessels will be required to do an integrity test later on. The criterion is a fast (in two minutes) decrease in pressure in every vessel. As a general rule can be said that for pressure drops higher than 5 % in 2 min, the vessel and therefore the modules in it must be repaired.
2. Extract from the vessels the modules to be repaired and clean them with water to remove impurities.
3. Submerge the modules in the tub and let the air flow through the modules for some minutes till is clear which fibres are broken.
4. Once identified the broken fibres, these must be temporally blocked with a plastic pin.
5. Remove the module from the water. Replace the temporal pins with new pines mixed with strong and fast glue. Put the pines with strength.
6. Verify that the broken fibres have been successfully blocked putting the module again in water and later on introduce air again.
7. Once all the modules were repaired, these must be placed in the pressure vessels again.
8. Closed all the piping and valves that were closed before the procedure.
9. Do the pressure test again for verifying the success in repairing the broken fibres.

3.2.6 Specific resistance of aluminium

3.2.6.1 Water Flux – Darcy's Law

The water flux through a membrane is proportional to the pressure gradient across the membrane & the **permeability** of the membrane (resistance model).

$$\text{Flux} = \frac{dV}{A dt} = J = \frac{K \Delta P}{\eta L} \quad \text{Darcy's law for laminar flow,}$$

V : filtrate volume (m³)

A : membrane area (m²)

L : membrane thickness (m)

P : pressure (Pa)

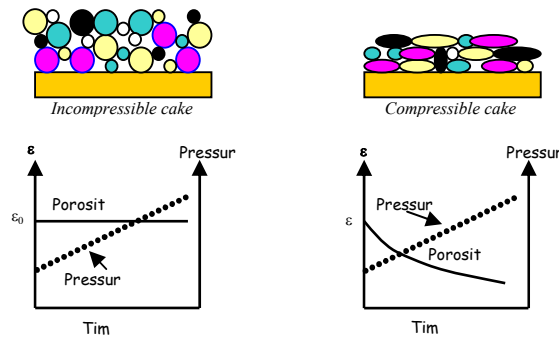
t: filtration time (s)

K: medium permeability

η : water viscosity (Pa.s)

3.2.6.2 Filter Cakes

- The cake can be classified as compressible or incompressible depending on the nature of the particles, such as shape, particle size distribution and rigidity.
- Incompressible cake: can withstand cumulative drag stresses or any other external stresses without any significant structural changes (specific cake resistance will be constant over time and as the porosity is pressure and time independent).
- Compressible cake: the drag stress will lead to a rearrangement of particles within the cake as internal stresses increase which means that the porosity of the cake will be at its minimum value.



3.2.6.3 Cake Filtration equations

Cake filtration is based on the fundamental equation for the rate of flow through a porous medium.

Flux is:

$$J = \frac{dV}{A dt} = \frac{\Delta P}{\eta R_{\text{total}}} = \frac{\Delta P}{\eta (R_m + R_b + R_c)}$$

Cake resistance is:

$$R_c = \frac{V}{A} \times I \quad [\text{m}^{-1}]$$

C_b = concentration of particles in feedwater, $[\text{kg}/\text{m}^3]$

I = index for the propensity of particles in water to form a layer with hydraulic resistance, $[\text{m}^{-2}]$

$$I = \alpha \cdot C_b, \text{ for incompressible cake}$$

$$I = \alpha_0 \Delta P_c^\omega C_b, \text{ taking into account cake compression}$$

where ω is the compressibility coefficient and α_0 a constant. For incompressible cakes, ω is zero and the higher the compressibility coefficient the more compressible the cake.

3.2.6.4 Specific cake resistance

The specific cake resistance is the term used to describe the resistance created by the deposited particles (cake).

Carmen equation is:

$$\alpha = \frac{180 (1 - \varepsilon)}{\rho_p d_p^2 \varepsilon^3} \quad [\text{m}/\text{kg}]$$

α	specific cake resistance [m/kg]
ε	cake porosity [-]
ρ_p	density of particles forming the cake [kg/m ³]
d_p	particle diameter, [m]
J	permeate water flux [m ³ /m ² s]

The resistance depends mainly on the characteristics of the cake layer particles, such as rigidity, shape and diameter and their relative arrangement in the cake. When the cake material is compressible, then the specific resistance is pressure dependent and the porosity will change with pressure.

For *constant flux*, the base equation is:

$$J = \frac{1}{\eta} \times \frac{\Delta P_t}{R_m + R_c}, \quad \Delta P_t = \text{pressure at time } t.$$

Substitution:

$$\frac{V}{A} = J \times t \quad \text{because} \quad \frac{1}{A} \times \frac{dV}{dt} = J = \text{constant}$$

$$\text{in: } R_c = \frac{I \times V}{A} = I \cdot J$$

$$\text{Results in: } J = \frac{1}{\eta} \times \frac{\Delta P_t}{R_m + I J}$$

$$\text{or } \Delta P_t = \eta R_m J + \eta I J^2 t$$

So ΔP_t is linear proportional with time and proportional with J^2 . As a consequence flux has a very dominant effect on the development of ΔP .

4 Results and Discussion

The schematic of the treatment process in Klazienaveen plant is shown in Figure 4-1. The units or treatment processes that were studied are coagulation/flocculation, ultra filtration and reverse osmosis.

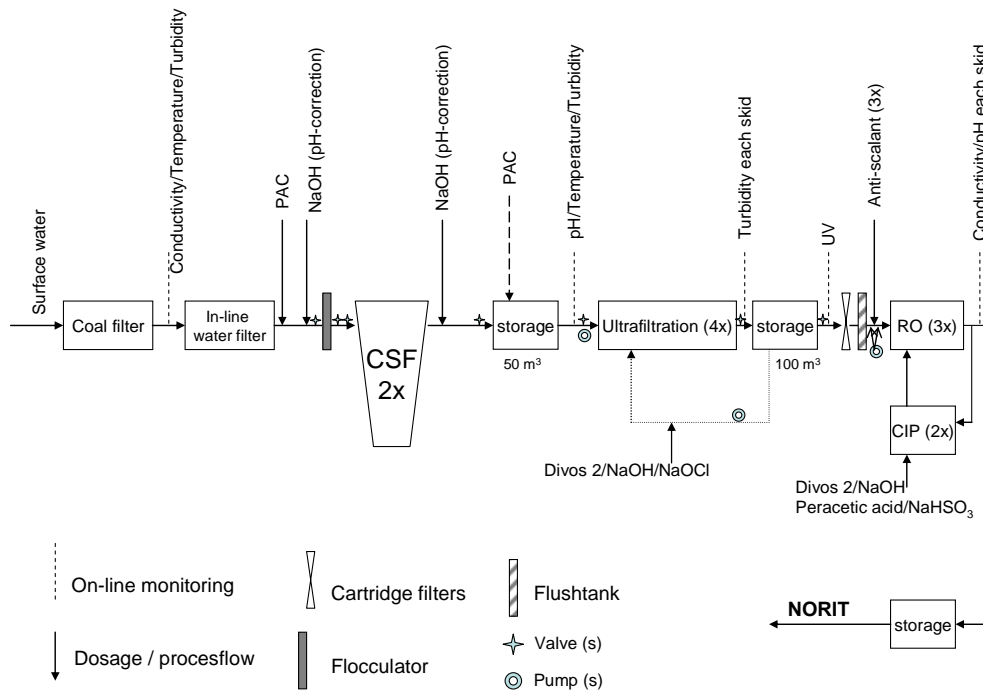


Figure 4-1 Treatment scheme – Klazienaveen Plant

The approach taken was firstly to analyse the available data from the WMD plant, then together with literature review try to verify the hypotheses formulated at the beginning of the project.

4.1 Rate of floc formation

The ability of macro-flocs to develop from the micro-flocs formed during coagulation is quite important. Floc settling rates are in general used to compare the effect of pH on macro-floc development.

Flocculation depends on collisions between particles, which are caused by their relative motion, mainly, diffusion and velocity gradients. The flocculation rate is determined by collision frequency induced by the relative motion (Zhang et al., 2004a).

On basis of literature review the following was found:

- ✓ The lower the pH, the lower the flocculation rate. This is illustrated in Figure 4-2.
- ✓ At low pH aluminium hydrolyzes and polymerizes more slowly and the formation of the precipitate is retarded. Flocculation rates are higher with Fe salts.
- ✓ The higher the dosage the higher the flocculation rate (Zhang et al., 2004a).

- ✓ Suitable increase in energy input and pH of the suspension can increase the flocculation rate.
- ✓ The higher the temperature the lower the optimum pH for coagulation (Mohtadi and Rao, 1973).
- ✓ The higher the temperature, the lower the coagulant dosage. However, a decrease in temperature does not necessarily mean an increase in the coagulant dosage provided the pH of the dispersion is maintained at the optimum value (Mohtadi and Rao, 1973).

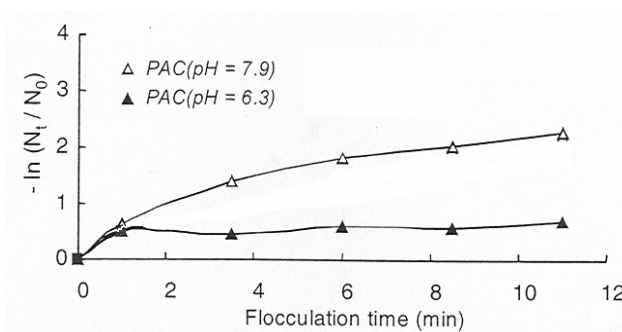


Figure 4-2 Influence of suspension pH on the flocculation rate (Zhang et al., 2004a)

Figure 4-2 compares the flocculation rate when the pH of the suspension was 6.3 and 7.9; the dosage of PAC was constant at 0.04 mmol/l Al (1 mg/l). At the lower pH of 6.3, the flocculation rate decreases compared with that at pH 7.9. At the lower pH the aluminium ions hydrolyze and polymerize more slowly and the formation of the precipitate is retarded.

The flocculation process (in front of the UF unit in the plant) was studied in terms of velocity gradient. As shown in the scheme of the treatment plant (Figure 4-1) there is a tank before UF where PAC is added (1 or 2 mg/l).

The data assumed and the results of this calculation are shown in next tables.

Table 4-1 Data and results. G, Gt estimation.

Parameter	Value	Unit	Parameter	Result	Accepted range
Temperature, T =	10	[°C]	Mean detention time, min	40	20 – 45
Flow, Q =	75	[m ³ /h]	G, s ⁻¹	12.5	20 – 74
Volume, V =	50	[m ³]	Gt	30017	20000 – 200000
Head loss, Δh =	0.05	[m]			
Gravity, g =	9.81	[m/s ²]			

The head loss is assumed. It was not possible to measure it in the plant. All the other assumed values are representative of the plant operation.

The results of this estimation give a G (mean velocity gradient) value of 12.5 when the minimum limit is 20 s⁻¹, this means that there is a poor floc formation in this step. Temperature and head loss in the storage time influence the flocculation process as was demonstrated by (Mohtadi and Rao, 1973) and (Zhang et al., 2004a). The process of calculation is shown in annex 7.1.3.

It was done a sensitivity analysis for the temperature and for the head loss. The higher the head loss, the higher the temperature the better the flocculation. A head loss higher than 17 cm is required to achieve the minimum G value when the temperature is 10 °C.

For a temperature of 25 °C is possible to achieve the minimum velocity gradient G for a head loss of 5 cm.

In practice, the flocculation kinetics is influenced by flocculation time, coagulant type, coagulant dosage, suspension characteristics and hydraulic conditions (Zhang et al., 2004a).

In conclusion, this section shows the influence of pH and temperature in flocculation processes. In “Norit” plant, the G estimated shows there is a poor floc formation in front of the UF unit. Although the dosage of coagulant is not as much as in front of the continuous sand filters, there is room for cost saving in coagulant.

4.2 PAC dose

The PAC dose added depends on the UV measurements after the UF system in “Norit” Klazienaveen Plant. According to the operators guidelines the UV reading should be less than 20 abs/m all the time. The ratio UV/DOC should be between 2 and 2.5 as a consequence of the dosage of coagulant and it is not used directly as guide for the PAC dosage.

Coagulant dosing control (CDC) is necessary to ensure stable treated water quality and to reduce chemical costs in treatment plants. The rapid development in online sensors and equipment as well as control strategies has triggered a significant development in CDC. The optimum CDC is quite dependent on the development, availability and adoption of the online water quality monitoring systems in the field. The main parameters in drinking water treatment plants remain flow, pH, turbidity/suspended solids, and colour. Flow, pH and conductivity have been measured at most DWTP for decades. Turbidity and suspended solids measurements have become fairly common in many large DWTP and operators have gained good operational experience. The need for monitoring residual aluminium (Maier et al., 2004) has increased the awareness among plant owners and researchers for using it as a parameter in coagulant control (van Leeuwin et al., 1999)

Ratnaweera (2004) described the coagulant dosing strategies in five types: simple dosing strategies, online water quality measurement, optical methods, streaming current detectors and charge titration units, mathematical models, neural networks and fuzzy logic.

According to the operation of the plant there is not a direct relation between PAC and UV readings after UF as was described by WMD (graph below). So, ultimately the PAC dose depends on other factors that are not clear so far but not directly on the UV value.

The outcome of a laboratory test done by WMD was a mathematical model for dosage of coagulant whose main objective was to achieve the target value of 20 abs/m. This formula is as follow:

$$Desired\ dose\ PAC = \frac{UV_{raw\ water} - UV_{guide\ value\ permeate}}{SUVA_{raw\ water} \times factor}$$

The specific ultra violet absorbance (SUVA) is UV/DOC ratio. The desired dose is calculated monthly and the coagulant dose is calculated weekly.

The *factor* value depends on the season of the year (temperature). For summer and spring, it is equal to one and for winter and autumn the factor is equal to 1.9. It is not

known if the coagulant used in the test is the same as is used in Klazienaveen plant nowadays.

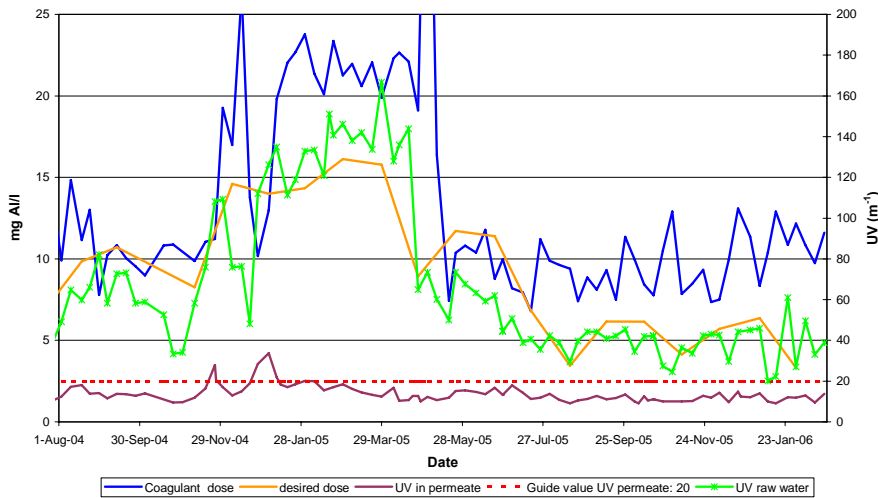


Figure 4-3 PAC dosage

The graph above shows the aluminium dosage and the “calculated” dosage of coagulant in mg/l and the UV absorbance versus time. UV absorbance and aluminium concentration are measured once a week while DOC is measured monthly. The desired dosage is calculated using the UV raw water for reducing it to the target value of 20 abs/m in the UF permeate. Nevertheless, the dosage used in the plant is higher than the one that is calculated as desired. In average, the UV removal up to UF permeate was 78 % in that period study and was found substantial over dose 89 % of the time.

In the graph, the PAC dose was obtained from the difference in mg/l of aluminium concentration before CSF and the raw water. This is,

$$\text{PAC dose} = \text{Al}_{\text{In CSF}} - \text{Al}_{\text{Raw water}}$$

The coagulant dose for several years is summarised in Table 4-2. The negative value in the dosage before UF means that the concentration of Al is lesser in feeding water of UF than after CSF (UF dose = $\text{Al}_{\text{feeding UF}} - \text{Al}_{\text{effluent CSF}}$).

Table 4-2 Average dose in mg Al/l

Year	CSF	UF
2005 (II)	9.6	0.5
2005 (I)	19.2	-1.8
2004	11.9	0.9
2003	9.3	1.4

Since 2003, the dosage of coagulant has been increased. In 2005(I), the dosage is significantly higher because of an “accident” in dosage (personal communication, 2005). During the second semester of 2005 some actions were taken in the operation of the plant, and the coagulant dosage was reduced considerably. The average dose of coagulant for 2005 was 14 mg/l and in 2006 the first two months had 11 mg/l of coagulant dose.

Coagulants have their own optimum pH ranges, with best utilisation of coagulants and working pH ranges. Beyond these ranges, the colloids remain stabilised or become re-stabilised. The simplest way to overcome this is to integrate a pH overrun function ensuring that dosing is controlled to be within this range (Ratnaweera, 2004). The turbidity, suspended solids, and colour measurements have become more reliable with

time and are now found in a few plants as control parameters integrated into the flow proportional dosing (Ratnaweera, 2004).

A number of researchers have worked with the development of coagulation models on a experimentation level. With the development of online water quality sensors, many treatment plants started to gather large amounts of operational data. The statistical processing of these data revealed various possibilities for optimising CDC. Using multivariate regression analysis, (Ratnaweera et al., 2002) presented a concept tested on full scale where the optimum coagulant dosage for WWTPs was estimated with online measurement of turbidity, coagulation pH, flow, conductivity, temperature, and time of day. In DWTPs, Nakamura (1974) and Kim and Kim (1993) set up the relationship equations between the raw water quality parameters and the coagulant dosage through a multivariable regression. The method was helpful in determining optimum coagulant dosage under rapidly varying conditions. Van Leeuwen et al. (2003) presented mathematical models for predicting alum and ferric chloride doses and pH control reagents that maximise removal of DOC and turbidity from raw waters, based on lab and pilot scale tests. Measurement of TOC in the raw water and dosage control to obtain the above relationship is proposed as a control strategy. Residual iron was correlated with the coagulant dosage, and a relationship was found for dosages below optimum dosage. Monitoring of residual iron and then controlling dosage proportionally to this parameter was suggested as another alternative for coagulant control.

The inconvenient with the formula found for the plant is that DOC is only available to measure in laboratory and this is done once a month for Klazienaveen plant. Since this point of view there is not a real dosage controlling strategy. Nevertheless, Flower (2004) demonstrated that UV absorbance of raw water is a good measure of the require dose coagulant, and that UV absorbance of treated water is an indication of residual organic matter (Swartz et al., 2004).

In case that the UV absorbance is more than the guide value, then the coagulant dosage is increased automatically with two pumps (one on stand by).

In conclusion, the strategy of coagulant dosing control in Klazienaveen plant is not optimal for coagulation because does not take into account pH for the calculation of the desired dose. The calculation of the desired dose is done a posteriori, because dependency on DOC delays the results. Under the actual coagulant dosage control there is a substantial over dose for reducing the UV absorbance to the target value. The effect of temperature should be added for dosage of the coagulant. Warm periods require fewer doses than cold periods. Because coagulation pH is so critical to optimum flocculation and colour removal, it should be included pH monitoring in a improved control system.

4.2.1 UV removal

The UV removal efficiency defines the amount of coagulant required for coagulation. Therefore, it is important to optimise this removal to reduce costs in the plant. UV is measured on-line for the UF permeate and is used to estimate coagulant dose.

The absorption of light by coloured waters is far higher at ultraviolet wavelengths than in the visible region and is caused by aromatic compounds and other organic substances with conjugated double bonds. It increases with decrease in wavelength available with no obvious peaks (Swartz et al., 2004). Next graph shows the UV removal in the plant up to UF product water.

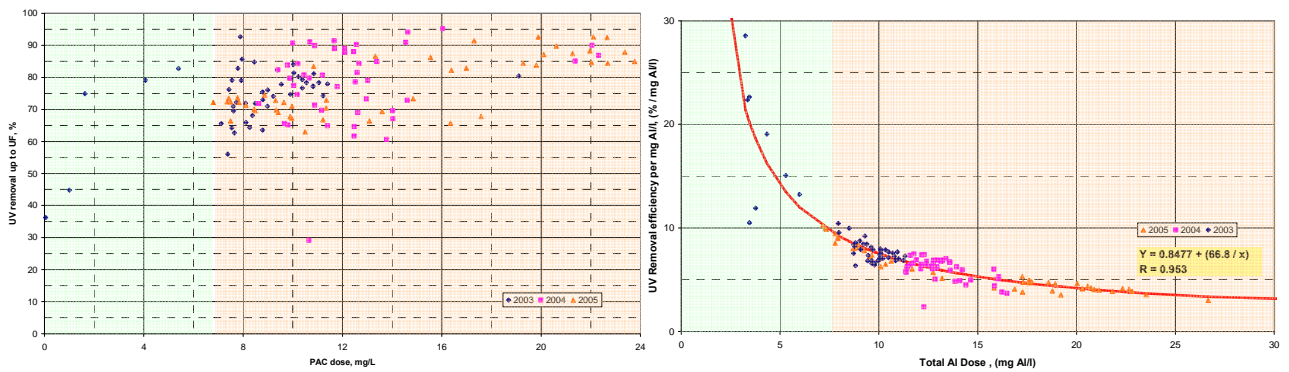


Figure 4-4 UV removal efficiency vs. PAC dose and Coagulant dose vs UV removal efficiency per mg of Al per litre

The available data for aluminium concentrations lower than 7 mg/l is very sparse. Aluminium concentrations are recorded weekly in the treatment plant.

It is possible to define in the graph two areas. The first region is defined for aluminium doses less than 7 mg/l, and shows higher removal with respect to doses between 1 to 7 mg/l. In the second zone, with Al doses higher than 7 mg/l, the UV removal is almost constant increasing the dose. Consequently, increasing the dose more than 7 mg/l shows no significant increase in UV removal.

To obtain the UV removal per milligram of aluminium per litre, the UV removal efficiency per milligram of aluminium was plotted in Figure 4-4. A regression was performed to obtain the best fit.

Summarizing the results of the graph:

Dose, mg/l	% UV removal / (mg/l)	Added value, % UV removal/(mg/l)
5	14	2.5
10	7.5	1.5
15	5.5	1
20	4.5	0.5

The difference between 20 mg/l and 10 mg/l is only 3 % of extra UV removal while for 15 and 10 mg/l the increment in removal is only 2 %.

The use of the first derivative is necessary to obtain the added value of every extra milligram of coagulant added.

The derivative is defined to be the instantaneous rate of change of a function. It gives the slope of the tangent to the graph of the function at a point. It provides a mathematical formulation of *rate of change*; it measures the rate at which the function's value changes (removal) as the function's argument changes (coagulant dose).

It is possible to do a similar approach obtaining the first derivative of the curve equation for obtaining the added value per extra milligram of coagulant dosed. Figure 4-5 shows this relation.

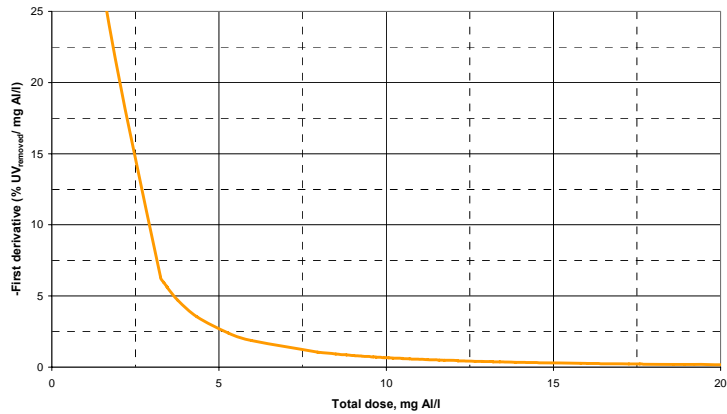


Figure 4-5 Added value of coagulant dosage

As can be seen in the graph and from the table above, beyond 5 mg/l of Al dose the additional increment in UV removal per extra milligram of coagulant per litre is less than 2.5 %. Therefore, for doses higher than 7 mg/l the UV removal is not significantly better than for 7 mg/l. Nevertheless, more data is required for the region of doses less than 7 mg/l to conclude with strength and it is assumed that UV readings are the same on-line as well as in laboratory.

4.2.2 DOC removal

In order to verify and study organic matter removal in the plant, DOC removal is used in first instance. According to the graph below showing data since 2002, there is a non-linear relation between aluminium dose and DOC removal.

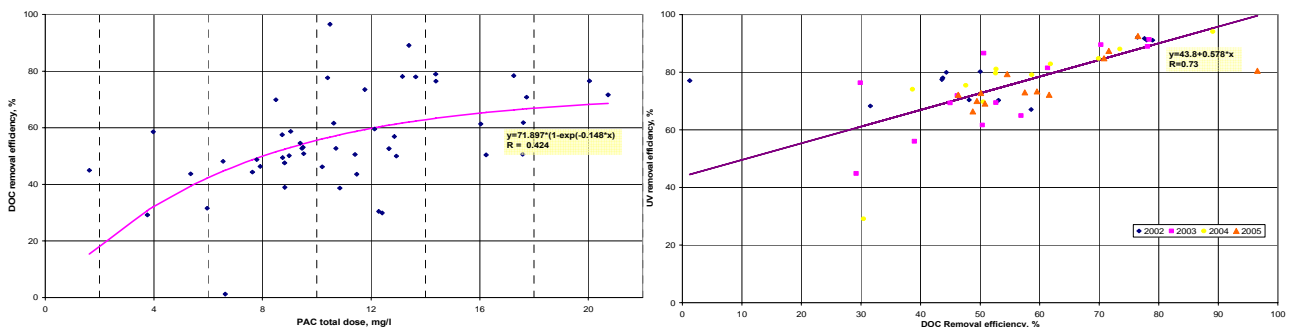


Figure 4-6 DOC removal vs. PAC dosage and DOC removal vs. UV removal

Above 10 mg/l Al, the removal is not significant although most data points are scatter. In comparison with UV removal it is necessary to use more coagulant to obtain more removal of organic matter in terms of DOC. Nevertheless, the removal efficiency is not as high as with UV for the same dose.

At this point is possible to compare the UV and DOC removals and joint them in a graph. Figure 4-6 right shows that UV removal is higher than DOC removal for the same dose of coagulant. In most of the cases the difference in removal is 20 % between UV and DOC removals.

According to the graph above high percentage of DOC has double bindings most likely the *humic* type. This is, because UV measures compounds with double binds that are mainly humic acids. UV absorbance at particular wavelengths can be related to the presence of specific chromophores. Absorbance at 254 nm can be mainly correlated to the amount of double bonds in aromatic rings (Pettersen et al., 1994) and, thus, to the aromaticity of a sample. HA is more aromatic than FA, and FA is more aromatic than

hydrophilic acids (Krasner et al., 1996). Absorbance was observed to be highly pH dependent (Abbt-Braun et al., 1990).

For monitoring and representing NOM concentration and the humic content or aromaticity of NOM, Ultraviolet absorbance at 254nm (UVA254) is used. The frequency of measurements of DOC is monthly while for UV is weekly. The UV absorbance is the only on-line measurement for organic matter available. DOC, AOC are costly and require a long time to obtain a result.

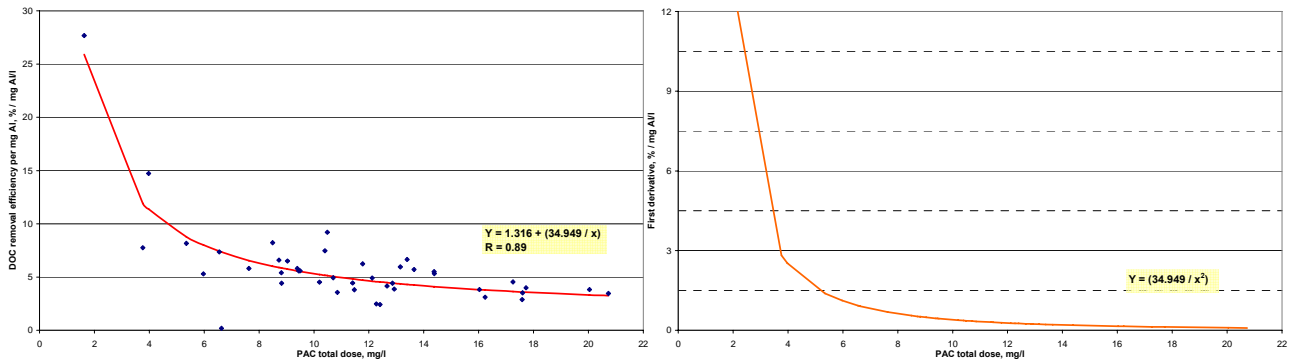


Figure 4-7 DOC removal (%) per mg of aluminium and Added value for DOC removal

Despite the limited data between 0 and 7 mg/l of coagulant, higher doses of PAC give very little additional DOC removal. For example, as shown in next table between 10 and 15 mg/l of coagulant dose the additional removal is only 1.5 % extra.

Dose, mg/l	% DOC removal / (mg/l)	Added value, % DOC removal/(mg/l)
5	8	1.5
10	5.5	0.5
15	4	0.25
20	3.5	0.15

From the above table, it can be seen that beyond 5 mg/l of Al dose the additional increment in DOC removal per extra milligram of coagulant per litre is less than 1.5 %. Nevertheless, the number of data is limited and it is difficult to conclude something with certainty.

The ratio of UV and DOC is an operational indicator of the nature of NOM and the effectiveness of coagulation in removing NOM (Edzwald and Benschoten, 1990). SUVA values offer a simple characterization of the nature of the NOM based on measurements of UV absorbance and DOC. Guidelines for the interpretation of SUVA values are presented in Table 2-1.

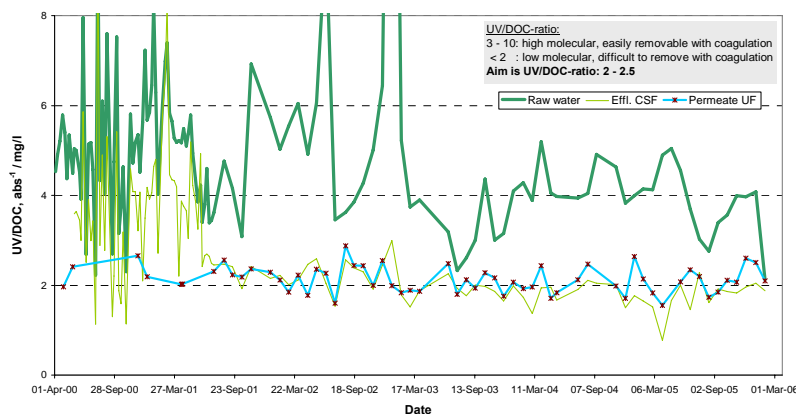


Figure 4-8 UV/DOC ratio

According to figure 4-8, and following the classification of (Edzwald and Tobiason, 1999) raw water composition ($SUVA > 4$) is mostly aquatic humics, with high hydrophobicity and high molecular weight, where NOM controls coagulation process. For supplies with low $SUVA$ (2 or less), TOC will not control coagulant dose. For water supplies with $SUVA$ greater than 2, the amount of NOM typically exerts a greater coagulant demand than the amount of particles. For these waters, the required coagulant dose increases with increasing TOC. Therefore, coagulation dosage should be focused in NOM removal, because of the raw water characteristics, this means that is required a lower pH than for particles removal.

4.3 Phosphate removal

Phosphates are not measured in “Norit” Klazienaveen treatment plant. Phosphates have an important influence for nutrients for micro organisms. The aim of finding an optimum dose is to get for the lowest dose the highest removal efficiency.

The aqueous chemistry of Al is complex and upon addition of an Al coagulant in water treatment, multiple reaction pathways are possible. For example, coordination between Al and inorganic ligands (e.g. PO_4^- , F^- , OH^- , SO_4^-) and organic ligands (e.g. humic materials) can occur as parallel competitive reactions. In addition, serial formation of Al monomers, Al polymers and $Al(OH)_3(s)$ may take place, depending on pH (vanBenschoten and Edzwald, 1990).

The pH of minimum solubility of $AlPO_4$ occurs at pH 6 which is one unit higher than that of $FePO_4(s)$ (pH 5). At higher pH values ($pH > 7$), the predominant phosphate precipitate is $Ca_{10}(PO_4)_6(OH)_2$ which has the lowest solubility among all the phosphate solids as shows next figure.

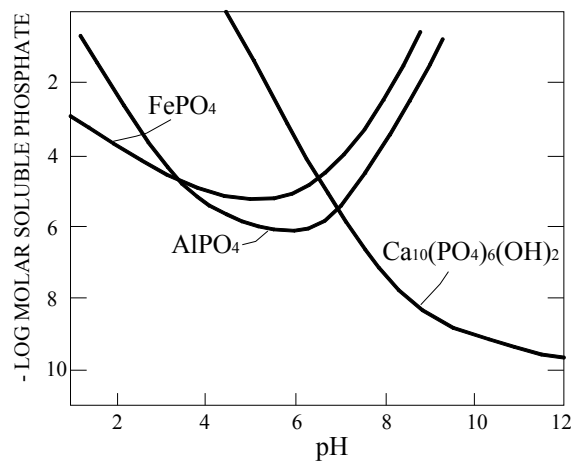


Figure 4-9 Solubility of metal phosphates (Stumm and Morgan, 1996)

Phosphate control is important in the study of biofouling on the membranes as hypothesis. Therefore, it is recommended to include phosphate tests for further study of biofouling in the plant.

In the same way, it is possible that aluminium solubility changes when aluminium is complexed with phosphates as was demonstrated by Stumm and Morgan in 1996.

4.4 Organic matter complexation with Aluminium

Organic matter could increase the solubility of aluminium due to complexation.

Optimum conditions for turbidity removal are not always the same as those for NOM removal, but provided the turbidity of the water is not excessive, the coagulant demand is governed by the concentration of NOM (Semmens and Field, 1980). It follows that the treatment process should be optimised for NOM removal where NOM is the major contaminant.

The mechanisms for coagulation described in literature review apply mainly to the removal of colloidal NOM, typically the higher molecular weight humic acids. These acids generally have low charge densities and therefore require low coagulant doses to induce destabilisation. However, the more soluble fraction of NOM (fulvic acids) has higher anionic charge densities that facilitate their dissolution. The *sweep coagulation* mechanism, which operates most effectively on colloidal NOM, is unlikely to be effective for these soluble fulvic acids. *Charge neutralisation* may remove soluble fulvic acids, but high doses of coagulant will be required to neutralize the high anionic charge, and the high coagulant dose required by soluble fulvic acids is likely to correspond to overdosing of humic acid colloids resulting in restabilisation of the colloids (Pernitsky and Edzwald, 2003).

A *fourth mechanism* that is occasionally alluded to is the chemical interaction of soluble NOM with soluble coagulant metal ions such as aluminium. The metal cation and chemically bound (complexed) NOM remain in solution until either the binding capacity of the NOM has been satisfied, or the solubility of the metal-NOM complex is exceeded. The complex does not need to be charge-neutral to precipitate.

The operational conditions for charge neutralisation, entrapment, adsorption, and complexing are not the same. Thus, it is unlikely that turbidity, colloidal NOM, and soluble NOM removal will be simultaneously accommodated during treatment. It is possible, however, to control the coagulation process to allow sequential interactions of coagulant with NOM and turbidity to effect their removal during coagulation/flocculation.

The solubility of natural organics is an important issue in membrane processes where concentration polarisation is a common effect. Concentration polarisation may lead to gel formation if the solubility is exceeded. Solubilities of mixtures are difficult to determine. Many parameters influence solubility; FA is, by definition, more soluble than HA at low pH. The complexation with metal ions also influences solubility.

Aggregation occurs due to an increase in ionic strength, which shields organic charge. The high MW components aggregate preferentially (Schafer, 2001). Calcium can enhance aggregation of NOM.

Concluding, it is necessary in WMD treatment plant to identify the nature of the organic matter present in the raw water and in some points along the treatment process. It is recommended to perform a LCOCD test for the points shown in the scheme in annex 7.1.5.

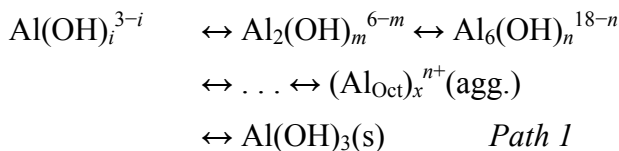
4.5 Characterising of the coagulant

4.5.1 Equations of aluminium species in PAC

Coagulants are one of the key factors in the coagulation process. Recently, based on conventional iron and aluminium salts, inorganic polymer flocculants (IPFs) have been developed rapidly and become applied widely. Among the IPFs, polyaluminium chloride (PAC) is one of the typical kinds. Little study has been focused directly on the features of chemical speciation during coagulation (Wang et al., 2004). There exist few established conclusions as to why their efficiency is superior to the traditional coagulants. It is generally thought that the pre-produced products contain species of superior quality and possess structure fairly stable to further hydrolysis and solution chemistry, resulting in higher coagulation efficiency.

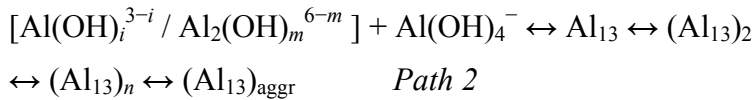
There are many excellent reviews with large amounts of literature on the aqueous chemistry of Al(III) and Fe(III) (Wang et al., 2004). However, there exist a few firmly established principles due to the complex nature of hydrolysis. The hydrolysis of Al(III) follows multiple pathways. A series of hydrolysis species can be formed depending on various factors such as aluminium concentration, sorts of bases adopted, methods of alkalization, speed for base addition, co-existing anions and particles. Therefore, the species formed are largely system specific and methodology dependent.

A review of aluminium hydrolysis chemistry reveals that two main kinds of mechanism for hydrolysis–polymerization exist. The most popular is the “core-link” or hexameric ring scheme, in addition to the more recent model of polynuclear formation involving a typical species of tridecameric, $\text{Al}_{13}\text{O}_4(\text{OH})_{24}^{7+}$ (also reported to range from 3^+ to 7^+ , normally simplified as Al_{13}^{7+}). The basic unit of the first model for aluminum polynuclear formation is either the $[\text{Al}_6(\text{OH})_{12}(\text{H}_2\text{O})_{12}]^{6+}$ (single ring) or the $\text{Al}_{10}(\text{OH})_{22}(\text{H}_2\text{O})_{16}^{8+}$ (double ring) species (Wang et al., 2004). The main feature of this mode is that the hydrolysis species may be continuously formed from monomer to polymer by bidimensional growth of the hexameric ring units. Therefore, many possible polynuclear species can be formed. The principal species will then depend mainly on the experimental conditions. In essence, the basic hexameric ring or “core-link” model was originally proposed as a logical extension of the solid state, crystalline aluminium trihydroxide structure. Although there is no direct verification of all of the possible structures, the model gains quite popular approval especially among the area of geochemistry and soil chemistry, since the resulting polymers prefigure the crystal structure of the aluminium trihydroxide polymorphs, gibbsite, bayerite, and nordstrandite. It is therefore possible to write the schematic reaction pathways from polymerization towards precipitation as Oct-Path 1:

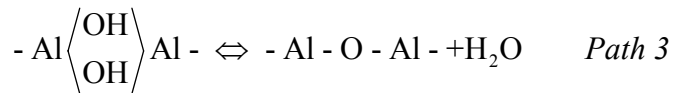


More recently, based on the direct measurement by ^{27}Al NMR and small angle X-ray diffraction, the polynuclear formation model was proposed. It is postulated that only several possible species in solution and direct transformation among them exist, such as monomers, dimers, tridecamer (Al_{13}), and aggregates. The existence of a tridecamer with a so-called Keggin structure has been verified by several investigators (Baes and Mesmer, 1976). This species forms rapidly and irreversibly when $\text{Al}(\text{OH})_4^-$ interacts with 12 octahedrally coordinated aluminium ions, and does not form on aging via polymer intermediates as suggested by (Baes and Mesmer, 1976). Akitt and Farthing

proposed a mechanism of Al₁₃ polynuclear formation whereby six dimeric species nucleate around Al(OH)₄⁻. However, several uncertainties remain in this model. It can not explain the entire process of species formation, distribution and transformation. There are some species beside the total aluminium concentration that can not be detected using the ²⁷Al NMR technique. And the mechanism for further transformation of Al₁₃ structure to aluminium trihydroxide is still to be confirmed, though some progress has been made in this regard (Wang et al., 2004). Regardless, based on the direct instrument detection, the Al₁₃ model has gained more and more approval. The possible schematic reaction pathways from polymerization towards precipitation involving Al₁₃ might be written as Tetra-Path 2:



It is therefore reasonable to infer a third pathway (Path 3) by mixing/combining Paths 1 and 2, with changes depending on the experimental conditions. For tailor-made PACls, the reaction scheme might follow Path 2 after dosing. However, the fast reacting polymeric species fraction is formed in situ through Path 3, in the main contribution from the monomeric species fraction in the original composition, as addressed previously. Upon aging, a structure rearrangement occurs rapidly through transformation of the hydroxy-bridge to an oxo-bridge:



There are several species of aluminium that can be formed dependent on the coagulant. It is not possible to take into account all the aluminium species. Laboratory analysis only presents a general value of aluminium concentration.

Aluminium salts are one kind of the most often used coagulants. Aluminium ions hydrolyse and polymerise into different species in water depending upon pH and aluminium concentration.

The Al₁₃ are regarded as the most efficient species for coagulation because of their high positive charge and large molecular weight (Tang and Luan, 1997). They can efficiently destabilise particles through adsorption and bridging in the coagulation process. During the application of conventional aluminium salts, rapidly formed aluminium species cannot be controlled and the more efficient Al₁₃ cannot be formed optimally. In order to improve coagulation efficiency and to suit different conditions, many inorganic polyaluminium chlorides with different OH/Al values have been produced and used (Gillberg, 1994; Shen and Dempsey, 1998).

The coagulant (PAC) characteristics used in klazienaveen treatment plant are as follow:

Molecular formula	AquaRhone® 18 D	Al(OH) _x Cl _y
pH	(20 °C)	1 ± 0.50
Specific gravity	(20 °C)	(gr/cm ³) 1.37 ± 0.02
Basicity (OH/3Al)	(%)	38 ± 5
Content:		
	Al ₂ O ₃	(%) 17.0 ± 0.5
	Al	(%) 9.0 ± 0.3
	Cl	(%) 21.5 ± 1.0

According to the classification done by (Pernitsky and Edzwald, 2003) AquaRhone® 18 D belongs to the range of medium basicity. With basis on the basicity (OH/Al) it is possible to determine the species that will be present in water as was described in the literature review section.

Figure 7-1 shows the different species that are common in PAC coagulants. This graph can be plotted using the equations below that were used by several authors (Pernitsky and Edzwald, 2003). Temperature plays a role in aluminium species concentrations as well as pH.

Table 4-3 Aluminium Species equations, log Al in mol/l

$T = 20\text{ }^{\circ}\text{C}$	$T = 5\text{ }^{\circ}\text{C}$
$\log \text{Al}(\text{OH})_4^- = \text{pH} - 12.7$	$\log \text{Al}(\text{OH})_4^- = \text{pH} - 13.4$
$\log \text{Al}_{13}^{7+} = -7*\text{pH} + 38.55$	$\log \text{Al}_{13}^{7+} = -7*\text{pH} + 41.45$
$\log \text{Al}(\text{OH})^{2+} = -2*\text{pH} + 5.7$	$\log \text{Al}(\text{OH})^{2+} = -2*\text{pH} + 6.3$

These equations agree with the chemical reactions for aluminium species using the correspondents Ksp (solubility product constant) that is found on literature, although are for standard laboratory conditions. For study purposes, were adopted the equations that produce the same solubilities as used in other publications for PAC coagulants.

Aluminium speciation is still a field for further research. Manufacturer of the coagulant does not specify the polymers or species dominant for each type of PAC. For the present study were used the three species summarized in Table 4-3.

4.6 Aggressivity against CaCO₃ (LSI) for permeate UF

Scaling is the deposition of sparingly soluble inorganic compounds on membranes. These compounds increase in concentration in the brine (concentrate). Theoretically precipitation may occur when the solubility is exceeded.

RO feed water is aggressive against calcium carbonate according to LSI calculations. Langelier saturation index (LSI) describes as negative the water that is under-saturated with calcium carbonate. As can be observed in the graph below, feed water of the RO is under-saturated varying the level of saturation with time.

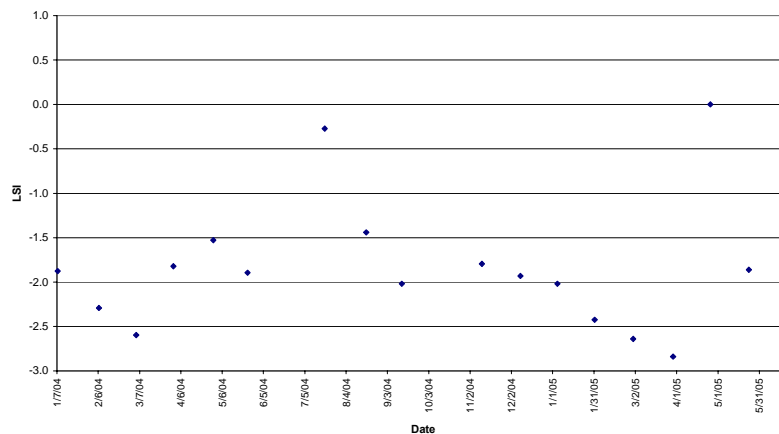


Figure 4-10 LSI in permeate UF

In case of scaling, this can be avoided not exceeding the solubility of any compound, dosing an acid to eliminate super saturation (this is only applicable for calcium carbonate), and dosing antiscalant.

For avoiding aggressivity against calcium carbonate it is necessary to increase the pH till reach the saturation pH (at that value there is no change of alkalinity). A positive value for SI indicates scale-forming tendencies, and a negative value indicates scale-dissolving or aggressive qualities. This is important during the filtration process with the reverse osmosis membranes.

4.7 Aluminium solubility changes in RO

Aluminium solubility is highly dependent upon pH of the solution as is shown in aluminium species equations (Table 4-3). In the same way, pH varies with the recovery of the RO system. Therefore in RO units, pH changes along the membranes and aluminium solubility changes because of its dependence on pH. Next equation shows the variation of pH in RO concentrate with the concentration factor.

$$pH_{concentrate} = \log CF_{hyp} + pH_{feed}$$

In this equation, concentration factor is described as hypothetical (CF_{hyp}) because it is assumed that the salt rejection (f) is equal to 100 %. Derivation of this formula is shown in annex 7.2.

The graph below shows the variation of the pH along a RO system for different pHs of feed water. When the recovery of the RO system is 75 % as is the case in Klazienaveen plant the change in pH in the concentrate is 0.6. For 50 % recovery the increase in pH is 0.5 and for 90 % is 1.

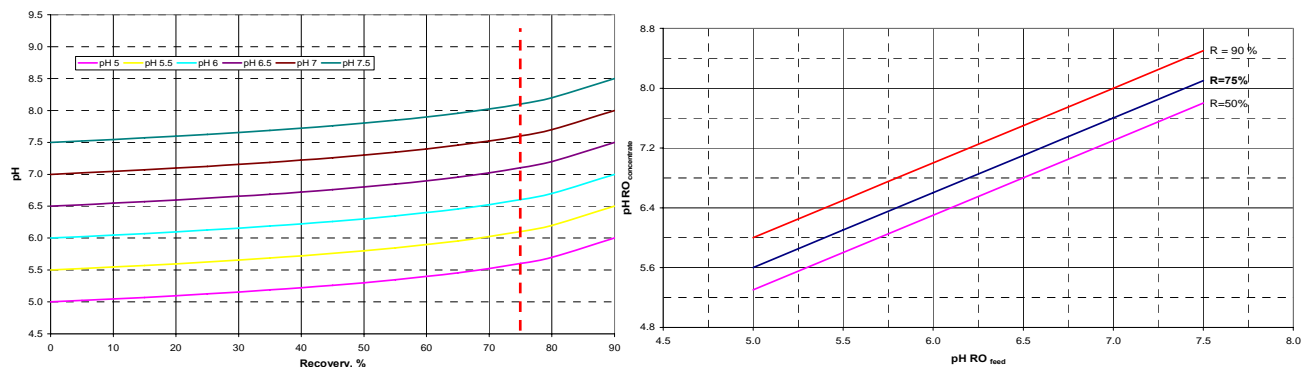


Figure 4-11 pH in RO concentrate vs Recovery and vs. pH RO feed

In conclusion, aluminium solubility changes for its several aluminium species because pH is increasing along the RO units.

4.8 Solubility of aluminium – UF permeate

4.8.1 Dependence on temperature

The total aluminium solubility changes with temperature (Pernitsky and Edzwald, 2003). For warm periods the total solubility is higher than in colder periods.

Next graph shows for theoretical species of aluminium the total solubility for different temperatures. Solubilities for 10 and 15 °C were interpolated.

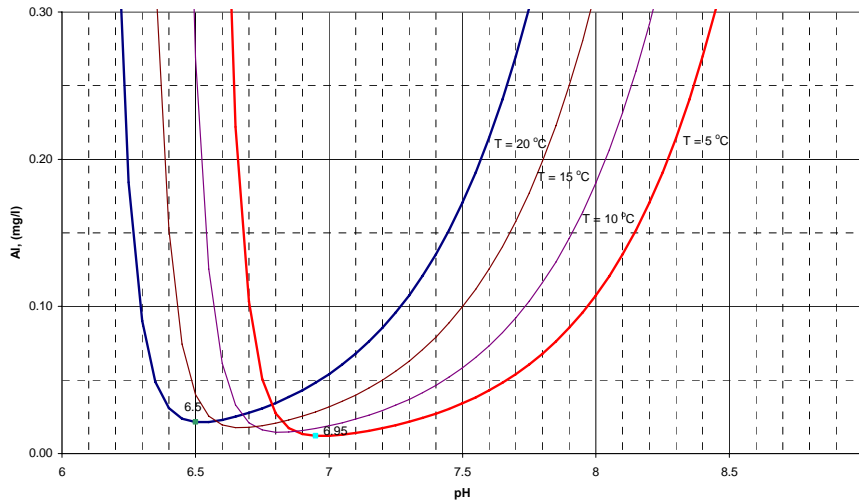


Figure 4-12 Total Aluminium solubility varying temperature

The higher the temperature, the higher the PAC solubility. In the same way the optimum pH for minimum solubility also changes with temperature, the higher the temperature the lower the pH. In warm periods (20 °C) the optimum pH is 6.5 and for colder periods (5 °C) is 6.95.

Now, it was assumed that all the aluminium in water is *soluble*; this is, “just saturated”. Therefore all non-soluble aluminium (flocs) is retained by the CSF and ultra filtration, and the aluminium remaining is soluble in the water. In annex 7.4 is shown an approximation for verifying that aluminium is soluble in the RO feed water (UF permeate). Figure 7-19 shows that water is just saturated with aluminium only in some periods of time; nevertheless, lack of data and availability of aluminium solubility for two temperatures makes difficult to conclude with strength.

It was plotted for different range of temperatures the aluminium concentration of the feed water in RO units in the treatment plant. Data points correspond to years since 2002 till June 2005. Measurements are done monthly for the UF permeate (RO feed water). Dots for temperatures higher than 20 °C are slightly right of the theoretical line for 20 °C. For temperatures lower than 10 °C dots have higher solubility than for higher temperatures and are not close to the theoretical line of 5 °C.

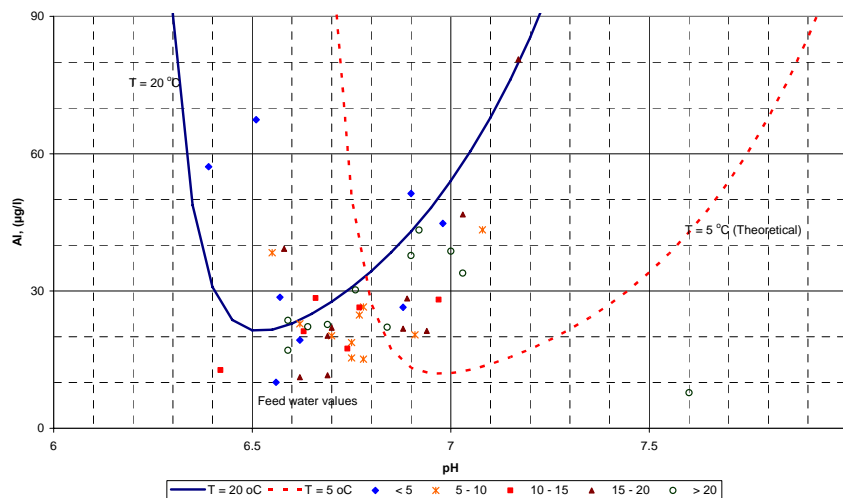


Figure 4-13 Aluminium concentration in RO feed water depending on temperature compared with theoretical PAC solubility

It was expected to obtain parallel lines from high to low temperatures. These differences could be because of leakages in the modules and that aluminium complexation with organic matter is occurring.

Concluding, it is very difficult to say if the aluminium is soluble or not. Data points are sparse (monthly measurements in five years); the equations available are only for 5 and 20 °C being the temperature of great influence on the solubility.

4.8.2 Optimum pH for coagulation

Klazienaveen plant deals with two water sources. Both sources have different properties in terms of optimum pH for coagulation. Defining November to March as winter water, and April to October as summer it was analysed the available data in terms of aluminium solubility versus its correspondent pH in UF permeate.

Data available for Al concentrations in UF permeate is monthly in the plant. The operational pH range is narrow and varies from 6.55 to 7.1 along all years. Dividing the data in two periods of time and analysing separately was found the following.

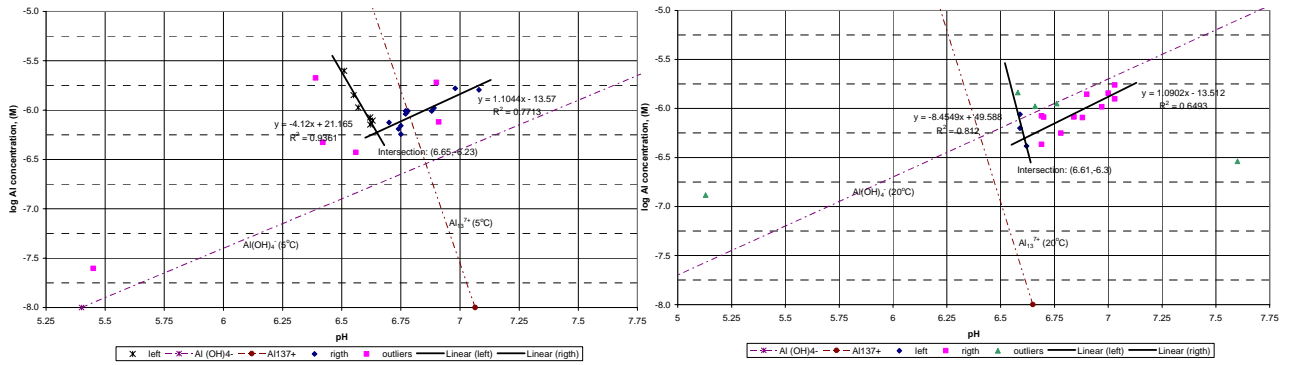


Figure 4-14 Solubility of Aluminium in permeate UF. November to April (“winter”) and May to October (“summer”)

Data points were divided in two groups in similar way as they were or Al(OH)_4^- and Al_{13}^{7+} . These species are the dominant for the pH range operated in the plant.

The intersection of the fitted lines to the data points produces the optimum pH for minimum solubility. For November to April the optimum pH is 6.65. Data points in this period were compared with theoretical species at 5 °C for Al(OH)_4^- and Al_{13}^{7+} . In case of summer period, data points were compared with the aluminium species at 20 °C. The intersection of the fitted lines gave the optimum pH for minimum solubility as 6.61 for summer period.

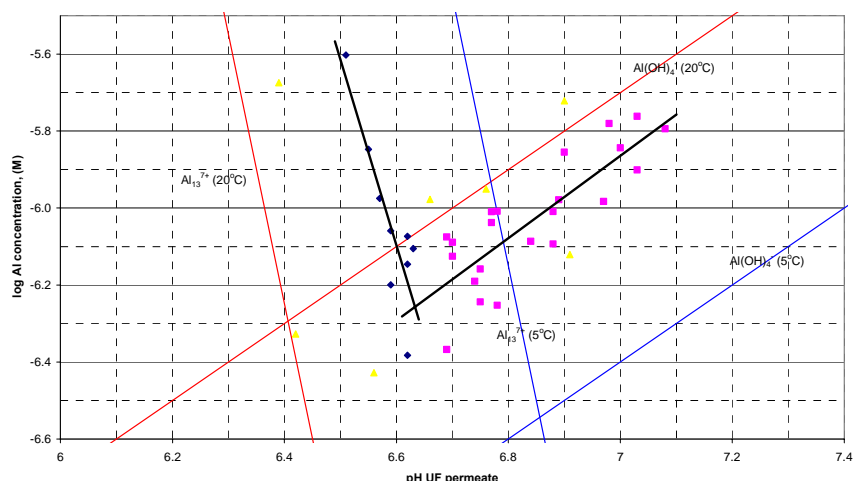


Figure 4-15 Optimum pH for minimum solubility of Aluminium.

In the figure, points represent aluminium solubility for different years of operation of the plant. The fitted lines for the total data lie between the theoretical lines for 20 and 5 °C because temperature was not normalized in the process.

The pH range is narrow for minimum solubility (6.6 to 6.7) and it is very important an adequate monitoring of pH before ultra filtration in order to reach the minimum solubility for aluminium.

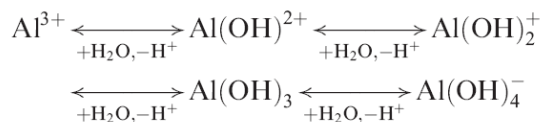
The correlations' coefficients should be as closer as 1 as possible for being the fitted equation acceptable and valid. The correlations are in general weak (0.77 and 0.65) even for limited data. Ideally, comparisons must be performed for data at approximately same temperature. Unfortunately there are not too many data points for this process.

Concluding, in case of “Norit” Klazienaveen plant on basis of available data (limited), there is no difference between the two water sources in the behaviour of aluminium solubility in permeate UF.

4.9 Simulation of Aluminium

4.9.1 Simulation of Aluminium solubility

After addition to water, Al coagulant dissociates and the Al^{3+} ions undergo the hydrolysis reactions as shown below (Exall and vanLoon, 2003):



The degree to which the reactions are proceeded and the nature of the produced species may depend on the Al ions concentration, pH, temperature and the presence of any other ions. Among the hydrolysis reaction products monomeric (Al^{3+} , $Al(OH)^{2+}$, $Al(OH)_2^+$, $Al(OH)_3$, $Al(OH)_4^-$) and polymeric ($Al_2(OH)_2^{4+}$, $Al_3(OH)_4^{5+}$, $Al_{13}O_4(OH)_{24}^{7+}$) forms may be detected (Duan and Gregory, 2003). In the solutions of the prehydrolyzed coagulants (PAC), the polymeric species with high positive charges occur more frequently among the hydrolysis products than in the solutions of the non-prehydrolyzed coagulants, which are added to water at a natural pH (Kabsch-Korbutowicz, 2005).

Polyaluminium chloride (PAC) has as predominant species Al_{13}^{7+} . Besides this species, there are other species that can be produced in the solution depending on the basicity of the coagulant and the pH of the solution.

Equations for determining the solubility of aluminium across the RO are summarized in Table 3-6. To simulate the change of solubility it was assumed that the aluminium concentration of aluminium in RO feed water is just saturated as was explained in the previous section.

The change in solubility for three different species is shown below when the RO feed water pH is 6.5 and the temperature of 20 °C.

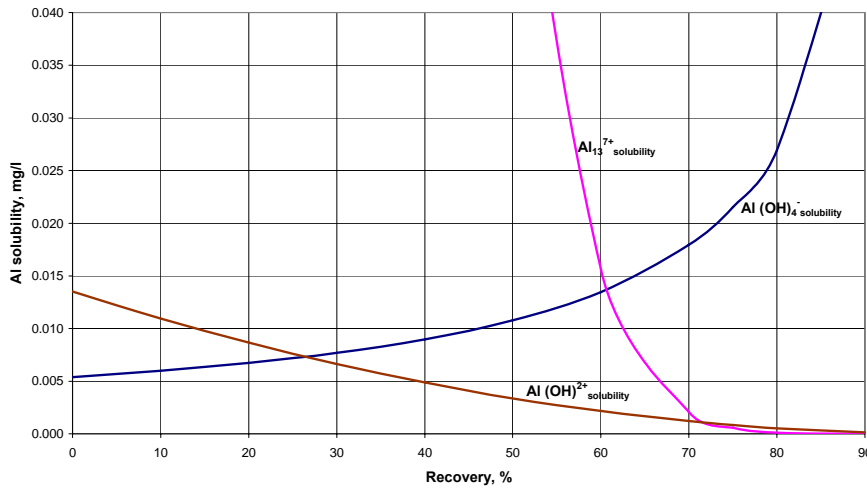


Figure 4-16 Simulation of solubility for $pH_{feed\ RO} = 6.5$ and $T = 20\ ^\circ C$

For this pH, Al_{13}^{7+} and $Al(OH)^{2+}$ decrease their solubilities when recovery was increased. While for $Al(OH)_4^-$ the solubility increases when recovery increases. The variation in the solubility for several pHs and temperatures is shown in annex 7.3. $Al(OH)^{2+}$ and $Al(OH)_4^-$ have very low (negligible) solubilities in the pH range of 6 to 7.5 (in the feed water of the R.O.)

Al_{13}^{7+} plays a dominant role at pH 6 since the concentrations are substantial in particular at 5 °C. So, substantial amounts of Aluminium theoretically might precipitate. At pH values 7 and 7.5 it is negligible. It is quite remarkable that the solubilities of $Al(OH)^{2+}$ and Al_{13}^{7+} are higher at lower temperatures and for $Al(OH)_4^-$ the solubility goes down at lower temperatures.

Now, it is possible to find the total aluminium solubility of PAC when recovery is changing. For this at the same pH, it was added the aluminium species solubility at every correspondent recovery and was obtained the total aluminium solubility as a function of the recovery. This result is shown in next figure.

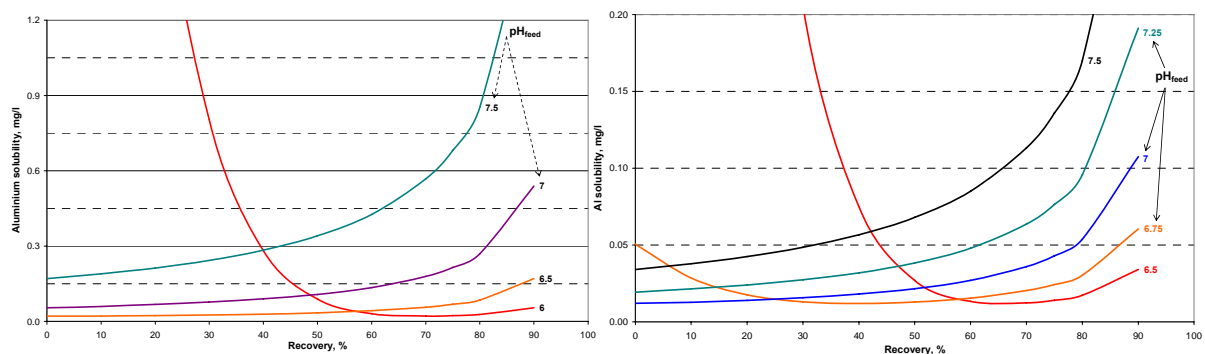


Figure 4-17 Simulation of Total Aluminium solubility, $T=20\ ^\circ C$ and $T=5\ ^\circ C$.

The solubility is higher for higher the temperature. When the temperature is 20 °C, aluminium solubility is increasing from pH 6.5 and decreases under this pH feed water. When the temperature is 5 °C, aluminium solubility increases from pH 6.85; and decreases with increasing the recovery under this feed water pH.

In conclusion, pH control is important in the change of solubility of aluminium along RO systems. Differences between pH 6 and 7.5 are huge in solubility of aluminium species.

4.9.2 Simulation of Aluminium concentration and solubility

It was compared the aluminium solubility with the change of aluminium concentration in RO systems. The outcome of this comparison procedure let identify the best and/or worst scenarios for aluminium precipitation in RO systems under theoretical assumptions.

The equations used for this simulation are summarised in Table 3-7.

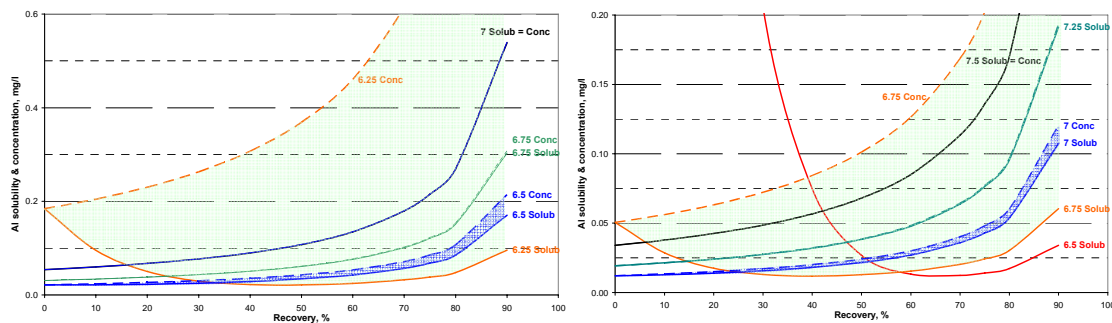


Figure 4-18 Simulation Aluminium solubility and concentration, T= 20 °C and T = 5 °C

The figure shows, the change in Al solubility and Al concentration for several feed water pHs versus recovery. Al concentration in all cases increases with increasing recovery, while Al solubility increases only for some pHs.

For temperature equal to 20 °C (left figure), when the pH is less than 6.25 the aluminium solubility decreases until 50 % recovery while for pH more than 6.5 the aluminium solubility increases from recovery 0 %.

It is expected that aluminium precipitation happens when the concentration is more than the solubility. Therefore, when feed water pH is lower than 6.75 it is possible to expect some aluminium precipitation on the RO membranes. For pH 7 the solubility is equal to the concentration and therefore in theory precipitation will not occur.

For a temperature of 5 °C it is required a higher pH for avoiding aluminium precipitation according to this simulation model. In the graph for pH 6.5, 6.75, and 7.0 it is occurring aluminium precipitation because the concentration is higher than the aluminium solubility; this is not the case for pH = 7.25 where both solubility and concentration are approximately the same for 75 % recovery.

Concluding, for temperatures as high as 20 °C it is required feed water pH in RO of 6.7 and for temperature of 5 °C it is necessary a pH of 7.2 to avoid aluminium precipitation on the membranes.

4.10 Aluminium scaling - precipitation

4.10.1 Particle Deposition Factor, Ω

The particle deposition factor represents the ratio of the particles deposited on the RO membrane to that in the feed water. Experimentally, the particle deposition factor is calculated from the relation between the aluminium concentration of the concentrate at recovery R of the RO system and the aluminium concentration of the feed water as follows.

$$\Omega = \frac{1}{R} + \frac{Al_{concentrate}}{Al_{feed}} \cdot \left(1 - \frac{1}{R}\right)$$

In the formula above is assumed that the salt rejection is 100 %, this is $f = 1$ and this influences the recovery factor. Therefore, the concentration factor is not the real one but a theoretical or hypothetical (CF_{hyp}). Rearrangement the above equation we have:

$$\Omega = \frac{1}{CF_{hyp} - 1} \cdot \left(CF_{hyp} - \frac{Al_{concentrate}}{Al_{feed}} \right)$$

It was calculated the concentrate concentration for different recoveries depending on the deposition factor starting with the average aluminium concentration in RO feed water.

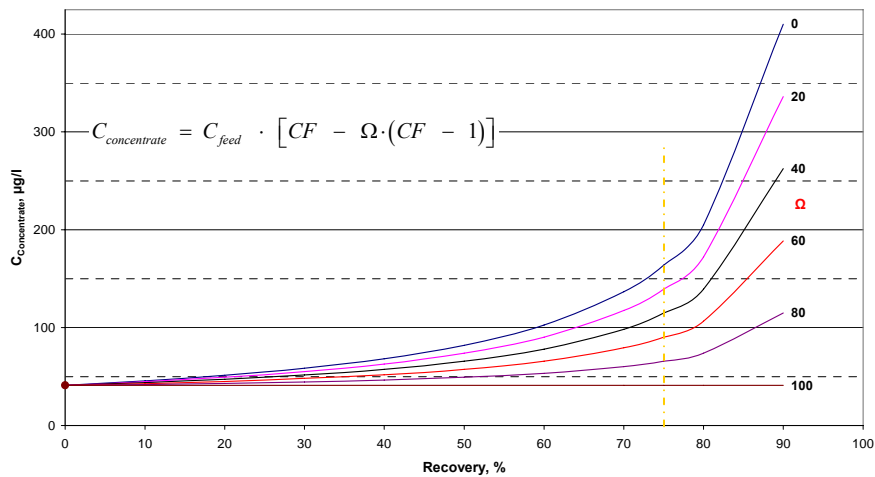


Figure 4-19 Recovery (%) vs. $C_{concentrate}$ ($\mu\text{g/l}$) for different Particle Deposition Factors (Ω)

For deposition factor equal to 100 %, the aluminium concentrate concentration is equal to the aluminium feed concentration, this mean that there is no rejection of the particles by the membranes. For deposition factor equal to 0 %, the concentrate concentration is the feed concentration times the concentration factor; in this case particles are rejected by the membranes. For deposition factors between 0 and 100 %, the rejection varies.

The results of the particle deposition factor in Klazienaveen plant are shown in Figure 4-20. A *positive* deposition factor indicates particles are being deposited as they pass through the system while a *negative* factor indicates the number of particles in the concentrate exceeds the incoming flux (taking into account the concentration factor) (Boerlage, 2001).

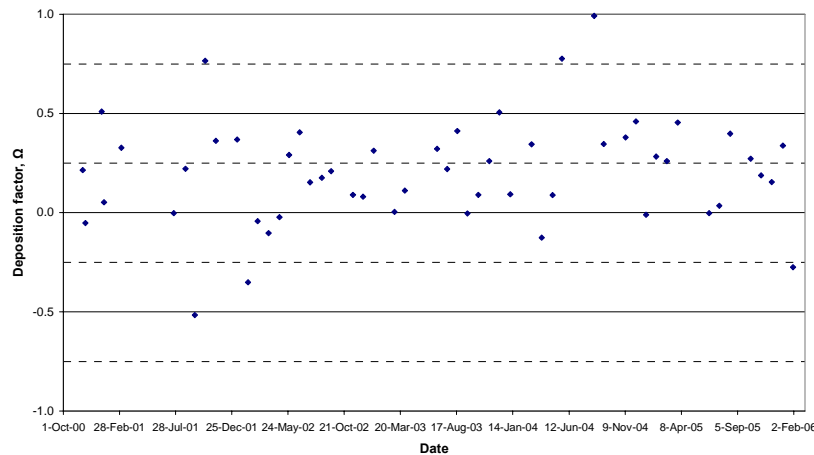


Figure 4-20 Deposition factor, Ω (Recovery = 75 %, CF = 4) (without outliers)

The particle deposition factor (Ω) varies in time and magnitude. Table 4-4 shows the range of values produced in Klazienaveen plant. In average 21 % of what is going through the RO system precipitated on the membranes when is calculated the average including negative values; but when only positive deposition factor were taken into account the average is 31 % of particle deposition.

It is possible to obtain deposition factors higher than 1 ($\Omega > 1$). The reason could be that there is accumulation of the salts in the spacer of the membranes, or because of a bad sampling or a bad laboratory analysis.

Table 4-4 Particle Deposition factor in Klazienaveen plant, Ω

	(+) ¹	(+ ^ -) ²
max	0.99	0.99
min	0.004	-0.52
avg	0.319	0.21

¹ Values calculated taking into account only positive values of Ω.

² Values calculated using all available data without outliers (neg. values < -1).

It was analysed the influence of pH and temperature on deposition factors results. The limited data made not possible to see a clear dependence on the results of deposition factor. These comparison graphs are shown in annex 7.5.

In conclusion, deposition factor is an appropriate indicator of aluminium particle deposition on the RO membranes. In 21 % average there was aluminium deposition on the membranes.

4.10.2 Modified Fouling Index (MFI)

To maintain membrane productivity, an increase in the applied pressure in combination with membrane cleaning is required, both of which increase energy costs. Therefore, methods to measure the particulate content of a feed water and to predict membrane fouling are important tools in the control of particulate fouling, both at the design stage and for monitoring during plant operation (Boerlage, 2001). Presently, the most widely applied fouling indices to measure the particulate fouling potential of membrane filtration feedwater are the Silt Density Index (SDI), the Modified Fouling Index (MFI_{0.45}) and more and more the MFI-UF (using a ultrafiltration membrane) that incorporate fouling due to smaller colloidal particles.

MFI can be determined in constant pressure mode or in constant flux mode.

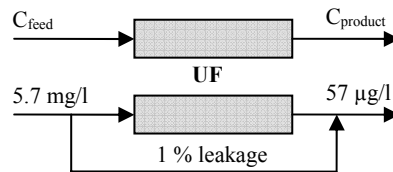
The height of the layer that will be formed during the period of time estimated is 29.2 nm per cm² of membrane. The porous size in an UF module can vary from 5 to 20 nm or even more.

In conclusion, the thin layer formed per square centimetre could be the reason for an often cleaning frequency in the RO skids.

4.10.4 Integrity tests

In case that UF membranes are leaking, then aluminium concentration in RO feed water is higher than suppose to be. MFI results were high after ultra filtration.

If exist a leakage in UF membranes of 1 %, and the UF feed water has a concentration in average of 5.7 mg/l, then the product water from the UF has a concentration of x + 1% of C_{feed UF}. This is 57 µg/l.



In the worst situation, aluminium concentration in UF feed water is as high as 19 mg/l and with a leakage of 1 % there is 190 µg/l of aluminium in UF product water. Aluminium concentration values in “Norit” Klazienaveen treatment plant are shown in annex 7.1. The characteristics of the UF membranes were summarised in Table 3-2 and an scheme of the UF units is shown below.

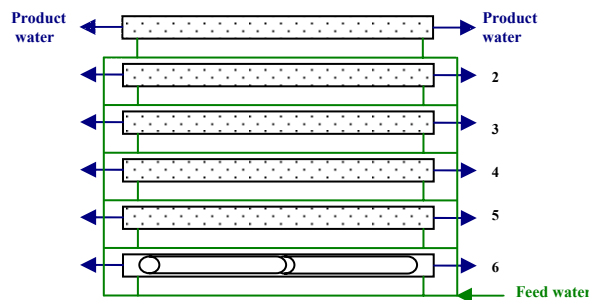


Figure 4-21 UF scheme – Klazienaveen plant

The results of detecting and blocking the broken fibres is as follow.

Table 4-6 Klazienaveen plant Integrity test results, 16/03/06

Vessel	Module 1	Module 2	Total
3.1	2 / 2	2 / 2	4
3.2	2 / 2	2 / 3	5
3.3	1 / 2	2 / 1	4
3.3	3 / 2	1 / 1	4
3.5	2 / 2	4 / 3	6
3.6	0 / 0	1 / 1	1
4.1	0 / 0	4 / 2	4
4.2	3 / 4	2 / 4	8
4.4	-	-	-
4.4	2 / 3	5 / 6	9
4.5	1 / 1	0 / 0	1
4.6	3 / 2	0 / 0	3

The table shows the number of broken fibres that were found per module and per vessel. Skid number 3 has a total of 24 broken fibres while skid number 4 has 25 broken fibres

as total. It was found some elements where the number of broken fibres is not the same at both sides; the reason could be that with the operation last repairing pins were released.

If we compared the number of broken fibres with the total in a UF module, the percentage in the worst case is 0.1 %.

5 Conclusions and Recommendations

5.1 Conclusions

- Expected G value is low (poor flocculation) and is recommended to be studied and if possible to increase it in a simple way (for example, increase headloss in tank by adding a barriers).
- Coagulant dosing control (CDC) was the focus of part of this study in Klazienaveen plant. The use of simple and robust online sensors like UV measurements allows an automatic dosing control. However, it was found that the actual target value of 20 Abs/m produces substantial over dose of coagulant – 90 % of the time – when UV removal is considered only.
- In case of employing more than 5 mg/l of coagulant, the additional removal of UV is less than 2.5 % (added value) per mg coagulant per litre. *Remark:* Dose in 2005 was 14 mg Al/l.
- Aluminium solubility is complex and changes along the RO system due to pH increase. The change in pH is according to next formula,
$$\text{pH}_{\text{concentrate}} = \text{pH}_{\text{feed}} + \log \text{CF}_{\text{hyp}}$$
 (at 75 % increase is 0.6)
- Simulation of aluminium change in solubility and in concentration in reverse osmosis systems on basis on theoretical Aluminium species showed that:
At 20 °C, if pH is higher than 6.5 then it is not Aluminium scaling expected.
At 5 °C, if pH is higher than 7.2 then it is not Aluminium scaling expected.
- The calculated deposition factor demonstrated that Aluminium may precipitate in the RO membranes - at least 21 % on average of the part that theoretically can precipitate.
- Integrity tests revealed that broken fibres were leaking in ultra filtration modules. Although the percentage is low, particles, colloids and micro-organisms may find their way into the RO feed and cause operational problems (*e.g.* membrane fouling).

5.2 Recommendations

For further research is possible to recommend:

- To extent the study to other metals that could be cause of fouling in the membranes as Manganese.
- Include pH of the solution in the coagulant dosing control for optimizing colour removal in warm periods and colloids in cold periods. For this, perform jar test
- Perform MFI-UF tests for verifying the particulate (colloidal) fouling in UF membranes.

6 References

- ABBT-BRAUN, G., FRIMMEL, F. H. & SCHULTEN, H. R. (1990) Strukturelle Charakterisierung isolierter aquatischer huminstoffe – Anwendbarkeit, Grenzen und Vergleich ausgewählter Methoden. *Vom Wasser*, 74, 325-338.
- AIKEN, G. & LEENHEER, J. (1993) Isolation and chemical characterization of dissolved and colloidal organic matter. *Chemistry and Ecology*, 8, 135-151.
- AMIRTHARAJAH, A. & MILLS, K. M. (1982) Rapid mix design for mechanisms of alum coagulation. *Journal of the American Water Works Association*, 74, 210-216.
- AWWA (2001) *NOM rejection by, and fouling of, NF and UF membranes*, USA.
- BAES, C. F. & MESMER, R. E. (1976) *The hydrolysis of Cations*, New York, Wiley.
- BOERLAGE, S. F. E. (2001) *Scaling and Particulate Fouling in Membrane Filtration Systems*. Delft, IHE-Delft / Wageningen University.
- BOTTERO, J. Y. & CASES, J. M. (1980) Studies of Hydrolyzed Aluminium Chloride Solutions. 1 Nature of aluminium species and composition of aqueous solutions. *Physical Chemistry*, 84, 2933-2939.
- CHO, J., AMY, G. & PELLEGRINO, J. (1998) Membrane filtration of natural organic matter: initial comparison of rejection and flux decline characteristics with ultrafiltration and nanofiltration membranes. *Water Res.*, 33, 2517-2526.
- CHO, J., AMY, G., PELLEGRINO, J. & YOON, Y. (1999) Characterization of clean and natural organic matter (NOM) fouled NF and UF membranes and foulants characterization. *Desalination*, 118, 101-108.
- CHO, J., AMY, G. A. & PELLEGRINO, J. (2000) Membrane filtration of natural organic matter: comparison of flux decline, NOM rejection, and foulants during filtration with three UF membranes. *Desalination*, 127, 283-298.
- CLARK, M. M. & JUCKER, C. (1993) Interactions between Hydrophobic Ultrafiltration Membranes and Humic Substances. *Membrane Technology*. Baltimore, MD.
- DELGADO, S., DIAZ, F., GARCIA, D. & OTERO, N. (2003) Behaviour of Inorganic Coagulants in Secondary Effluents from a Conventional Wastewater Treatment Plant. *Filtration+separation*, 1, 42-46.
- DEMPSEY, B. A. (1994) Production and utilization of Polyaluminium Sulfate. *AWWA Research Foundation*, 71.
- DUAN, J. & GREGORY, J. (2003) Coagulation by hydrolysing metal salts. *Adv. Colloid Interface Sci.*, 100-102 475-502.
- EDZWALD, J. K. & BENSCHOTEN, J. E. V. (1990) Aluminum Coagulation of Natural Organic Matter, Chemical water and wastewater treatment. *Chemical water and wastewater treatment*, 341-359.
- EDZWALD, J. K. & TOBIASON, J. E. (1999) Enhanced Coagulation: USA requirements and a broader view. *Removal of Humic substances from water*. Trondheim, Norway, IAWQ/IWSA Joint specialist group on particle separation.
- ELIMELECH, M., CHEN, W. H. & WAYPA, J. J. (1994) Measuring the zeta (electrokinetic) potential of reverse osmosis membranes by a streaming potential analyzer. *Desalination*, 95, 269-286.
- EXALL, K. N. & VANLOON, G. W. (2003) Effects of raw water conditions on solute-state aluminium speciation during coagulant dilution. *Water Res.*, 37, 3341-3350.

- GREGOR, J. E., NOKES, C. J. & FENTON, E. (1997) Optimising natural organic matter removal from low turbidity waters by controlled pH adjustment of aluminium coagulation. *Wat. Res.*, 31, 2949-2958.
- GREGORY, J. & DUAN, J. (2001) Hydrolyzing metal salts as coagulants. *Pure Appl. Chem.*, 73, 2017-2026.
- HONG, S. & ELIMELECH, M. (1997) Chemical and physical aspects of natural organic matter (NOM) fouling of nanofiltration membranes. *Membr. Sci.*, 132, 159-181.
- KABSCH-KORBUTOWICZ, M. (2005) Effect of Al coagulant type on natural organic matter removal efficiency in coagulation/ultrafiltration process. *Desalination*, 185, 327-333.
- KRASNER, S. W., CROUE, J. P., BUFFLE, J. & PERDUE, E. (1996) Three approaches for characterizing NOM. *Journal AWWA*, 66-79.
- MALLEVIALLE, J., ODENDAAL, P. E. & WIESNER, M. R. (1996) *Water Treatment Membrane Processes*, McGraw-Hill.
- MOHTADI, M. F. & RAO, P. N. (1973) Effect of Temperature on Flocculation of Aqueous Dispersions. *Water Research*, 7, 747-767.
- NEWLOGICRESEARCHINC. (2003) Feed Water Treatment for Industrial Boilers & Power Plants. *Filtration+Separation*, 1, 28-29.
- ODEGAARD, H. J. & FETTIG, J. (1990) Coagulation with prepolymerized metal salts. *Chemical Water and wastewater treatment*, 189-220.
- PARTHASARATHY, N. & BUFFLE, J. (1985) Study of polymeric aluminum (III) hydroxide solutions for application in waste water treatment. Properties of the polymer and optimal conditions of preparation. *Water Research*, 19, 25-36.
- PERNITSKY, D. J. & EDZWALD, J. K. (2003) Solubility of Polyaluminium coagulants. *Journal of Water Supply: Research and Technology-AQUA*, 52.6, 395-406.
- PETTERSON, C., EPHRAIM, J. & ALLARD, B. (1994) On the composition and properties of humic substances isolated from deep groundwater and surface waters. *Organic Geochemistry*, 21, 443-451.
- RATNAWEERA, H. (2004) Coagulant Dosing Control. IN HAHN, H. H., HOFFMANN, E. & ODEGAARD, H. (Eds.) *Chemical Water and Wastewater Treatment*. Orlando, Florida, USA, IWA Publishing.
- RATNAWEERA, H., LEI, L. & LINDHOLM, O. (2002) Simulation program for wastewater. *Water Science and technology*, 46, 27-33.
- SCHAFFER, A. I. (2001) *Natural Organics Removal using membranes*, Technomic Publishing Co, Australia.
- SCHIPPERS, J. C. & BUIITEMAN, J. P. (2005) *Conventional water treatment technology*, Delft, The Netherlands.
- THURMAN, E. M. (1985) *Organic Geochemistry of Natural Waters*, Dordrecht., Martinus Nijhoff/Dr Junk W Publishers.
- VANBENSCHOTEN, J. E. & EDZWALD, J. K. (1990) Chemical aspects of coagulation using Aluminum salts I. Hydrolytic reactions of alum and polyaluminum chloride. *Wat. Res.*, 24, 1519-1526.
- WANG, D., SUN, W., XU, Y., TANG, H. & GREGORY, J. (2004) Speciation stability of inorganic polymer flocculant-PAC. *Colloids and Surfaces A*, 243, 1-10.
- WEISNER, M. R. & KLUTE, R. (1997) *Properties and measurements of particulate contaminants in water in treatment process selection for particle removal*, AWWARF.

- YANGALI, V. A. (2005) Colloidal and Non colloidal fouling of UF membranes: Analyses of membrane fouling and cleaning. *Municipal Water and Infrastructre*. Delft, Unesco-IHE.
- ZHANG, P., HAHN, H. H. & HOFFMANN, E. (2004a) Study on Flocculation Kinetics of Silica Particle Suspensions. IN HAHN, H. H., HOFFMANN, E. & ODEGAARD, H. (Eds.) *Chemical Water and Wastewater Treatment*. First ed. Orlando, Florida, USA, IWA Publishing.
- ZHANG, P., HAHN, H. H., HOFFMANN, E. & ZENG, G. (2004b) Influence of some additives to aluminium species distribution in aluminium coagulants. *Chemosphere*, 57, 1489–1494.

7 Appendixes

7.1 Annex 1

7.1.1 Summary of chemical parameters analysis

Compound	Unit	Raw water			Feeding UF			Permeate UF		
		min	Avg	max	min	Avg	max	min	Avg	max
pH	-	6.1	6.9	7.6	5.5	6.7	7.7	5.1	6.7	7.6
Temperature	oC	0.8	11.9	25.5	1.3	12.4	23.7			
E. Conductivity	mS/m							17.7	42.9	73.0
Aluminium, Al ³⁺	µg/L	55.3	320.2	5336.0	134.8	5741.9	19081.0	3.5	37.2	413.1
Iron, Fe ²⁺	mg/L	1.11	4.16	9.51	0.05	1.79	6.65	0.01	0.02	0.13
Mn ²⁺	mg/L	0.06	0.15	0.35				0.0	0.1	0.3
Barium, Ba ²⁺	µg/L							1.8	19.6	65.1
Calcium, Ca ²⁺	mg/L							0.1	24.5	52.9
Sr ²⁺	µg/L	69.0	81.2	104.0				0.0	79.3	217.4
Silicium, Si ³⁺	mg/L							0.1	3.5	8.1
HCO ₃	mg/L							4.3	69.4	150.3
Chloride, Cl ⁻	mg/L							27.0	69.3	111.0
SO ₄ ²⁻	mg/L							12.8	40.6	79.4
ATP	ng/L				0.0	70.4	973.0	0.0	9.0	304.0
Chlorofyl	µg/L	1.2	39.3	104.8						
Turbidity	FTU	7.2	25.6	136.5	0.6	17.6	98.4	0.0	0.0	0.6
Suspended Solids	mg/L	1.4	13.4	49.6	0.0	20.7	103.1			
DOC	mg/L	6.1	20.2	42.7	4.0	12.8	39.9	0.4	8.0	14.2
UVA254	abs/m	19.5	88.8	242.4	7.8	26.1	183.2	2.1	17.8	67.3
UV/DOC	abs.L/m.mg	2.1	4.9	23.2	0.8	2.9	9.6	1.6	2.1	2.9

Summary until February 2006.

7.1.2 Ionic Balances

The ionic balance was calculated for permeate of the UF, for 21/06/05 is:

Positive ions												
	[Al ³⁺]	[Ba ²⁺]	[Ca ²⁺]	[Mg ²⁺]	[Na ⁺]	[NH ₄ ⁺]	[Fe ²⁺]	[Mn ²⁺]	[Si ³⁺]	[Sr ²⁺]	[H ⁺]	Σ _{pos}
C (mg/L)	0.01704	0.01263	27.48				0.052	0.0872	2.54	0.07962		
M (mg/mmol)	27	137	40	24	23	18	56	55	28	88		
C (mmol/L)	0.001	0.000	0.687	0.000	0.000	0.000	0.001	0.002	0.090	0.001	2.6E-04	
Valency	3	2	2	2	1	1	2	2	3	2	1	
meq/L	0.00	0.00	1.37	0.00	0.00	0.00	0.00	0.00	0.27	0.00	2.6E-04	1.65
eq/L	1.9E-06	1.8E-07	1.4E-03	0.0E+00	0.0E+00	0.0E+00	1.9E-06	3.2E-06	2.7E-04	1.8E-06	2.6E-07	0.001655
												0.001383

Negative ions												
	[Cl ⁻]	[SO ₄ ²⁻]	[HCO ₃ ⁻]	[F ⁻]	[NO ₃ ⁻]	[PO ₄ ³⁻]					[OH ⁻]	Σ _{neg}
C (mg/L)	68.2	39.69	58.99									
M (mg/mmol)	35.5	96	61	19	62	95						
C (mmol/L)	1.92	0.41	0.97	0.00	0.00	0.00					3.9E-05	
Valency	1	2	1	1	1	3					1	
meq/L	1.92	0.83	0.97	0.00	0.00	0.00					3.9E-05	3.72
eq/L	1.9E-03	8.3E-04	9.7E-04	0.0E+00	0.0E+00	0.0E+00					3.9E-08	0.00372

$S_{pos} - S_{neg} = -2.06 \text{ meq/L}$ $(S_{pos} - S_{neg})/S_{pos} = -125 \%$
 $-2.1E-03 \text{ eq/L}$ **Generally: < 10 %**

Summary of ionic balances differences between negative and positive ions:

Date	Difference, %
21/06/05	-125
23/05/05	-407
25/04/05	-479
29/03/05	-169
28/02/05	-131
31/01/05	-125
4/1/2005	-92
8/12/2004	-155

All the time negative ions are higher than the positive ions.

7.1.3 Flocculation, G & Gt values

Temperature, T = 10 [°C]
 Flow, Q = 75 [m³/h] = 0.0208 [m³/s]
 Volume, V = 50 [m³]
 Head loss, Δh = 0.05 [m]
 Gravity, g = 9.81 [m/s²]

Answer

According to temperature, kinematic viscosity is:

$$\nu = 1.31 \times 10^{-6} \text{ [m}^2\text{/s]}$$

mean detention time is:

$$t = V / Q$$

$$t = 2400 \text{ [s]}$$

$$t = 40 \text{ [min]} \quad \text{ok}$$

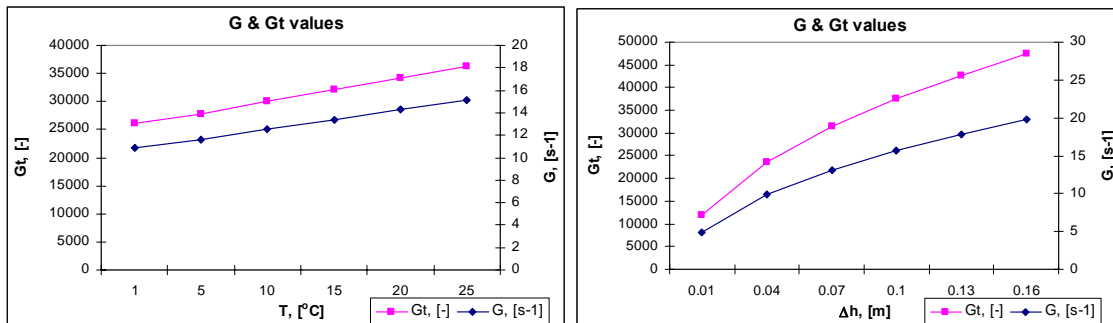
so,

$$G = 12.5 \text{ [s}^{-1}\text{]}$$

Not ok, low value

$$Gt = 30017$$

ok, in the range



7.1.4 Theoretical Solubility of Aluminium

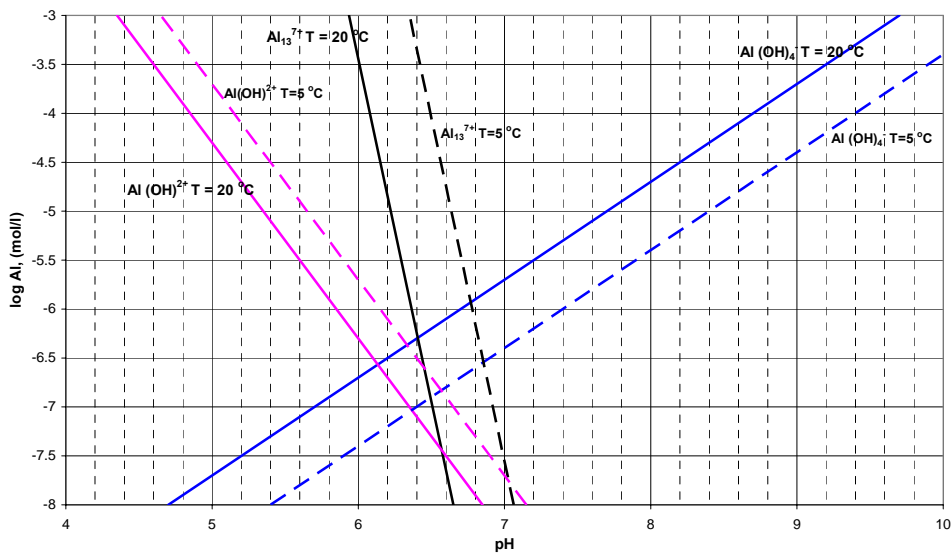


Figure 7-1 Theoretical solubility for Al species in equilibrium with Al(OH)₃(am) indicated by solid (20°C) and dashed (5°C) lines. (Pernitsky et al., 2003)

Table 7-1 Summary of Coagulant solubility

Coagulant	Minimum Solubility			
	20 °C		5 °C	
	pH	µg/L Al	pH	µg/L Al
Alum	6	16	6.2	3
Polyaluminium Sulfate (PAS)	6	28	6.4	6
PAC low basicity non sulfated (LBNS)	6.2	27	6.7	4
PAC medium basicity sulfated (MBS)	6.3	29	6.5	4
PAC high basicity non-sulfated (HBNS)	6.4	36	6.8	9
PAC high basicity sulfated (HBS)	6.4	52	6.9	5
Aluminium-Chlorohydrate (ACH)	6.7	101	7.6	53

Source: Pernitsky et al. (2003)

7.1.5 Sampling Points for LCOCD test

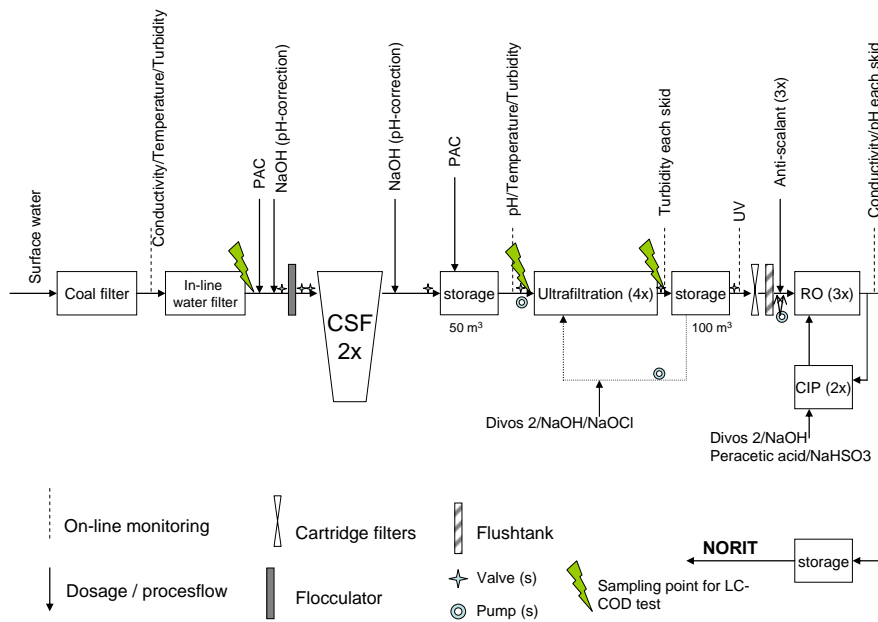


Figure 7-2 Proposed sampling points for LC-COD test

7.2 Annex 2 - Equations for aluminium solubility and concentration along R.O. systems

Data:

Parameter	Comment
Recovery, R	It is desired a range from zero to ninety percent for the calculations.
Rejection, f	It is assumed that the salt rejection is equal to 100 %. This makes the calculations “theoretical” or “hypothetical”.
Salt Passage, SP	Because of the assumed salt rejection, the salt passage is zero.
Temperature, T	It has an important effect in the concentration of aluminium species but not in the pH RO concentrate.
pH _{feed}	pH value that enters the RO unit.
[HCO ₃ ⁻]	Feed concentration in RO units.

Determining pH RO concentrate

- Concentration Factor, CF $CF = \frac{1-R \cdot (1-f)}{(1-R)}$

- pK

$$pK = f\{\text{Temp}\}$$

T, °C	pK
5	6.52
10	6.46
15	6.42
20	6.38
25	6.35

Doing a regression for the table we have,

$$pK = 6.5784174 - 0.012885537 \cdot \text{Temp} + 0.00014834711 \cdot (\text{Temp})^2$$

- $[\text{CO}_2]_{\text{concentrate}}$

$$pH = pK + \log\left(\frac{[\text{HCO}_3^-]}{[\text{CO}_2]}\right)$$

$$pH = pK + \log[\text{HCO}_3^-] - \log[\text{CO}_2]$$

$$\log [\text{CO}_2] = pK - pH + \log [\text{HCO}_3^-]$$

$$[\text{CO}_2]_{\text{concentrate}} = 10^{\left[pK - pH_{\text{feed}} + \log(\text{HCO}_3^-)_{\text{feed}}\right]}$$

- $[\text{HCO}_3^-]_{\text{concentrate}}$

$$[\text{HCO}_3^-]_{\text{concentrate}} = CF_{\text{hyp}} \times [\text{HCO}_3^-]_{\text{feed}}$$

- $pH_{\text{concentrate}}$

$$pH_{\text{concentrate}} = pK + \log \frac{(\text{HCO}_3^-)_{\text{concentrate}}}{(\text{CO}_2)_{\text{concentrate}}}$$

$$pH_{\text{concentrate}} = pK + \log \frac{CF_{\text{hyp}} \times (\text{HCO}_3^-)_{\text{feed}}}{(\text{CO}_2)_{\text{concentrate}}}$$

$$pH_{\text{concentrate}} = pK + \log CF_{\text{hyp}} + \log (\text{HCO}_3^-)_{\text{feed}} - \log (\text{CO}_2)_{\text{concentrate}}$$

$$\text{CO}_2_{\text{concentrate}} = \text{CO}_2_{\text{feed}}$$

So,

$$pH_{\text{concentrate}} = \log CF_{\text{hyp}} + pH_{\text{feed}}$$

Temperature doesn't play a role in the calculation of pH concentrate.

7.2.1 Determining aluminium species solubility

For every Recovery (%) correspond a $pH_{\text{concentrate}}$ (assuming $f = 1$).

For $T = 20^\circ\text{C}$



With the $\text{pH}_{\text{concentrate}}$

$$\log \text{Al(OH)}_4^- = \text{pH}_{\text{concentrate}} - 12.7 \quad \text{in mol/l}$$

$$\text{Al(OH)}_4^- = 10^{\text{pH}_{\text{concentrate}}} \times \left(\frac{1}{10^{12.7}} \right) \quad \text{in mol/l}$$

With the pH_{feed}

$$\log \text{Al(OH)}_4^- = (\log \text{CF}_{\text{hyp}} + \text{pH}_{\text{feed}}) - 12.7 \quad \text{in mol/l}$$

$$\log \text{Al(OH)}_4^- = \log \text{CF}_{\text{hyp}} + \text{pH}_{\text{feed}} - 12.7 \quad \text{in mol/l}$$

$$\text{Al(OH)}_4^- = \text{CF}_{\text{hyp}} \times 10^{\text{pH}_{\text{feed}}} \times \left(\frac{1}{10^{12.7}} \right) \quad \text{in mol/l}$$



With the $\text{pH}_{\text{concentrate}}$

$$\log \text{Al}_{13}^{7+} = -7 \times \text{pH}_{\text{concentrate}} + 38.55 \quad \text{in mol/l}$$

$$\text{Al}_{13}^{7+} = [10^{(-7)}]^{\text{pH}_{\text{concentrate}}} \times 10^{38.55} \quad \text{in mol/l}$$

With the pH_{feed}

$$\log \text{Al}_{13}^{7+} = -7 \times (\log \text{CF}_{\text{hyp}} + \text{pH}_{\text{feed}}) + 38.55 \quad \text{in mol/l}$$

$$\log \text{Al}_{13}^{7+} = -7 \times \log \text{CF}_{\text{hyp}} - 7 \times \text{pH}_{\text{feed}} + 38.55 \quad \text{in mol/l}$$

$$\text{Al}_{13}^{7+} = \frac{[10^{(-7)}]^{\log(\text{CF}_{\text{hyp}})}}{[10^7]^{\text{pH}_{\text{feed}}}} \times 10^{38.55} \quad \text{in mol/l}$$



With the $\text{pH}_{\text{concentrate}}$

$$\log \text{Al(OH)}^{2+} = -2 \times \text{pH}_{\text{concentrate}} + 5.7$$

$$\text{Al(OH)}^{2+} = [10^{(-2)}]^{\text{pH}_{\text{concentrate}}} \times 10^{5.7}$$

With the pH_{feed}

$$\log \text{Al(OH)}^{2+} = -2 \times (\log \text{CF}_{\text{hyp}} + \text{pH}_{\text{feed}}) + 5.7 \quad \text{in mol/l}$$

$$\log \text{Al(OH)}^{2+} = -2 \times \log \text{CF}_{\text{hyp}} - 2 \times \text{pH}_{\text{feed}} + 5.7 \quad \text{in mol/l}$$

$$\text{Al(OH)}^{2+} = \frac{[10^{(-2)}]^{\log(\text{CF}_{\text{hyp}})}}{[10^2]^{\text{pH}_{\text{feed}}}} \times 10^{5.7} \quad \text{in mol/l}$$

For $T = 5^\circ\text{C}$



With the $\text{pH}_{\text{concentrate}}$

$$\log \text{Al(OH)}_4^- = \text{pH}_{\text{concentrate}} - 13.4 \quad \text{in mol/l}$$

$$Al(OH)_4^- = 10^{pH_{concentrate}} \times \left(\frac{1}{10^{13.4}} \right) \quad \text{in mol/l}$$

With the pH_{feed}

$$\log Al(OH)_4^- = (\log CF_{hyp} + pH_{feed}) - 13.4 \quad \text{in mol/l}$$

$$\log Al(OH)_4^- = \log CF_{hyp} + pH_{feed} - 13.4 \quad \text{in mol/l}$$

$$Al(OH)_4^- = CF_{hyp} \times 10^{pH_{feed}} \times \left(\frac{1}{10^{13.4}} \right) \quad \text{in mol/l}$$

$$\mathbf{Al_{13}^{7+}}$$

With the $pH_{concentrate}$

$$\log Al_{13}^{7+} = -7 * pH_{concentrate} + 41.45 \quad \text{in mol/l}$$

$$Al_{13}^{7+} = [10^{(-7)}]^{pH_{concentrate}} \times 10^{41.45} \quad \text{in mol/l}$$

With the pH_{feed}

$$\log Al_{13}^{7+} = -7 \times (\log CF_{hyp} + pH_{feed}) + 41.45 \quad \text{in mol/l}$$

$$\log Al_{13}^{7+} = -7 \times \log CF_{hyp} - 7 \times pH_{feed} + 41.45 \quad \text{in mol/l}$$

$$Al_{13}^{7+} = \frac{[10^{(-7)}]^{\log(CF_{hyp})}}{[10^7]^{pH_{feed}}} \times 10^{41.45} \quad \text{in mol/l}$$



With the $pH_{concentrate}$

$$\log Al(OH)^{2+} = -2 * pH_{concentrate} + 6.3$$

$$Al(OH)^{2+} = [10^{(-2)}]^{pH_{concentrate}} \times 10^{6.3}$$

With the pH_{feed}

$$\log Al(OH)^{2+} = -2 \times (\log CF_{hyp} + pH_{feed}) + 6.3 \quad \text{in mol/l}$$

$$\log Al(OH)^{2+} = -2 \times \log CF_{hyp} - 2 \times pH_{feed} + 6.3 \quad \text{in mol/l}$$

$$Al(OH)^{2+} = \frac{[10^{(-2)}]^{\log(CF_{hyp})}}{[10^2]^{pH_{feed}}} \times 10^{6.3} \quad \text{in mol/l}$$

Now, for every species of Aluminium it is possible to find its correspondent concentration in the RO concentrate in mol/l and later on in mg/l.

Conversion from mol/l to mg/l of aluminium:

Aluminium molecular weight = 27 gr/mol

mg Al/l = 27 gr/mol \times 1000 mg/gr \times mol Al/l

7.2.2 Determining aluminium species concentration

It is expected that the aluminium concentration after coagulation will be equal to the solubility of aluminium. Therefore for calculating the aluminium concentration in the RO it is assumed that the initial concentration is that one for R = 0 %.

For every Recovery (R) corresponds a CF_{hyp}

Initial concentration of aluminium:

$$Al_{\text{feed concentration}} = Al_{\text{solubility for R = 0\%}}$$

$$Al_{\text{concentration}} = CF_{hyp} \times Al_{\text{feed concentration}}$$

Therefore, we have:

For $T = 20 \text{ } ^\circ\text{C}$



With the $pH_{\text{concentrate}}$

Initial concentration (solubility for R=0%):

$$\left[Al(OH)_4^- \right]_{R=0\%} = 10^{(pH_{\text{concentrate}})_{R=0\%}} \times \left(\frac{1}{10^{12.7}} \right) \quad \text{in mol/l}$$

$pH_{\text{concentrate}}$ corresponds to the one in R = 0 %.

$Al(OH)_4^-$ concentration as function of recovery is:

$$\left[Al(OH)_4^- \right] = CF_{hyp} \times \left[Al(OH)_4^- \right]_{R=0}$$

With the pH_{feed}

Initial concentration (solubility for R=0%):

$$Al(OH)_4^- = CF_{hyp} \times 10^{pH_{\text{feed}}} \times \left(\frac{1}{10^{12.7}} \right) \quad \text{in mol/l}$$

But $CF_{hyp} = 1$ for Recovery = 0 % (initial concentration condition)

$$\left[Al(OH)_4^- \right]_{R=0\%} = 1 \times 10^{pH_{\text{feed}}} \times \left(\frac{1}{10^{12.7}} \right) \quad \text{in mol/l}$$

$Al(OH)_4^-$ concentration as function of recovery is:

$$\left[Al(OH)_4^- \right] = CF_{hyp} \times \left[Al(OH)_4^- \right]_{R=0}$$

$$\left[Al(OH)_4^- \right] = CF_{hyp} \times \left[1 \times 10^{pH_{\text{feed}}} \times \left(\frac{1}{10^{12.7}} \right) \right] \quad \text{in mol/l}$$

$$\therefore \left[Al(OH)_4^- \right]_{\text{concentration}} = \left[Al(OH)_4^- \right]_{\text{solubility}}$$

$$Al_{13}^{7+}$$

With the $pH_{\text{concentrate}}$

Initial concentration (solubility for R=0%):

$$\left[Al_{13}^{7+} \right]_{R=0\%} = \left[10^{(-7)} \right]^{(pH_{\text{concentrate}})_{R=0\%}} \times 10^{38.55} \quad \text{in mol/l}$$

$\text{pH}_{\text{concentrate}}$ corresponds to the one in $R = 0\%$.

Al_{13}^{7+} concentration as function of recovery is:

$$[\text{Al}_{13}^{7+}] = \text{CF}_{\text{hyp}} \times [\text{Al}_{13}^{7+}]_{R=0\%} \quad \text{in mol/l}$$

With the pH_{feed}

Initial concentration (solubility for $R=0\%$):

$$\text{Al}_{13}^{7+} = \frac{[10^{(-7)}]^{\log(\text{CF}_{\text{hyp}})}}{[10^7]^{\text{pH}_{\text{feed}}}} \times 10^{38.55} \quad \text{in mol/l}$$

But $\text{CF}_{\text{hyp}} = 1$ for Recovery = 0 % (initial concentration condition)

$$\text{Al}_{13}^{7+} = \frac{[10^{(-7)}]^{\log(1)}}{[10^7]^{\text{pH}_{\text{feed}}}} \times 10^{38.55} \quad \text{in mol/l}$$

$$[\text{Al}_{13}^{7+}]_{R=0\%} = \frac{10^{38.55}}{[10^7]^{\text{pH}_{\text{feed}}}} \quad \text{in mol/l}$$

Al_{13}^{7+} concentration as function of recovery is:

$$[\text{Al}_{13}^{7+}] = \text{CF}_{\text{hyp}} \times [\text{Al}_{13}^{7+}]_{R=0\%}$$

$$\therefore [\text{Al}_{13}^{7+}] = \text{CF}_{\text{hyp}} \times \frac{10^{38.55}}{[10^7]^{\text{pH}_{\text{feed}}}} \quad \text{in mol/l}$$



With the $\text{pH}_{\text{concentrate}}$

Initial concentration (solubility for $R=0\%$):

$$[\text{Al(OH)}^{2+}]_{R=0\%} = [10^{(-2)}]^{(\text{pH}_{\text{concentrate}})_{R=0\%}} \times 10^{5.7} \quad \text{in mol/l}$$

$\text{pH}_{\text{concentrate}}$ corresponds to the one in $R = 0\%$.

Al(OH)^{2+} concentration as function of recovery is:

$$[\text{Al(OH)}^{2+}] = \text{CF}_{\text{hyp}} \times [\text{Al(OH)}^{2+}]_{R=0\%} \quad \text{in mol/l}$$

With the pH_{feed}

Initial concentration (solubility for $R=0\%$):

$$\text{Al(OH)}^{2+} = \frac{[10^{(-2)}]^{\log(\text{CF}_{\text{hyp}})}}{[10^2]^{\text{pH}_{\text{feed}}}} \times 10^{5.7} \quad \text{in mol/l}$$

But $\text{CF}_{\text{hyp}} = 1$ for Recovery = 0 % (initial concentration condition)

$$\text{Al(OH)}^{2+} = \frac{[10^{(-2)}]^{\log(1)}}{[10^2]^{\text{pH}_{\text{feed}}}} \times 10^{5.7} \quad \text{in mol/l}$$

$$\left[Al(OH)^{2+} \right]_{R=0\%} = \frac{10^{5.7}}{\left[10^2 \right]^{pH_{feed}}} \quad \text{in mol/l}$$

$Al(OH)^{2+}$ concentration as function of recovery is:

$$\left[Al(OH)^{2+} \right] = CF_{hyp} \times \left[Al(OH)^{2+} \right]_{R=0\%}$$

$$\therefore Al(OH)^{2+} = CF_{hyp} \times \frac{10^{5.7}}{\left[10^2 \right]^{pH_{feed}}} \quad \text{in mol/l}$$

For $T = 5^\circ C$



With the $pH_{concentrate}$

Initial concentration (solubility for $R=0\%$):

$$\left[Al(OH)_4^- \right]_{R=0\%} = 10^{(pH_{concentrate})_{R=0\%}} \times \left(\frac{1}{10^{13.4}} \right) \quad \text{in mol/l}$$

$pH_{concentrate}$ corresponds to the one in $R = 0\%$.

$Al(OH)_4^-$ concentration as function of recovery is:

$$\left[Al(OH)_4^- \right] = CF_{hyp} \times \left[Al(OH)_4^- \right]_{R=0}$$

With the pH_{feed}

Initial concentration (solubility for $R=0\%$):

$$Al(OH)_4^- = CF_{hyp} \times 10^{pH_{feed}} \times \left(\frac{1}{10^{13.4}} \right) \quad \text{in mol/l}$$

But $CF_{hyp} = 1$ for Recovery = 0 % (initial concentration condition)

$$\left[Al(OH)_4^- \right]_{R=0\%} = 1 \times 10^{pH_{feed}} \times \left(\frac{1}{10^{13.4}} \right) \quad \text{in mol/l}$$

$Al(OH)_4^-$ concentration as function of recovery is:

$$\left[Al(OH)_4^- \right] = CF_{hyp} \times \left[Al(OH)_4^- \right]_{R=0}$$

$$\left[Al(OH)_4^- \right] = CF_{hyp} \times \left[1 \times 10^{pH_{feed}} \times \left(\frac{1}{10^{13.4}} \right) \right] \quad \text{in mol/l}$$

$$\therefore \left[Al(OH)_4^- \right]_{concentration} = \left[Al(OH)_4^- \right]_{solubility}$$



With the $pH_{concentrate}$

Initial concentration (solubility for $R=0\%$):

$$\left[Al_{13}^{7+} \right]_{R=0\%} = \left[10^{(-7)} \right]^{(pH_{concentrate})_{R=0\%}} \times 10^{41.45} \quad \text{in mol/l}$$

$pH_{concentrate}$ corresponds to the one in $R = 0\%$.

Al_{13}^{7+} concentration as function of recovery is:

$$[Al_{13}^{7+}] = CF_{hyp} \times [Al_{13}^{7+}]_{R=0\%} \quad \text{in mol/l}$$

With the pH_{feed}

Initial concentration (solubility for $R=0\%$):

$$Al_{13}^{7+} = \frac{[10^{(-7)}]^{\log(CF_{hyp})}}{[10^7]^{pH_{feed}}} \times 10^{41.45} \quad \text{in mol/l}$$

But $CF_{hyp} = 1$ for Recovery = 0 % (initial concentration condition)

$$Al_{13}^{7+} = \frac{[10^{(-7)}]^{\log(1)}}{[10^7]^{pH_{feed}}} \times 10^{41.45} \quad \text{in mol/l}$$

$$[Al_{13}^{7+}]_{R=0\%} = \frac{10^{41.45}}{[10^7]^{pH_{feed}}} \quad \text{in mol/l}$$

Al_{13}^{7+} concentration as function of recovery is:

$$[Al_{13}^{7+}] = CF_{hyp} \times [Al_{13}^{7+}]_{R=0\%}$$

$$\therefore [Al_{13}^{7+}] = CF_{hyp} \times \frac{10^{41.45}}{[10^7]^{pH_{feed}}} \quad \text{in mol/l}$$



With the $pH_{concentrate}$

Initial concentration (solubility for $R=0\%$):

$$[Al(OH)^{2+}]_{R=0\%} = [10^{(-2)}]^{(pH_{concentrate})_{R=0\%}} \times 10^{6.3} \quad \text{in mol/l}$$

$pH_{concentrate}$ corresponds to the one in $R = 0\%$.

$Al(OH)^{2+}$ concentration as function of recovery is:

$$[Al(OH)^{2+}] = CF_{hyp} \times [Al(OH)^{2+}]_{R=0\%} \quad \text{in mol/l}$$

With the pH_{feed}

Initial concentration (solubility for $R=0\%$):

$$Al(OH)^{2+} = \frac{[10^{(-2)}]^{\log(CF_{hyp})}}{[10^2]^{pH_{feed}}} \times 10^{6.3} \quad \text{in mol/l}$$

But $CF_{hyp} = 1$ for Recovery = 0 % (initial concentration condition)

$$Al(OH)^{2+} = \frac{[10^{(-2)}]^{\log(1)}}{[10^2]^{pH_{feed}}} \times 10^{6.3} \quad \text{in mol/l}$$

$$[Al(OH)^{2+}]_{R=0\%} = \frac{10^{6.3}}{[10^2]^{pH_{feed}}} \quad \text{in mol/l}$$

$Al(OH)^{2+}$ concentration as function of recovery is:

$$[\text{Al}(\text{OH})^{2+}] = CF_{\text{hyp}} \times [\text{Al}(\text{OH})^{2+}]_{\text{R}=0\%}$$

$$\therefore \text{Al}(\text{OH})^{2+} = CF_{\text{hyp}} \times \frac{10^{6.3}}{[10^2]^{pH_{\text{feed}}}} \quad \text{in mol/l}$$

7.3 Annex 3 – Simulation of Al solubility and concentration

7.3.1 T = 20°C

It is important to remark that in all cases the initial concentrations of aluminium species are equal to solubility of each species. This is done for understanding the behaviour of aluminium with pH and recovery. It is important to notice that real concentration in RO concentrate is 120 µg/l in average.

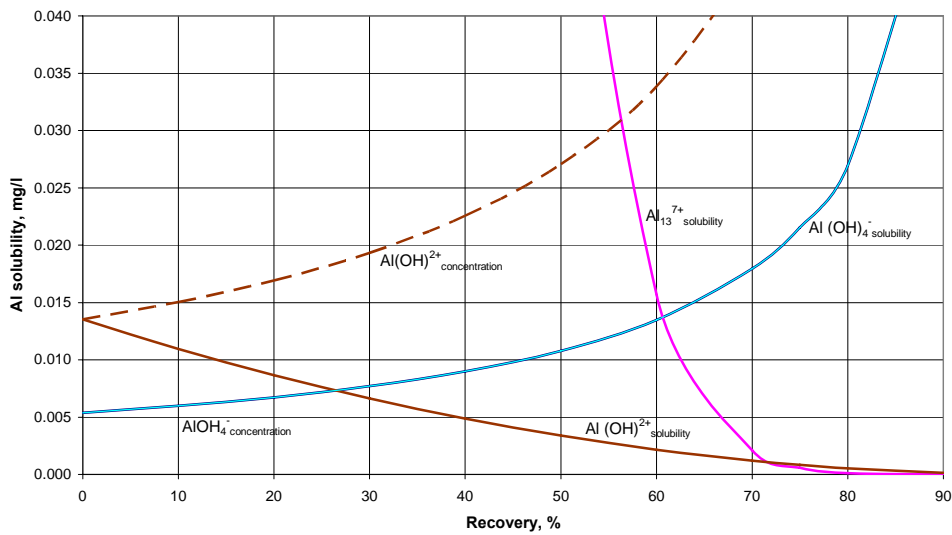


Figure 7-3 Simulation Al solubility and Al concentration (pH_{feed RO} = 6), T = 20°C (a)

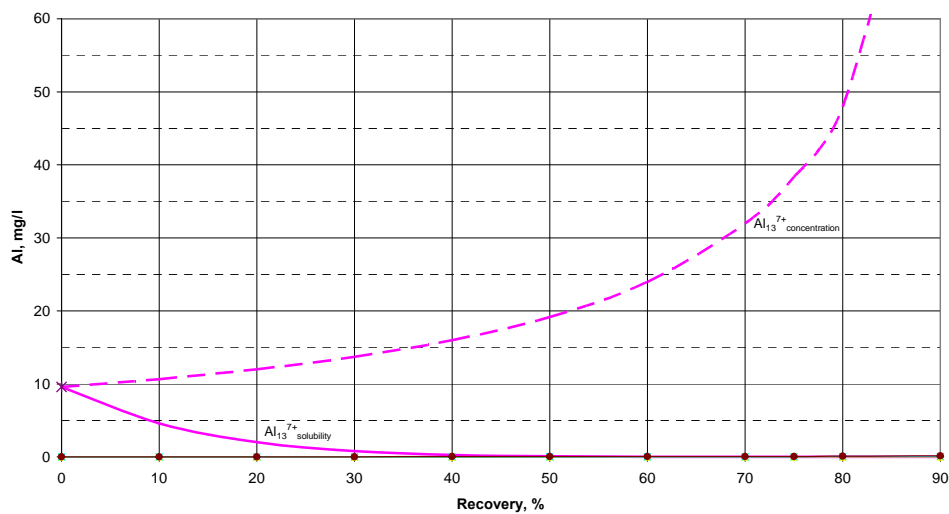


Figure 7-4 Simulation Al solubility and Al concentration (pH_{feed RO} = 6), T = 20°C (b)

For $\text{Al}(\text{OH})_4^-$ the concentration and the solubility overlap and increase with increasing recovery. For Al_{13}^{7+} , solubility decreases rapidly while its concentration is increasing.

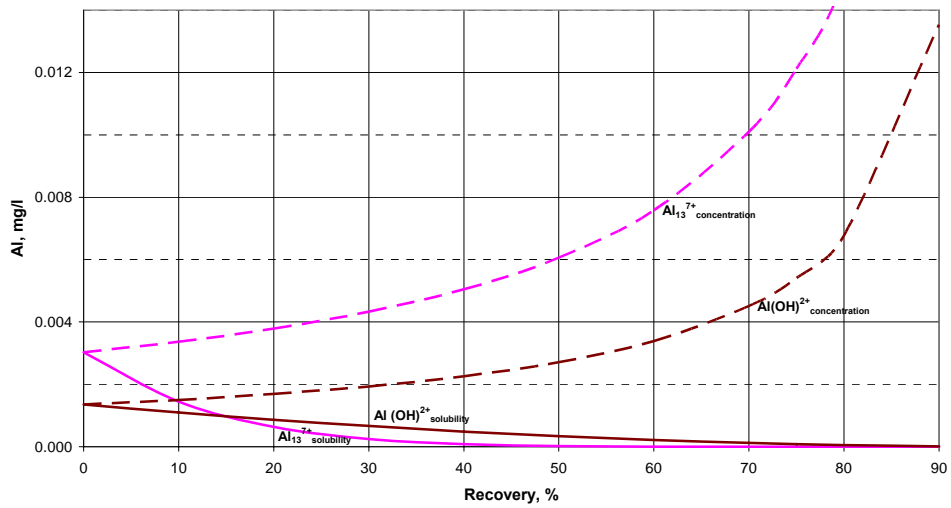


Figure 7-5 Simulation Al solubility and Al concentration ($\text{pH}_{\text{feed RO}} = 6.5$), $T = 20^\circ\text{C}$ (a)

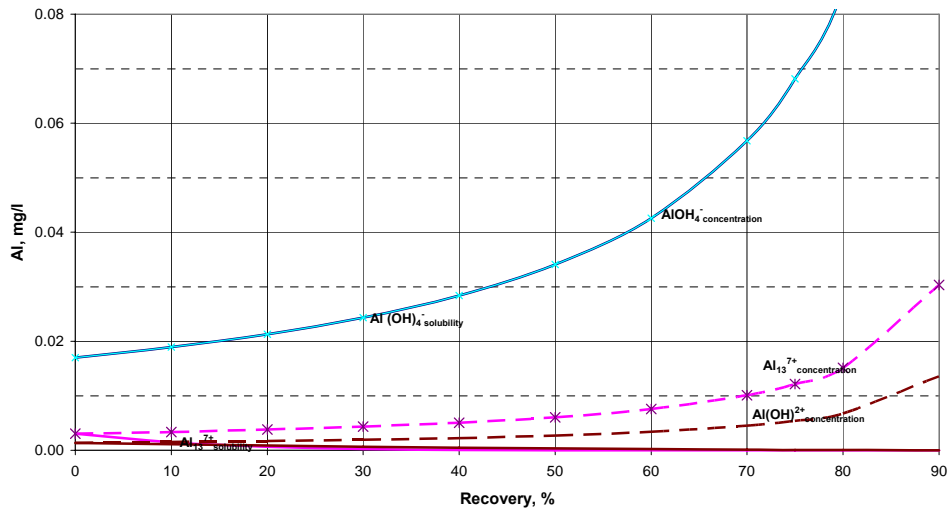


Figure 7-6 Simulation Al solubility and Al concentration ($\text{pH}_{\text{feed RO}} = 6.5$), $T = 20^\circ\text{C}$ (b)

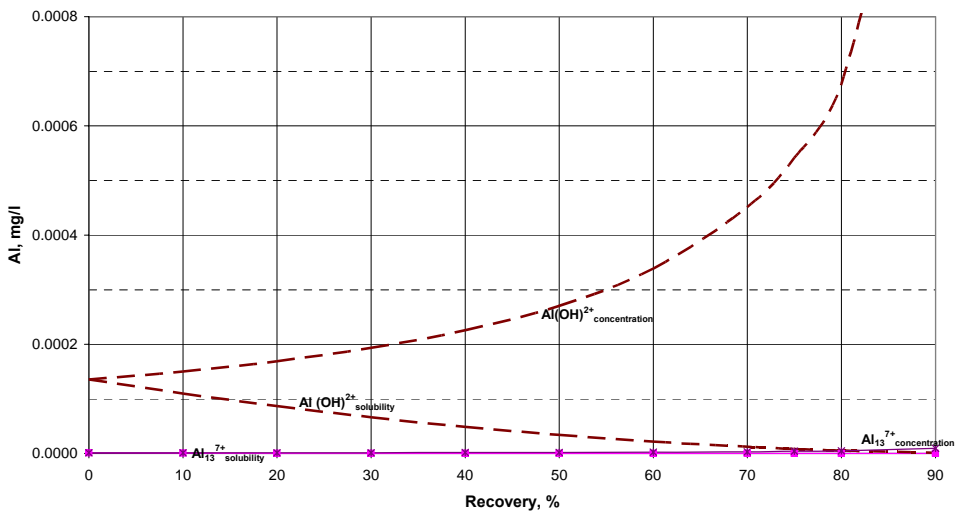


Figure 7-7 Simulation Al solubility and Al concentration ($\text{pH}_{\text{feed RO}} = 7$), $T = 20^\circ\text{C}$ (a)

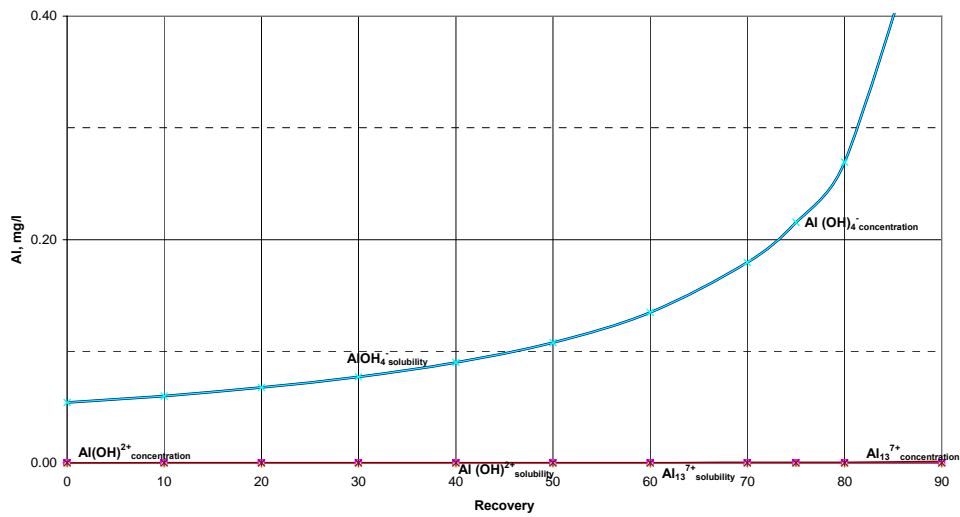


Figure 7-8 Simulation Al solubility and Al concentration ($\text{pH}_{\text{feed RO}} = 7$), $T = 20^\circ\text{C}$ (b)

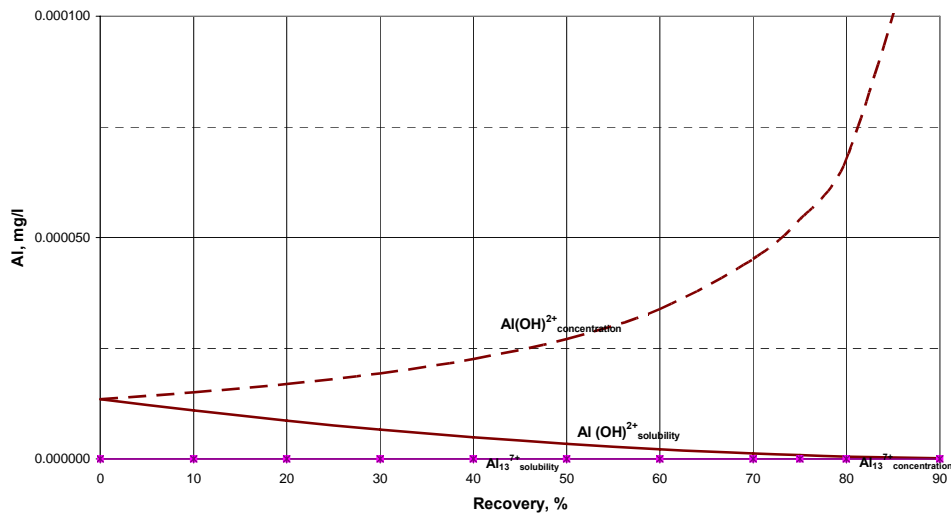


Figure 7-9 Simulation Al solubility and Al concentration ($\text{pH}_{\text{feed RO}} = 7.5$), $T = 20^\circ\text{C}$ (a)

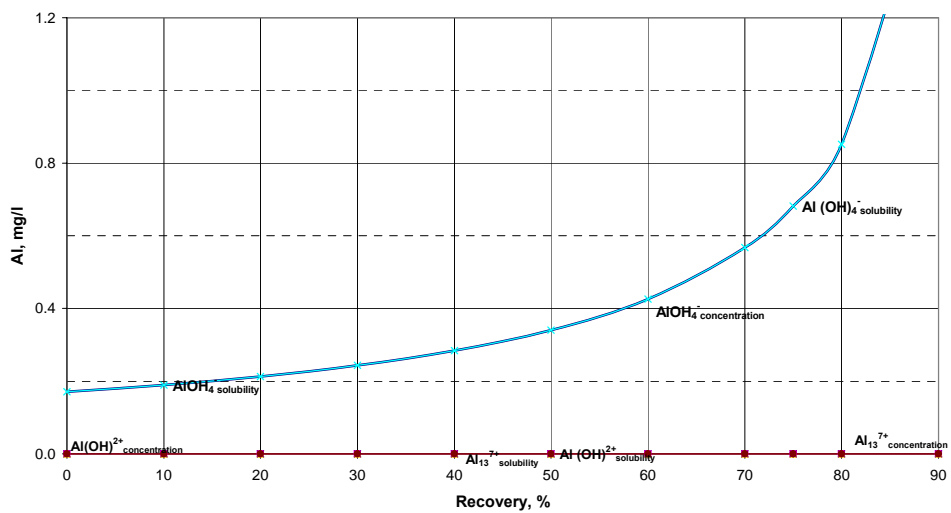


Figure 7-10 Simulation Al solubility and Al concentration ($\text{pH}_{\text{feed RO}} = 7.5$), $T = 20^\circ\text{C}$ (b)

7.3.2 T = 5°C

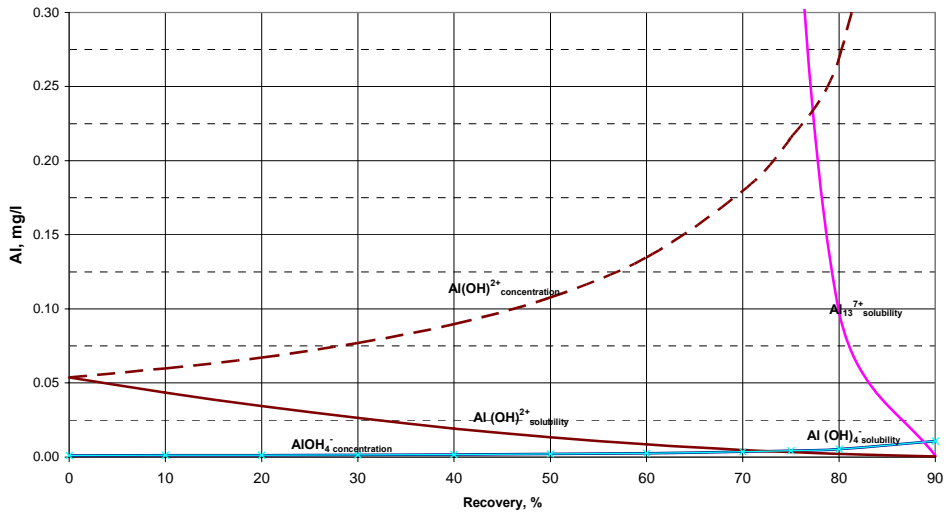


Figure 7-11 Simulation Al solubility and Al concentration (pH_{feed RO} = 6), T = 5 °C (a)

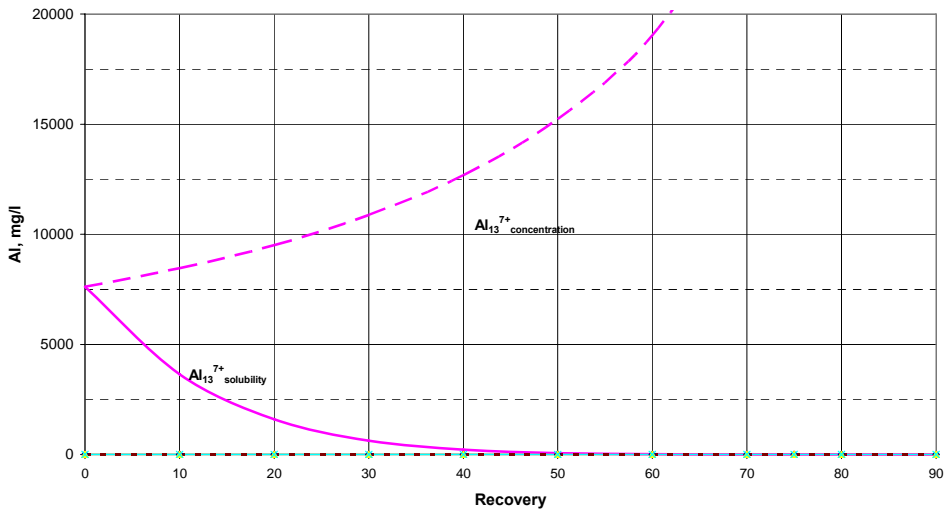


Figure 7-12 Simulation Al solubility and Al concentration (pH_{feed RO} = 6), T = 5 °C (b)

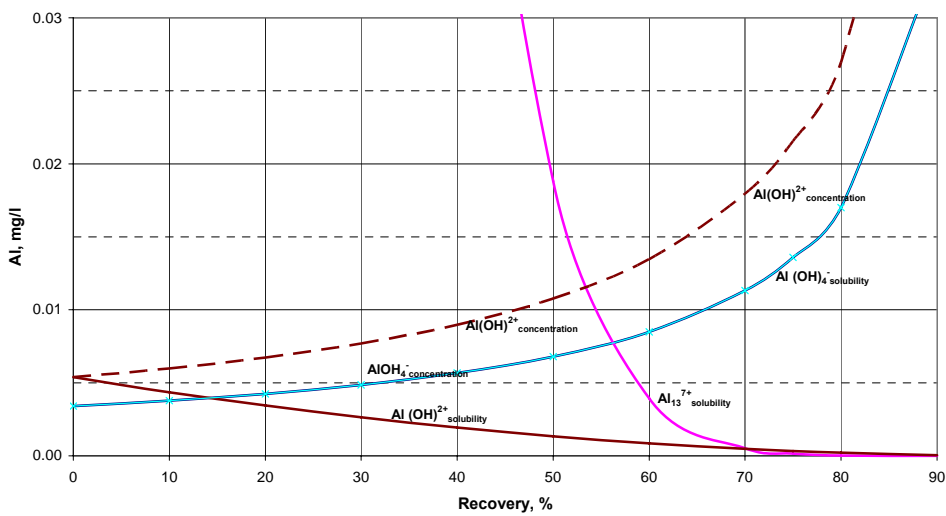


Figure 7-13 Simulation Al solubility and Al concentration (pH_{feed RO} = 6.5), T = 5 °C (a)

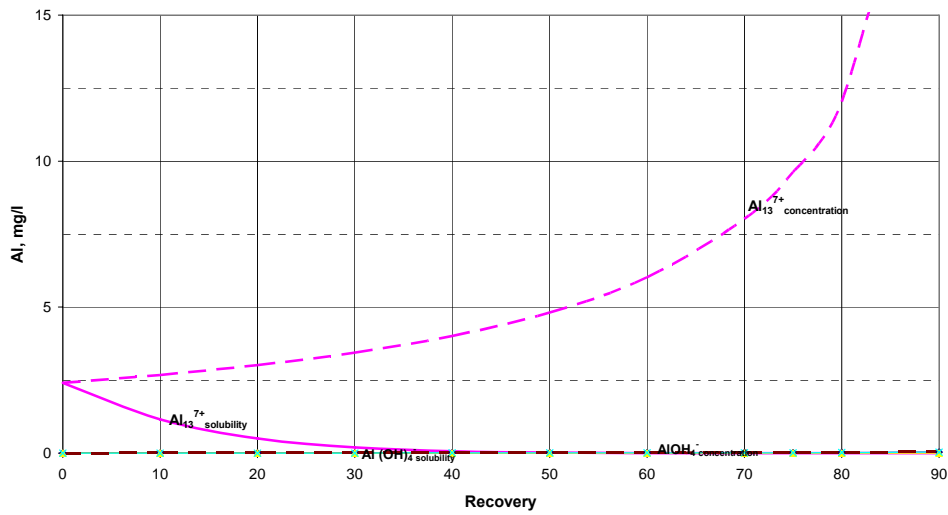


Figure 7-14 Simulation Al solubility and Al concentration ($\text{pH}_{\text{feed RO}} = 6.5$), $T = 5\text{ }^\circ\text{C}$ (a)

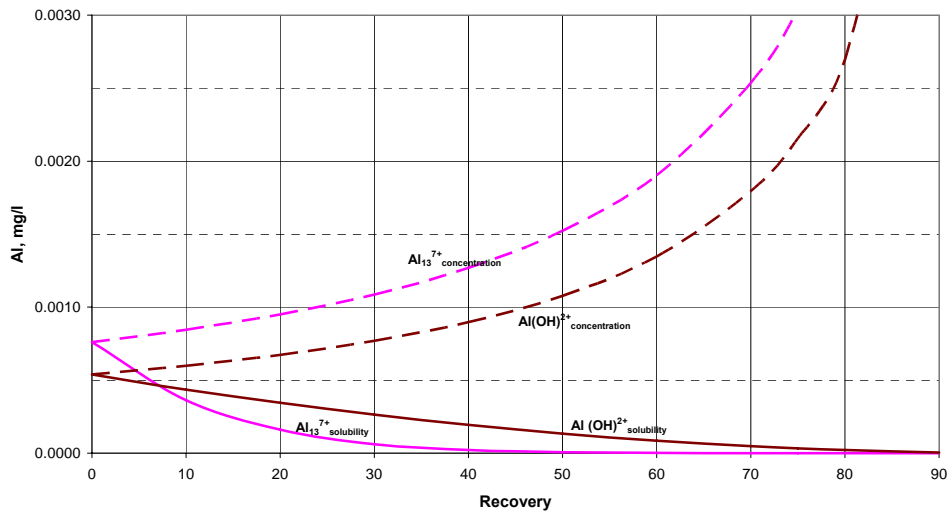


Figure 7-15 Simulation Al solubility and Al concentration ($\text{pH}_{\text{feed RO}} = 7$), $T = 5\text{ }^\circ\text{C}$ (a)

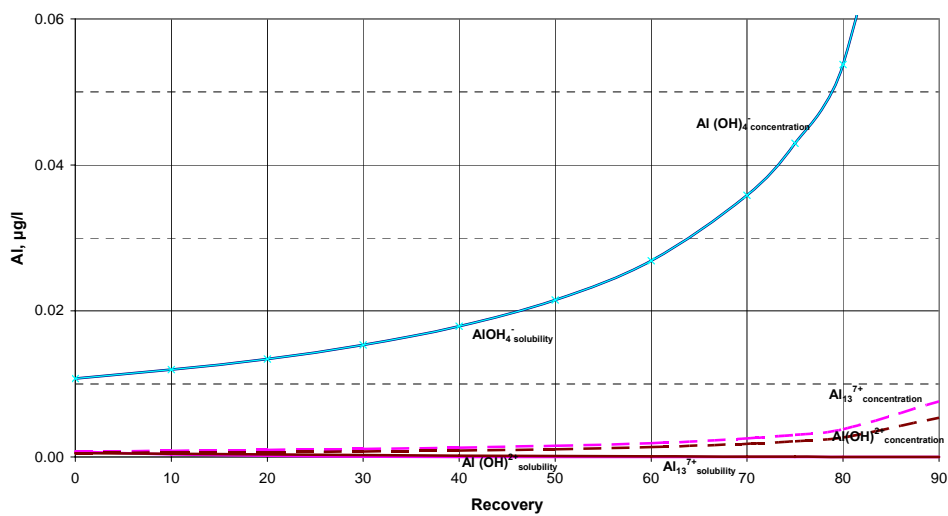


Figure 7-16 Simulation Al solubility and Al concentration ($\text{pH}_{\text{feed RO}} = 7$), $T = 5\text{ }^\circ\text{C}$ (b)

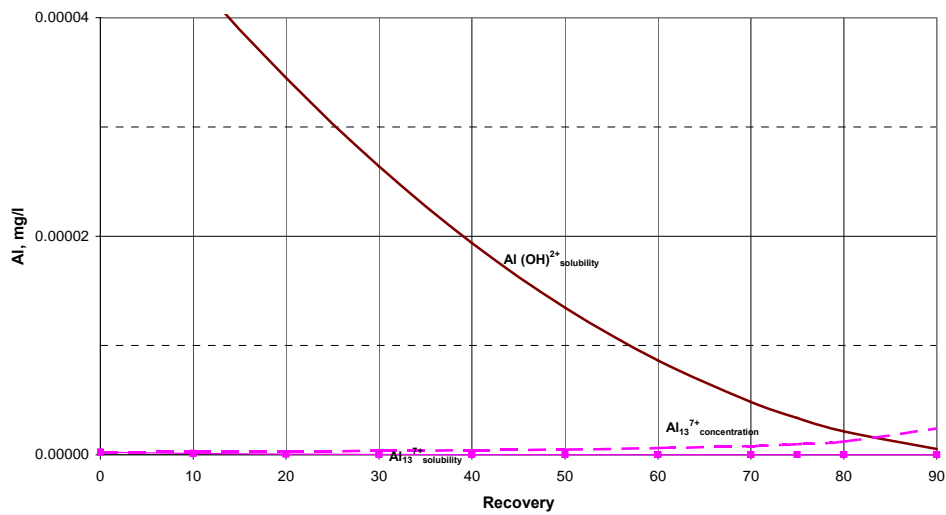


Figure 7-17 Simulation Al solubility and Al concentration ($\text{pH}_{\text{feed RO}} = 7.5$), $T = 5\text{ }^\circ\text{C}$ (a)

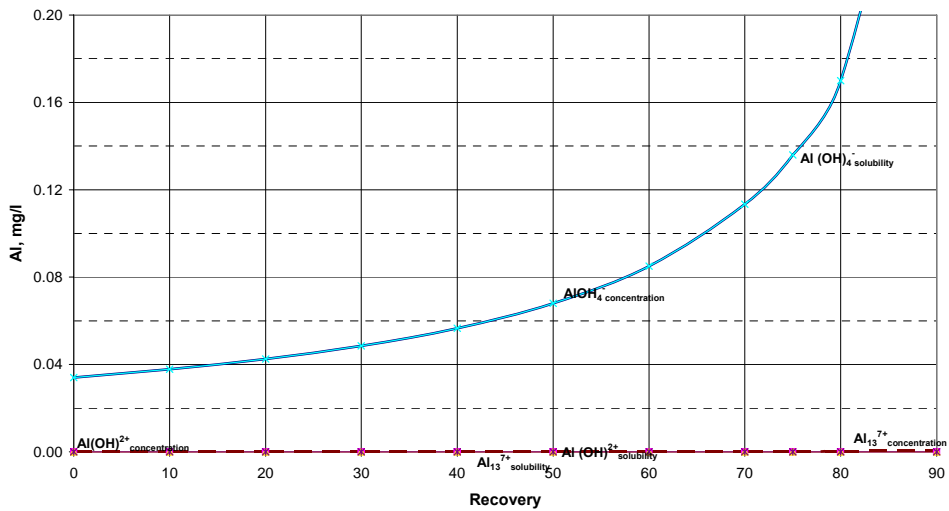


Figure 7-18 Simulation Al solubility and Al concentration ($\text{pH}_{\text{feed RO}} = 7.5$), $T = 5\text{ }^\circ\text{C}$ (b)

7.4 Annex 4. Aluminium soluble in water

As it is available for two temperatures (5 and 20 °C) the solubility concentrations it was defined two ranges, lower and higher than 12 °C for using the formulas for the Al species. After this, with the pH was calculated the total solubility and compared later on with the aluminium concentration in RO feedwater and concentrate water.

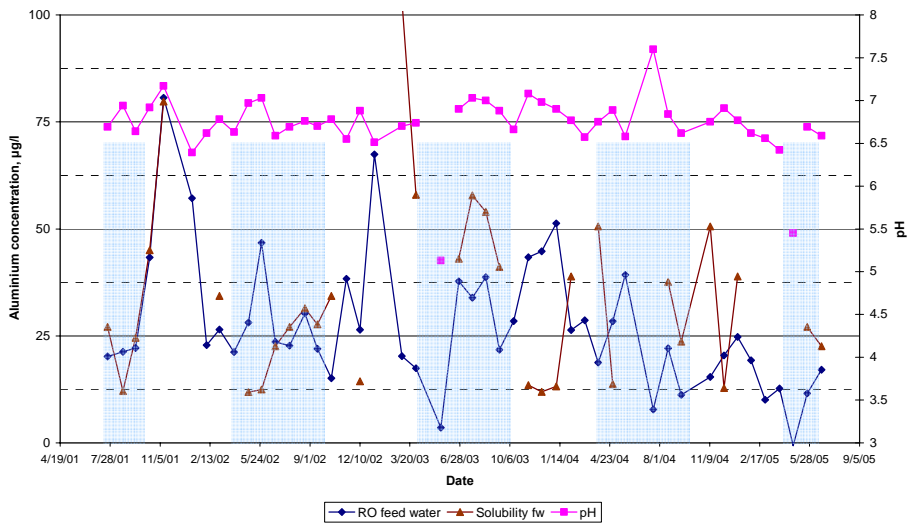


Figure 7-19 Aluminium concentration (data) and Al solubility in RO feed water, µg/l

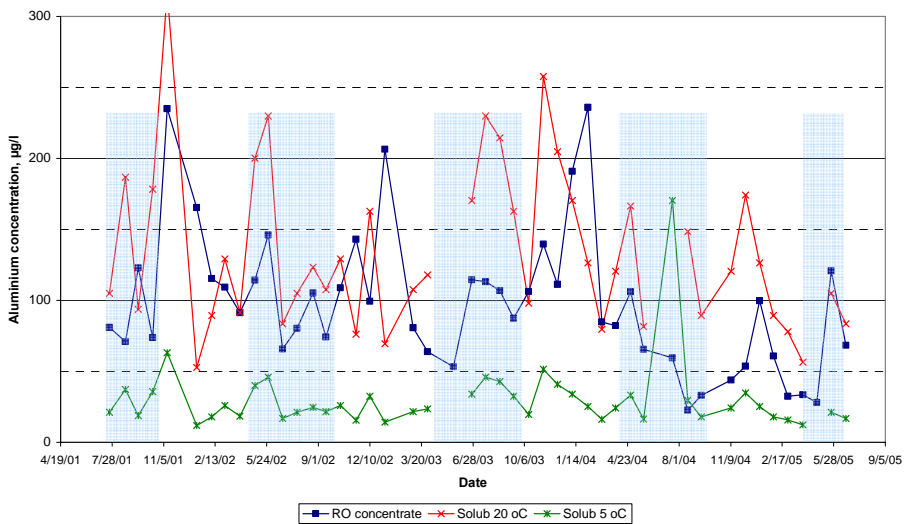


Figure 7-20 Aluminium concentration and Al solubility in RO concentrate water, µg/l

Most of time the concentrate water in the RO is supersaturated with aluminium. There are some extreme values for the solubility that can be caused by differences of temperature and pH that could be defined as outliers. It is in “winter” periods where the concentration exceeds the solubility in majority.

7.5 Annex 5. Deposition factor, pH and Temperature

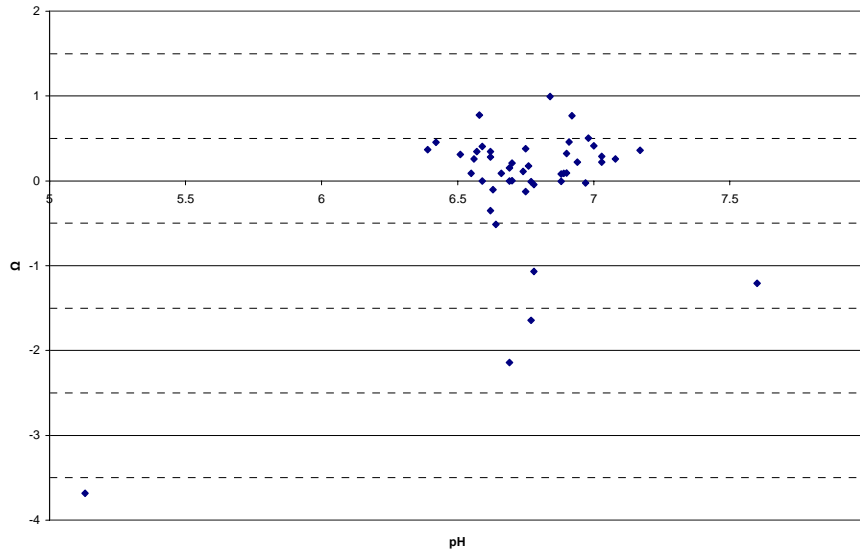


Figure 7-21 Deposition factor (Ω) as function of pH (Recovery = 75 %, $CF_{hyp} = 4$)

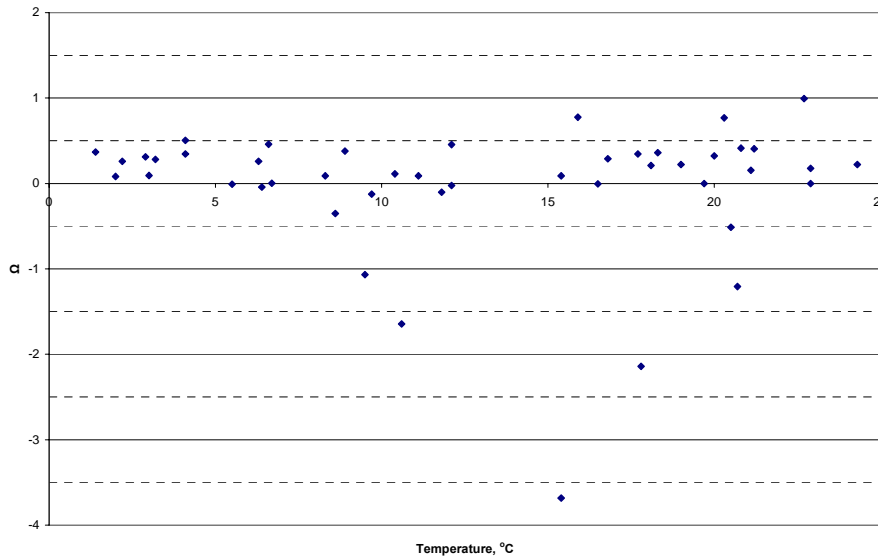


Figure 7-22 Deposition Factor (Ω) as function of Temperature (Recovery = 75 %, $CF_{hyp} = 4$)

7.6 Annex 6 - The Modified Fouling Index (MFI)

Cake Filtration equations

The MFI can be determined under constant flux filtration. In this mode the permeate flux is kept constant and the pressure is increasing to maintain a constant flux.

Cake filtration is based on the fundamental equation for the rate of flow through a porous medium.

Flux is:

$$J = \frac{dV}{A dt} = \frac{\Delta P}{\mu R_{total}} = \frac{\Delta P}{\mu (R_m + R_b + R_c)}$$

Cake resistance is: $R_c = \frac{V}{A} \times I$, [m⁻¹]

V = filtrate volume, [m³]

A = membrane surface area, [m²]

C_b = concentration of particles in feed water, [kg/m³]

I = index for the propensity of particles in water to form a layer with hydraulic resistance, [1/m²]

$I = \alpha \cdot C_b$, for incompressible cake

$I = \alpha_0 \Delta P_c^\omega C_b$, taking into account cake compression

where ω is the compressibility coefficient and α_0 a constant. For incompressible cakes, ω is zero and the higher the compressibility coefficient the more compressible the cake.

And the specific cake resistance (Carman eq.) is:

$$\alpha = \frac{180(1-\varepsilon)}{\rho_p d_p^2 \varepsilon^3}, [\text{m/kg}]$$

Integrating results in:

$$\frac{t}{V} = \frac{\mu R_0}{\Delta P A} + \frac{\mu \alpha C_b}{2 \Delta P A^2} V$$

The MFI determined in Constant Pressure Mode

The modified Fouling Index (MFI) is based on cake filtration, whereby, particles are retained on the membrane during filtration by a mechanism of surface deposition. The MFI can be measured at constant pressure using the well known cake filtration equation where the MFI is defined as the gradient of the linear region found in the plot of t/V versus V:

$$\frac{t}{V} = \frac{\eta R_m}{\Delta P A} + \frac{\eta I}{2 \Delta P A^2} V \quad \text{Eq. 1}$$

↑
(MFI)

where V is filtrate volume, t filtration time, ΔP the applied transmembrane pressure, η the water viscosity and A the membrane surface area. The MFI is calculated at standard reference values of ΔP (2 bar), η ($\eta_{20^\circ\text{C}}$) and A the surface area of the 0.45 μm test membrane ($13.8 \times 10^{-4} \text{ m}^2$). I in equation 6 refers to the fouling index which is a measure of the fouling potential of the feedwater. The fouling index I is defined as the product of α the specific resistance of the cake deposited and C_b the concentration of particles in the feedwater (Equation 7). An advantage of using the fouling index I is that most cases it is impossible to determine C_b and α accurately.

$$I = \alpha C_b \quad \text{Eq. 2}$$

Equation 2 is for an incompressible cake. However, the MFI is also valid for compressible cakes as when the pressure drop over the cake ΔP_c is dominant, a linear relationship between t/V versus V will appear and the MFI value can then be determined. The fouling index I taking into account cake compression is defined as follows:

$$I = \alpha_0 \Delta P_c^\omega C_b \quad \text{Eq. 3}$$

Where w is the compressibility coefficient and α_0 a constant. For incompressible cakes, ω is zero and the higher the compressibility coefficient the more compressible the cake. Substitution of the Carman-Kozeny relationship for the specific resistance of a cake composed of spherical particles in the MFI gives:

$$\alpha = \frac{180(1-\varepsilon)}{\rho_p d_p^2 \varepsilon^3} \quad (\text{Carman-Kozeny Equation})$$

$$MFI = \frac{\eta_{20^\circ C} 90(1-\varepsilon)C_b}{\rho_p d_p^2 \varepsilon^3 \Delta P_0 A_0^2} \quad \text{Eq. 4}$$

Thus, the MFI is a function of the dimension and nature of the particles forming a cake on the membrane, and directly correlated to the concentration of particles in a feedwater. At the fixed reference values of ΔP_0 , $\eta_{20^\circ C}$ and A_0 , the MFI can be used to characterize and compare the fouling potential of feedwater containing particles.

The MFI Determined in Constant Flux Mode

The MFI can also be determined under constant flux filtration. In this mode of filtration the permeate flux is kept constant and the pressure is increasing to maintain a constant flux. Taking the standard equation describing the flux through a membrane:

$$\frac{dV}{A dt} = \frac{\Delta P}{\eta(R_m + R_c)} \quad \text{Eq. 5}$$

And substituting J for flux and R_c by:

$$R_c = \frac{V}{A} \times I \quad \text{Eq. 6}$$

The following equation is obtained:

$$J = \frac{\Delta P}{\eta \left(\frac{V}{A} \cdot I + R_m \right)} \quad \text{Eq. 7}$$

Rewriting V/A as Jt and rearranging gives:

$$\Delta P = J \eta R_m + J^2 \eta I t \quad \text{Eq. 8}$$

The following index I can then be determined from the slope of the linear region in a plot of ΔP versus time which corresponds to cake filtration or by manipulation of Equation 13. The MFI can be calculated using I (from Equation 13) for standard reference conditions as follows:

$$MFI = \frac{\eta_{20^\circ C} I}{2 \Delta P_0 A_0^2} \quad \text{Eq. 9}$$

MFI-UF Determination

Constant pressure mode

$$MFI-UF = \frac{\eta_{20^\circ C}}{\eta_r} \left(\frac{\Delta P}{\Delta P_0} \right)^{1-\omega} \left(\frac{A}{A_0} \right)^2 \frac{d \frac{t}{V}}{dV} \quad \text{Eq. 10}$$

The global pressure correction (ω) value of 0.75 was applied to correct for cake filtration effects. The MFI-UF reported represents the average calculated over the stable region (corresponds to cake filtration) of the MFI-UF over time in a single test.

Constant Flux Mode

To determine the MFI-UF of a feedwater in the constant flux mode, the pressure reducing valve of the MFI-UF equipment was manually adjusted to maintain the required applied flux at a constant value. The fouling index I was calculated at time (t) by manipulation of Equation 8 which gives:

$$I = \frac{\Delta P - J \eta_{20^\circ C} R_m}{J^2 \eta_{20^\circ C} t} \quad \text{Eq. 11}$$

Where J is the applied flux corrected to 20°C and R_m is the membrane resistance at the beginning of the test. The fouling index I was input into Equation 9 to determine the MFI-UF at standard reference conditions.

Symbols

A	membrane surface area, [m ²]
A ₀	reference surface are of a 0.45 m membrane filter [13.8x10 ⁻⁴ m ²]
C _b	concentration of particles in feedwater [kg/m ³]
d _p	particle diameter, [m]
I	index for the propensity of particles in water to form a layer with hydraulic resistance [m ⁻²]
J	permeate water flux [m ³ /m ² s]
ΔP	applied transmembrane pressure [bar] or [N/m ²]
ΔP _c	pressure drop over the cake [bar] or [N/m ²]
ΔP ₀	reference applied transmembrane pressure [2 bar]
R	resistance to filtration [m ⁻¹]
R _b	resistance due to blocking [m ⁻¹]
R _c	resistance of the cake [m ⁻¹]
R _m	membrane filter resistance [m ⁻¹]
V	filtrate volume, [m ³]
α	specific cake resistance [m/kg]
ε	cake porosity [-]
η	fluid viscosity [Ns/m ²]
ω	compressibility coefficient [-]
ρ _p	density of particles forming the cake [kg/m ³]

7.7 Annex 7 - Specific Resistance

Data:

Flux, J =	20	[l/m ² hr]	5.56E-06	[m ³ /m ² s]	(Operation: Flux is constant in the plant)
ΔP =	200000	[N/m ²]	2	[bar]	(Assumed increment average)
Temperature, T =	10	[°C]			
Viscosity water, =	1.31E-03	[Ns/m ²]			

$$R_{total} = \frac{\Delta P}{\mu \cdot J} \quad \text{So,} \quad R_{total} = 2.76E+13 \text{ [m}^{-1}\text{]}$$

Concentration of particles, C _b =	0.0000372	[kg/m ³]	Min = 0.000035	Max = 0.000413
Cake porosity, ε =	0.5	[-]	Min = 0.25	Max = 0.75
(Range assumed based on "experience knowledge")				
Particle density, ρ _p =	2700	[kg/m ³]	(Value correspondant to aluminium density)	
Particle diameter, d _p =	1.25E-08	[m]	Min = 5.00	Max = 20.00
(Depend on UF pore size in nm)				

Membranes

Diameter:	8	[inch]		
Area/element:	37.16	[m ²]		
total membrane area per skid:	1114.8	[m ²]		
total membrane area installation:	3344.5	[m ²]		
Flow, Q =	743.2	[l/hr]	per element	
Filtrate volume, V =	374.59	[m ³]	in three weeks cycle	

Constant Flux Mode

This means that the pressure is varying and increasing with time.

Now, $\alpha = \frac{180(1-\varepsilon)}{\rho_p d_p^2 \varepsilon^3}$ $I = \alpha \cdot C_b$ $R_c = \frac{V}{A} \times I = J \cdot t \cdot I$

α =	1.71E+15	[m/kg]	α = specific resistance of the cake per unit of weight
I =	6.35E+10	[m ²]	Fouling Index
R _c =	6.40E+11	[m ⁻¹]	

Now, $C_b \times J \times t = \text{mg/l} \times (\text{l/m}^2 \cdot \text{hr}) \times \text{hr} = \text{mg/m}^2$

Deposition factor =	0.21			
t =	3	week		
	504	hr	μg Al/cm ² =	7.87
C _b =	0.0372	mg/l	μm Al/cm ² =	0.0292 <i>dividing by density</i>
mg Al/m ² =	375.0		nm Al/cm ² =	29.2 <i>in time "t"</i>
mg Al/m ² =	78.7	<i>considering deposition factor</i>		

